Integration of PV with CSP and Thermal Storages in Solar Power Plants

Investigations about Synergies by close Coupling

Final report of the research project: IntegSolar

Grant numbers:
DLR e.V.: 03EE5011A
Dornier Suntrace GmbH: 03EE5011B

Supported by:

Federal Ministry
for Economic Affairs
and Climate Action

on the basis of a decision
by the German Bundestag

Contributors

Jürgen Dersch, DLR

Luca Schomaker, Dornier Suntrace

Javier Inigo Labairu, DLR

Sujay Mhaske, Dornier Suntrace

Lukas Pfundmaier, Dornier Suntrace

Martin Schlecht, Dornier Suntrace

Felix Zimmermann, Dornier Suntrace

Acknowledgements

This work was funded by the German Federal Ministry for Economic Affairs and Energy (Funding reference number: 03EE5011). The responsibility for the content is solely by the authors. The authors gratefully acknowledge the funding.

Suggested Citation

Dersch, Juergen; Schomaker, Luca:

Integration of CSP and PV Power Plants, Cologne, Germany. Final report of the research project "IntegSolar" No. 03EE5011, https://elib.dlr.de/188367/

Table of Contents

1. Introduction

The project IntegSolar investigated the hybridization options for Concentrating Solar Power (CSP) and Photovoltaic (PV) power plants combining benefits of both systems by deeper integration. PV-CSP hybrid power plants are an attractive option for supplying cheap and dispatchable solar electricity. Through this project, a techno-economic analysis of these hybrid power plants was carried out in search of those combinations which provide lowest LCOE (under certain boundary conditions), and the results were compared with other technologies.

One of the main objectives of the project was the evaluation of the synergy effects produced by the hybridization of the CSP plant with a PV plant. CSP systems with integrated thermal storage offer a cost-effective way to generate solar power even after sunset and at times of low solar radiation, while photovoltaic systems offer lower costs for solar power generation during daytime hours. Therefore, there are currently approaches to integrate both types of power plant and thereby use the respective advantages to offer cost-effective solar power generation with high security of supply and high solar coverage. In this project, a close coupling between both technologies is proposed to increase the advantages of this integration. Understanding and optimizing this integration and the synergies produced was one of the biggest challenges of the project as they were dependent on the boundary conditions and were not always obvious.

The impact of boundary conditions on the optimum configurations was another fundamental aspect of the investigation. Different locations with different radiation and latitude conditions were simulated. The influence of different demand curve profiles was also investigated, and systematic sensitivity analyses were carried out through the variation of the cost assumptions. The most suitable plant types and configurations for the given boundary conditions were considered.

The hybrid systems analysed were the parabolic trough CSP plant in combination with a PV plant and the central receiver system also together with a PV plant. These systems were optimized and compared with other technologies like pure CSP plants, PV with battery storage and PV with electric heaters, thermal storage and power block. The optimization was performed not only to achieve the lowest solar electric costs for the systems but also to increase the proportion of electricity delivered to the grid during the hours when the sun is not shining.

The software greenius was used by DLR for the simulations. Some modifications were done during the project to enable the simulation of all systems, especially hybrid PV-CSP plants. Dornier Suntrace developed and used its proprietary HYPPO software that also allows the calculation of hybrid PV-CSP plants, and the results of both tools were compared. Both tools permit a flexible and efficient optimization of the plant and its economic evaluation and deliver comparable results.

There are currently approaches to integrate both types of power plant and thus to use the respective advantages. Some publications show the research carried out on hybrid PV-CSP plants in recent years. DLR participated in THERMVOLT project [1], where the combination of CSP, PV, thermal storage, battery storage and backup combined cycle power plants was examined. The focus was on fulfilling representative load curves while at the same time limiting the specific CO2 emissions in kg/kWh of produced electricity. Grid coupling of the systems was also investigated, but without deep integration like in this project. Starke et al. [2] conducted a techno-economic analysis for the evaluation of the performance of hybrid PV-CSP plants in northern Chile. The parametric analysis and optimization showed high potential in this region for the installation of hybrid PV-CSP plants due to

the high levels of irradiation. Zhai et. al [3] proposed a thermal storage PV-CSP plant and calculated the annual hourly performance of the system. Two different dispatch strategies were studied: a conventional strategy in which the PV and CSP system operate independently and a constant-output strategy that integrated both systems producing some synergies. Lower LCOEs were presented by the constant-output strategy that resulted in a more fluid and stable power output. Zurita et al. [4] performed a techno-economic evaluation of a hybrid PV-CSP plant integrated with a thermal energy storage and a large-scale battery energy storage for base generation in northern Chile. LCOE and the capacity factor were used to evaluate the performance of the plant identifying the configurations with a minimum LCOE. Results showed that battery costs should be reduced by approximately 60-90% to attain competitive LCOEs in comparison to hybrid plants. Riffelmann et al. [5] studied different options to combine benefits of PV and CSP technologies. A small PV plant that supplied the own consumption of the CSP plant, hybrid CSP-PV plants with optional electric heater and a PV system with additional electrical heater were simulated for different scenarios. For a Spanish location, the most economic configuration combined a CSP plant that charged the thermal storage during daytime and produced electricity during night time and a PV system that delivered electricity at day hours charging additionally the thermal storage with an electric heater. In contrast, the calculation of the best configuration in a high DNI site like South Africa resulted in a system without electric heater. For both locations, the electricity produced with the CSP plant and thermal storage was more economic than the one originated from the PV system with electric heater. Mata-Torres et al. [6] assessed the impact of solar irradiation and plant location for a hybrid PV-CSP plant integrated to a multi-effect distillation plant for simultaneous power generation and seawater desalination. A techno-economic analysis was performed at different locations to determine the most suitable sites for this kind of plant showing that inland locations with considerable increase of DNI with respect to the coast (over 300 kWh/m^2-yr), distances from the sea of no more than 60 km and altitudes up to 750-1000 m presented the most appropriate conditions. Richter et al. [7] defined a predictive storage strategy for an optimal design of hybrid PV-CSP plants with immersion heater. It was proven that the strategy had a huge impact on the output of the plant and the subsystem sizing.

Moreover, some hybrid plants are already under construction or operational. Phase 4 of MBR Solar Park in Dubai is under construction and will combine 600MW (three units of 200MW each) parabolic trough, 100MW molten salt solar power tower and 250MW photovoltaic plant [8]. Noor Midelt 1 in Morocco will have a total installed capacity of 800MW and hybridise concentrated solar power and photovoltaic technologies with a 5 hours thermal storage [9]. Cerro Dominador was inaugurated in Chile in 2021 and has a 110 MW central tower and a 100 MW photovoltaic field [10]. Additionally, 4 projects that combine CSP and PV has been started in China. Each project will include 100 MW of CSP and 900 MW of PV [11].

2. Technologies and Plant Concepts

2.1. Benefits and Challenges of hybridizing CSP and PV projects

Different plant concepts using CSP, or PV technology were analysed. The deployment of these technologies represents several general advantages.

CSP power plants with thermal energy storage are a cost-effective option for storing renewable energy for use after sunset. Thermal energy storage is economical and due to its easy scale-up has low marginal cost. The power block can work efficiently in a wide range of part-load conditions and is relatively flexible in terms of dispatchability (generation on-demand). At the same time, CSP solar fields can generate heat very efficiently.

PV plants, on the other hand, have low electricity generation costs. PV is the cheapest source of electricity during daytime in regions with high solar irradiation and its direct generation of electricity allows flexible use (direct electricity sale, P2H, P2G, auxiliary supply, etc.).

Two different options for the integration of PV and CSP technologies in solar hybrid power plants are generally possible. The first option can be called “grid-integrated” hybrid plants. The hybridization takes place on grid level where the electrical power output of both subsystems is “hybridized” in the transmission grid and the grid operator is responsible for controlling the separate plant outputs. In this strategy the plants could even be in different locations, connected to the same branch of a transmission grid. In the case of solar plants located remotely or in great distance to each other, the grid capacity may be a limiting factor, or grid capacity may have to be oversized in order to avoid curtailment of renewable generation.

The second option includes “fully-integrated” hybrid plants. The different technologies are hybridized on system level or in other words “inside the fence”. These plants have only one common grid-access point. Here the plant operator is responsible for controlling the separate subsystem outputs, their interactions, and their contribution to the grid power (and ancillary services) supply. Electrical and thermal energy is enabled to flow between subsystems in order to provide charging power to energy storage systems or for unidirectional supply of auxiliary power. Many synergies are possible. Firstly, if the CSP system does not produce electricity during the day, it would charge the thermal storage system having its own electrical requirements to operate the solar field. The daily demand can be then covered by the coupled PV system. Secondly, the self-consumption of the CSP systems reaches the range of 10% of their nominal power. However, steam turbines often cannot be operated at this low partial load point. Therefore, covering self-consumption with the CSP system in standalone operation is not trivial and the integrated PV plant may be used for this purpose. If the PV system supplies excess electricity that the grid cannot consume at the time, this could be stored in the thermal storage system of the CSP power plant using power-to-heat technologies. This energy could be used at a later time instead of being dumped. Finally, the physical proximity and the integration reduce the grid load and eases coordinated operation and production planning for the next few days. A solar hybrid power plant fully integrated on system level benefits from multiple synergies, but also comes with more challenges due to a higher number of degrees of freedom in the system design and operating strategy. In this project only the second option (“fully-integrated” hybrid plants) was evaluated.

The combination of both systems would not lead to lower electricity generation costs compared to standalone PV plants. However, the generation of solar power at times of the day when the sun does not shine cannot be covered by the PV plant without storage. In this respect, storing energy in the heat storage tank should be viewed in comparison to an alternative storage concept. A joint optimization of PV and CSP to a specific power generation profile will therefore lead to electricity generation costs that will lie between those of pure PV (without battery) and the pure CSP power plant. A shift in power generation from the CSP power plant to the evening hours can result, for example, in this CSP power plant having a smaller solar field than with a pure CSP plant that also supplies electricity during the day. In this case, the storage size and the power plant unit remain basically unchanged. Savings are therefore primarily made in the solar field, which may account for about 50% of the investment costs of the CSP power plant (this is given here only as an indicative value, since the cost fraction of the solar field depends on the storage size).

2.2. Plant concepts

The following systems were analysed in this study:

- **Parabolic trough hybrid power plant:**
  - PV injects electricity into the grid during the day.
  - The power block generates electricity at night from the thermal storage.
  - The electric heater is connected in series to the CSP field and works as a booster for the parabolic trough cycle increasing the TES inlet temperature and thus improving PB efficiency and increasing the TES energy capacity.
  - Priority Order for the use of PV output power:
    1. Auxiliary Supply: cover the auxiliary consumption of the CSP solar field (pumps, auxiliary heating)
    2. Booster function: increase the temperature of the molten salt from nominal outlet temperature of the parabolic trough solar field (385°C) to the nominal temperature of the hot tank (565°C),
    3. Excess electricity is delivered to the grid.
  - Thermal storage upper HFT temperature is equal to central receiver plant temperature levels (565°C).
  - Steam generator is always operated with hot salt in this variant. Direct use of thermal oil to generate steam does not make any technical or economic sense because a second steam generator would be required, and the turbine would have to be operated with significantly reduced live steam parameters.

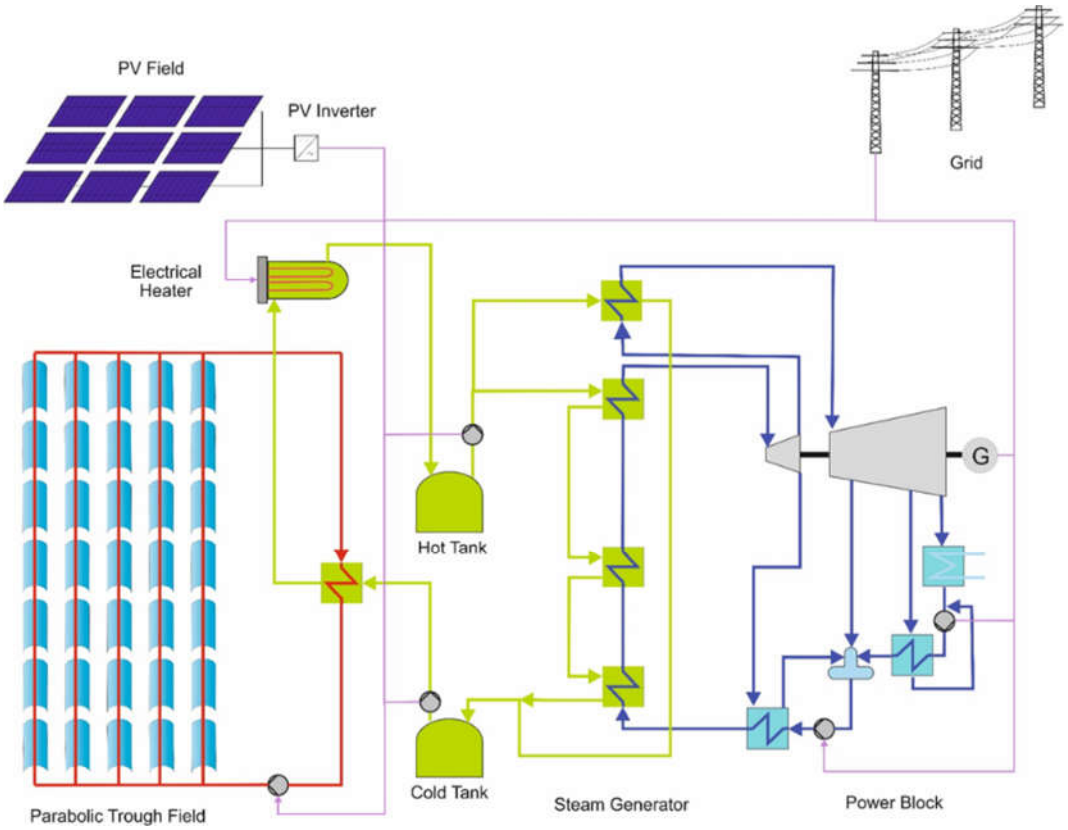

Figure 1: Parabolic trough hybrid power plant

- **Tower hybrid power plant without electric heater**
    - PV injects electricity into the grid during the day.
    - The power block generates electricity at night from the thermal storage.
    - PV provides auxiliary power to CSP plant (pumps, heliostat tracking, PB startup auxiliaries).
    - Priority Order for the use of PV output power:
        1. Auxiliary Supply: PV power is used to cover auxiliary requirements of the CSP plant.
        2. Direct Grid injection.

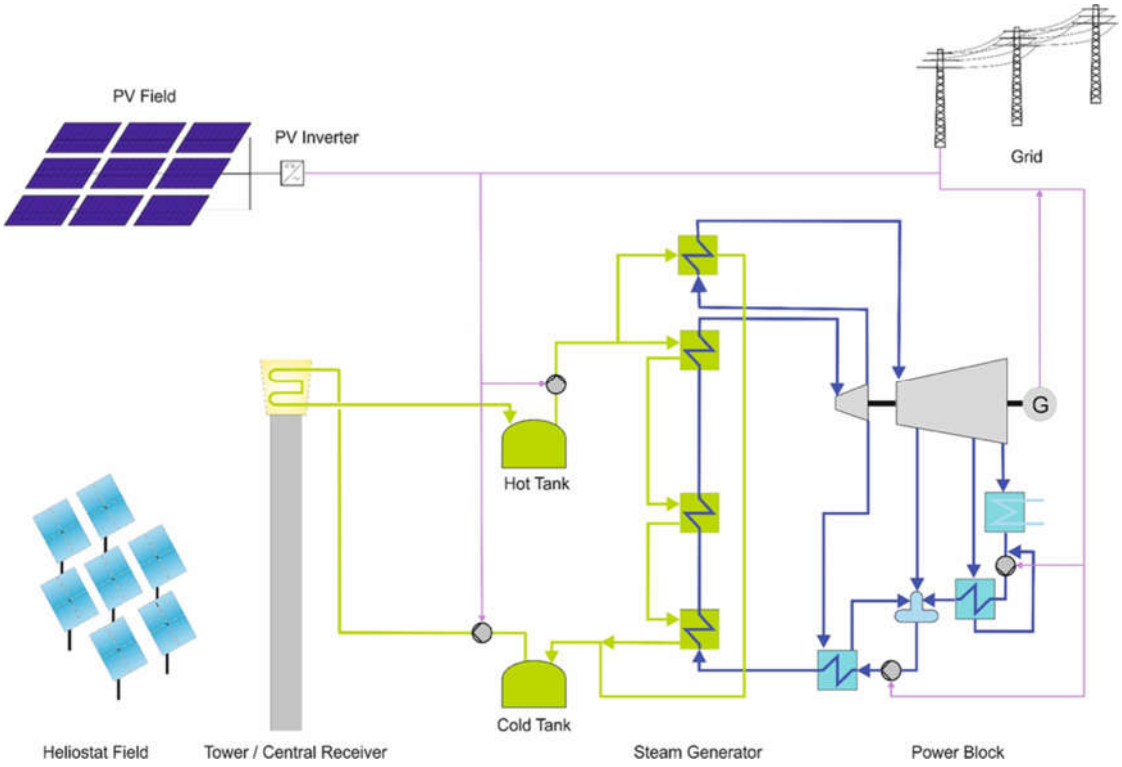

Figure 2: Tower hybrid power plant without electric heater

- **Tower hybrid power plant with electric heater**
    - PV injects electricity into the grid during the day.
    - The power block generates electricity at night from the thermal storage.
    - PV provides auxiliary power to CSP plant (pumps, heliostat tracking, PB startup auxiliaries).
    - PV excess power can be converted to heat (electrical heater) and stored in the thermal storage.
    - Priority Order for the use of PV output power:
        1. Auxiliary Support: PV power is used to cover auxiliary consumption of the solar field,
        2. Direct Grid injection
        3. Power to Heat: remaining excess PV power is converted to heat and stored in the thermal storage by heating up additional molten salt.
    - The electric heater is connected in parallel to the CSP field.
    - Using the ERH as a booster is not considered in tower systems, since they heat the molten salt directly and can easily bring it to its maximum temperature, which is determined by the physical limits of the molten salt.

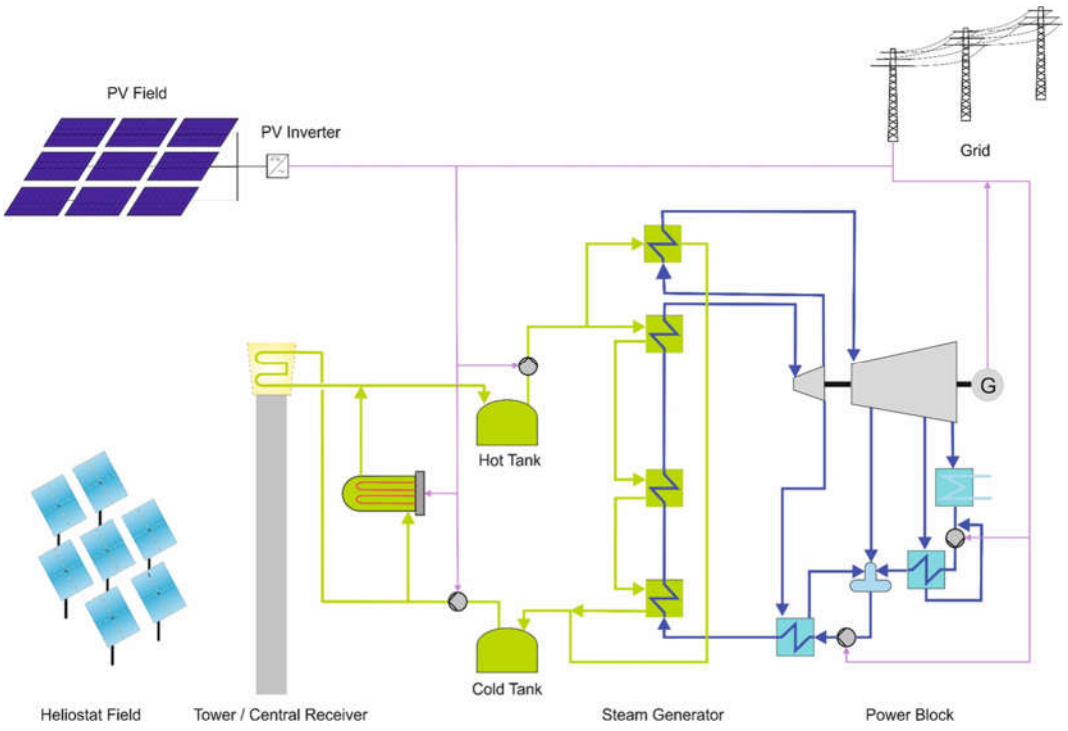

Figure 3: Tower hybrid power plant with electric heater

- **Standalone tower power plant (as a “classical CSP” reference)**
    - They have no PV-field.
    - Two tank molten-Salt thermal energy storage (TES).
    - The CSP power block (Steam Turbine) runs during day and night.
    - Cost-effective electricity during night time.

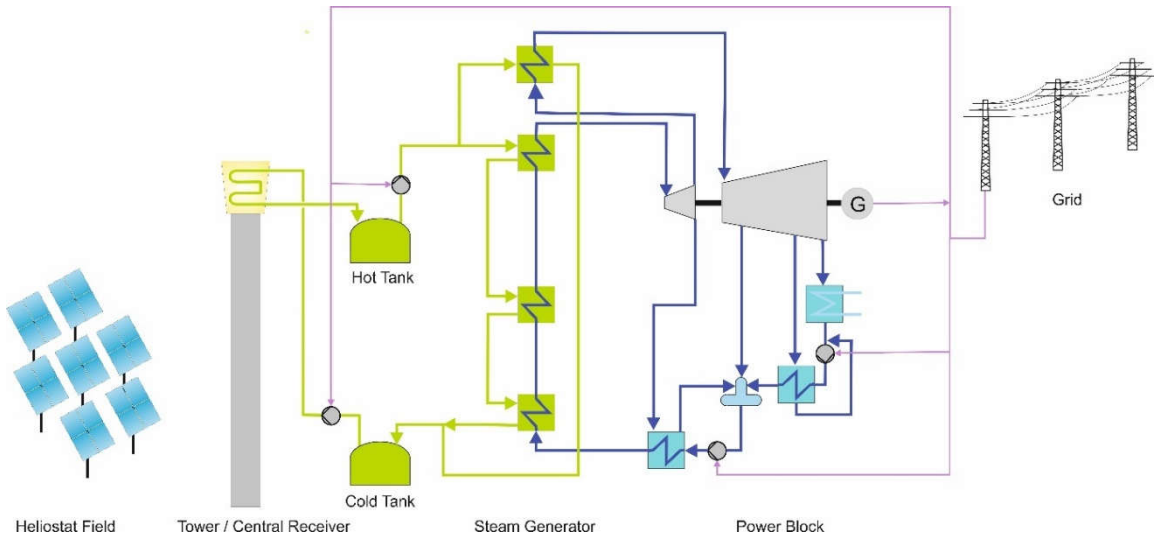

Figure 4: Standalone tower plant concept

- **Standalone parabolic trough power plant**
    - They have no PV-field.
    - Two tank molten-Salt thermal energy storage (TES).
    - The CSP power block (Steam Turbine) runs during day and night.
    - Cost-effective electricity during night time.

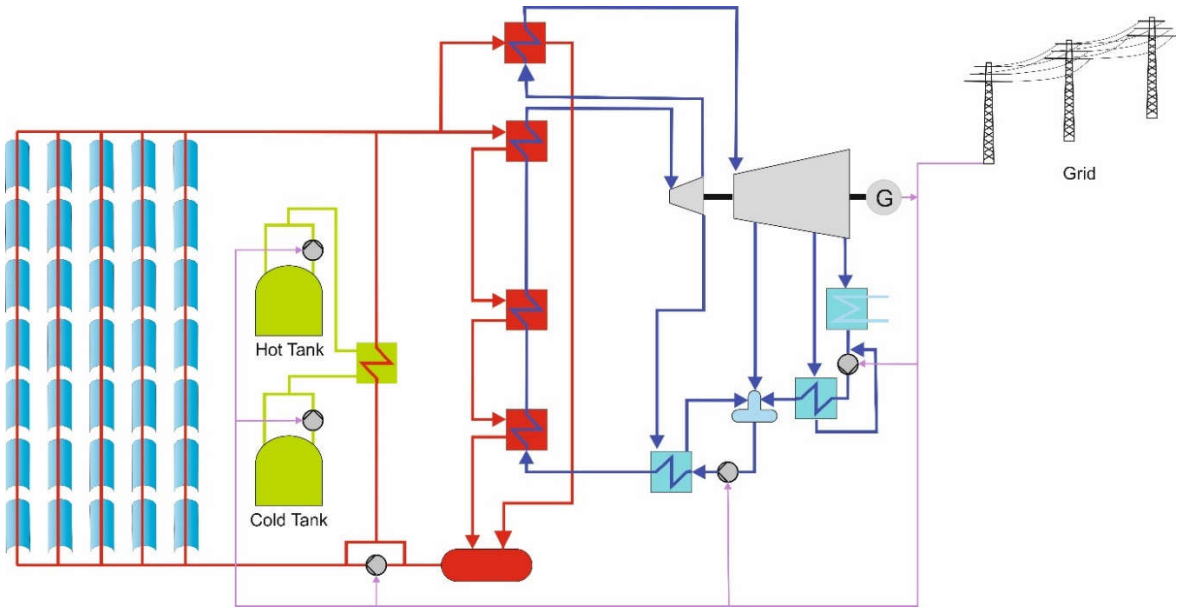

Figure 5: Standalone parabolic trough concept

- **PV with battery (standalone plant for comparison):**
    - No CSP field.
    - Battery as storage, discharges to the grid during night-time.
    - Priority Order for the use of PV output power:
        1. Direct Grid injection: PV injects electricity into the grid during the day
        2. Charging BESS: PV excess power is stored in the battery, which generates electricity during the night.
    - Low-cost electricity can be used with flexibility and BESS is a highly efficient and flexible storage.

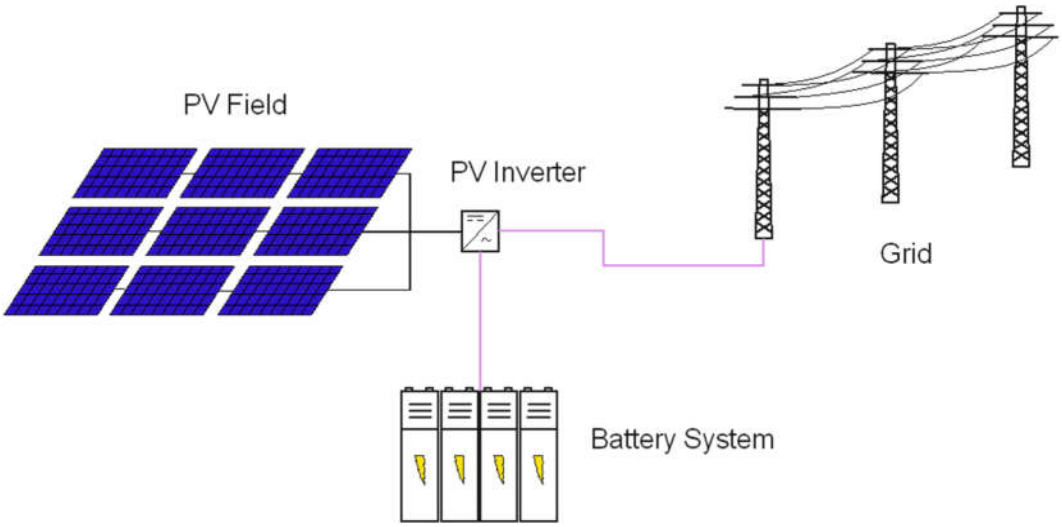

Figure 6: PV with battery concept

- **PV without battery:**
    - Low values of LCOE but without storage or night-time supply.

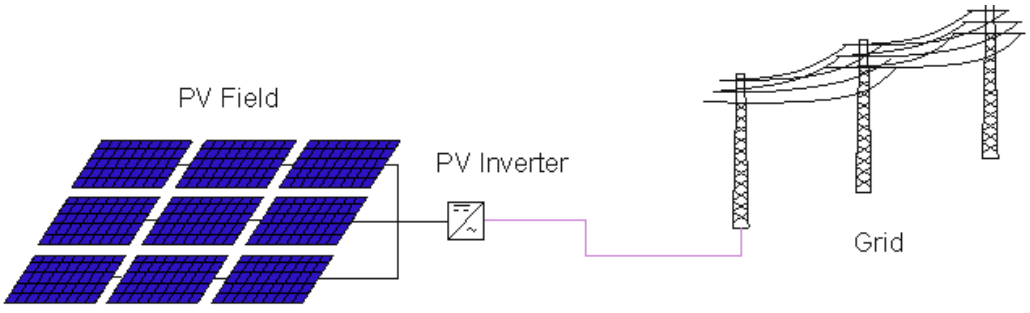

Figure 7: PV without battery concept

PV with electrical heater (P2H), thermal energy storage and power block

- No CSP field.
- PV power is used by an electric heater to charge the thermal storage during the day.
- PV excess power is injected to the grid during the day.
- TES storage is cost-effective for longer storage durations.
- The power block generates electricity at night from the thermal storage.
- Two different operating strategies were analysed:

  Option a) – Night-time electricity is prioritized (Higher Night-time Fraction)

  Priority Order for the use of PV output power (Option a)

  - Auxiliary Supply
  - Power to Heat: Charge the thermal storage with the electric heater (incl. related auxiliaries)
  - Direct grid injection: excess power is delivered to the grid.

  Option b) – Daytime grid injection is prioritized (Higher direct feed-in)

  Priority Order for the use of PV output power (Option b)

  - Direct Grid Injection: excess power is delivered to the grid.
  - Auxiliary supply
  - Power to Heat: Charge the thermal storage with the electric heater (incl. related auxiliaries)

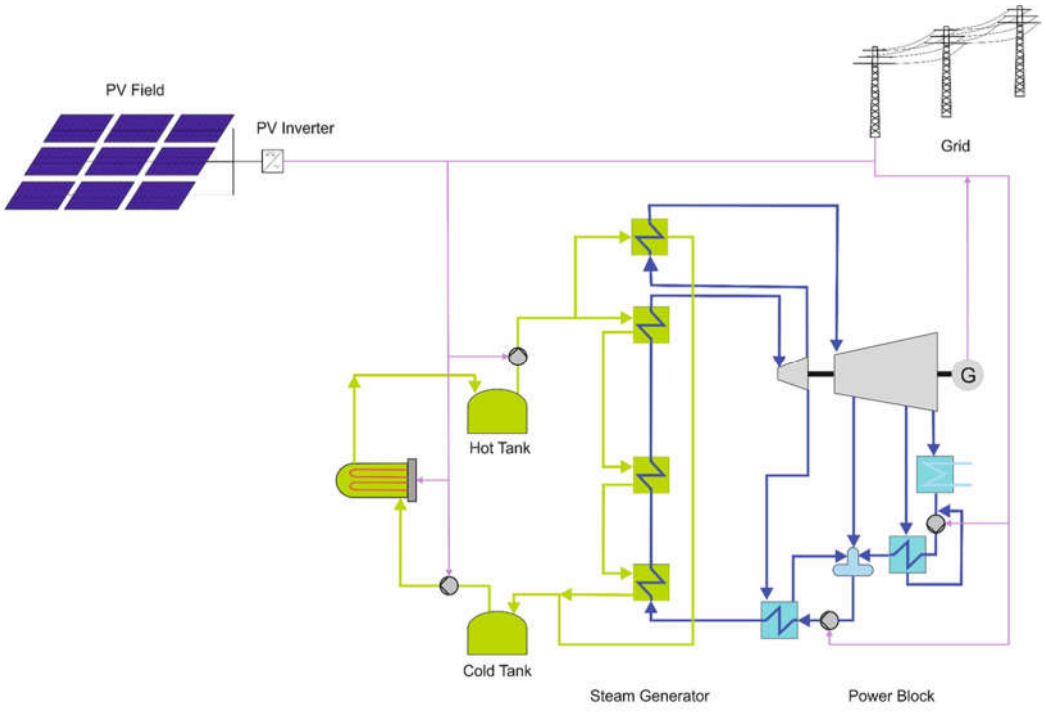

Figure 8: PV+ERH+PB concept

2.3. Summary PV power operating strategies

Not all systems have the same operating strategy. The priority order in which PV power is delivered varies for each system. Here the priorities for all evaluated plant topologies are summarized.

- Hybrid parabolic trough
    1. CSP/PB Auxiliary Supply
    2. Power to Heat: Boosting TES inlet temperature
    3. Direct Grid Injection
- Hybrid tower without electric heater
    1. CSP/PB Auxiliary Supply
    2. Direct Grid Injection
- Hybrid tower with electric heater
    1. CSP/PB Auxiliary Supply
    2. Direct Grid Injection
    3. Power to Heat for thermal storage
- PV with battery
    1. Direct Grid Injection
    2. Charging Battery storage
- PV without battery
    1. Direct Grid Injection
- PV + ERH + PB: Two different operating strategies were investigated
    1. Operating strategy 1: Priority for night-time electricity
        1. Auxiliary Supply
        2. Power to Heat for thermal storage
        3. Direct Grid Injection
    2. Operating strategy 2: Priority for grid injection
        1. Direct Grid Injection
        2. Auxiliary Supply
        3. Power to Heat for thermal storage

2.4. Auxiliary Demand

The CSP solar fields have the highest auxiliary power demand of the evaluated systems. For Parabolic Trough plants the HTF pumps moving thermal oil through the solar collector field create the biggest demands. The molten salt pumps moving salt from the cold tank up to the receiver on top of the tower is the largest auxiliary power for central receiver systems. Significant amounts of electrical power are also required for pumping the molten salt trough the ERH for Parabolic Trough systems. Further, all piping containing molten salt require active electrical heating during standby in order to prevent freezing.

The power block has significant auxiliary power demand that usually is covered from the gross output of the generator. During standby or start-up periods, the remaining auxiliary demand of the power block (keeping the turbine warm, circulation pumps, other demands) can be covered directly from PV, as the power block is usually in stand-by during the daytime.

The thermal energy storage can have significant auxiliary power demands related to pumping the molten salt as well as emergency heating as part of the storage freeze protection. The pumping energy is considered relative to the thermal charging/discharging power. Simulations for the project locations considered for this study showed that energy demands for freezing protection/emergency heating is negligible. However, the simulation models allow to consider this energy demand.

The electrical heaters have low auxiliary power demands as the molten salt pumps are not considered part of this system, but rather part of the CSP/TES systems. Auxiliary power demands for electrical heaters are therefore neglected in this study.

The PV system has some auxiliary power demands during the night as well. As these demands are small compared to the CSP solar fields and the power block, they are neglected in this study.

The BESS can have significant auxiliary energy demands related to cooling the battery cells. This auxiliary demand is covered by the energy used to charge the BESS and is accounted for in the battery's roundtrip efficiency. BESS auxiliary demands not covered by this assumption (e.g. in case of a system shutdown) are neglected in this study.

3. Simulation and optimization tools

The project partners adapted existing yield models to expand them for use in the project and new models were created from scratch. DLR used and adapted greenius for the simulation and optimization of the systems. Dornier Suntrace created the HYPPO tool for use in this study and to enable extended simulation and optimisation services as part of their commercial activities. Additional models in EBSILON®Professional, PVSyst and NREL's System Advisor Model were also used to generate input data.

3.1. Greenius

The software tool greenius [12] has been developed at DLR since several years and it is customized to perform fast calculation of the technical performance and economical figures of merit for different renewable energy systems. The software itself as well as more details about the models are available from the website [12]. The calculation is done on an hourly basis for a full year using a typical meteorological data set with this temporal resolution for the specific site of interest. Finer time resolutions of 30, 15, or 10 minutes are also possible, as well as multi-year simulations.

Annual performance modelling of CSP plants is not yet standardized but several approaches and models exist, most of them not publicly available but undisclosed by the owners. Currently there is no official standard for annual performance modelling of CSP plants available but there is a guideline published by SolarPACES (SolarPACES, 2017) [13]. greenius is following this guideline to a large extend but not completely since it has been designed and implemented years before the publication of this guideline.

In the past, validation tests have been done by comparing greenius results with operational results from SEGS VI. Another validation was a model comparison performed under the auspices of SolarPACES in 2010 and 2011 where 10 annual performance models for parabolic trough plants from different research organizations and companies have been compared. The results of this model benchmarking were undisclosed due to the preferences of some companies involved in this

comparison. Two benchmarking rounds have been done in guiSmo and greenius was involved in both rounds. The first round showed that input data and boundary conditions must be defined very carefully in order to get comparable results. The second round revealed a range of ± 6.5 % between the calculated annual gross and net output of 7 models. Actual measurements of the annual performance were not available for this benchmarking since the simulation was not based on real operation conditions. greenius' results were about 2 % lower than the mean annual output of the 7 models considered in the final comparison. For solar tower systems there was no distinct benchmarking but greenius has been used in several solar tower projects (e.g. due diligence studies) in which annual performance data was provided by potential suppliers. Comparison of greenius results with this undisclosed supplier's data makes us confident that the greenius results for solar towers are within a similar accuracy as those for parabolic trough power plants.

3.2. HYPPO

HYPPO (**Hy**brid **P**ower **P**lant **O**ptimization) is a tool that uses a particle swarm optimization algorithm to optimize the size of the relevant main components of a hybrid power plant. The tool is realized as a Python script and can be flexibly extended with additional models and control strategies to meet specific project requirements. It takes input data from industry standard simulation tools for the independent components (PV, PT and CRT) as well as site- and project-specific information to model the specific boundary conditions. Currently the HYPPO tool can be used to optimize the following plant topologies (as described in section 2.2, some cases (CRT standalone, PV standalone) are not available in HYPPO):

1. Parabolic Trough (PT) – Photovoltaic (PV) hybrid plant
2. Central Receiver Tower (CRT) – PV hybrid plant
3. PT stand-alone plant (only night-injection, as a reference)
4. PV – Electrical Heater (EH) hybrid plant
5. PV – Battery plant

This tool was created by Felix Zimmermann (M.Sc.) as a master's thesis for the M.Sc. Renewable Energies program at Hamburg University of Technology, in collaboration with Dornier Suntrace GmbH, as part of the IntegSolar project. The sizes of the various components are optimized using a multi-objective optimization with the two objective functions capacity factor (CF) and Levelized Cost of Electricity (LCOE). The results provide a more detailed understanding of how the LCOE of different plant topologies behaves with increasing CF, as well as which plant topology is the most cost-effective solution for a specific targeted CF. To compare the hybrid plants more appropriately, it is also possible to calculate the energy generated during the night hours, which are defined below for each individual location. The optimization is carried out for various sites as well as different cost assumptions for plant components reflecting the expected cost for the years 2021 and 2030.

The tool optimizes the nominal power/capacity of the following components:

- CSP Solar Field (PT and CRT, incl. Tower)
- Photovoltaic System
- Thermal Energy Storage
- Electrical Heater
- Battery Energy Storage

- Power Block

The main advantage of HYPPO is that it provides results in the form of a 2D-Pareto frontier, displaying the trade-off between LCOE and capacity factor. The configurations with the lowest LCOE for a CF are displayed and the sizes of the main components are saved to an output file. For each of the optimized configurations the hourly (alternatively: 15 min, 1 min) energy yield and other operational parameters are available. This tool can be extremely useful for project developers or consultants in the early stages of hybrid CSP projects to assess the most appropriate plant topology based on site conditions and requirements, resulting in the most cost-effective development solution with the individual equipment sizes. Dornier Suntrace GmbH will use HYPPO for commercial applications such as consultancy services and will make it available to third parties as part of service contracts.

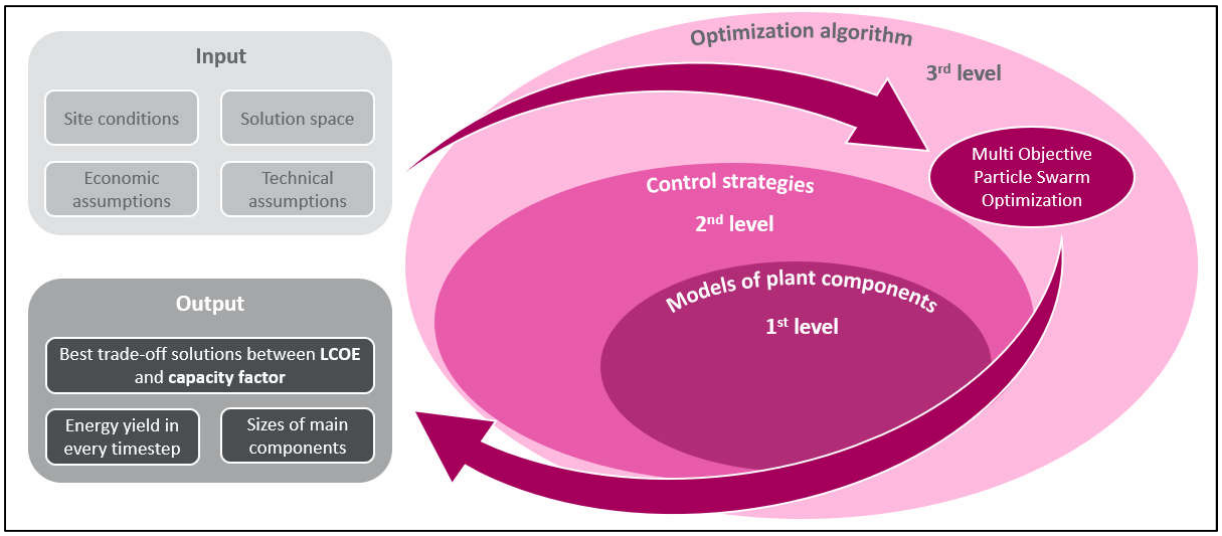

Figure 9: General Structure – HYPPO simulation tool

3.2.1. 1st Level: Model Plant Components

Parabolic Trough System:

The CSP solar field is simulated with System Advisor Model (SAM) to get the necessary data for a simplified surrogate model for each project location. The surrogate model consists of approximation functions calculating all relevant plant parameters (aperture area, tower height, etc.) based on the nominal thermal plant capacity (CSP or Receiver thermal power). Scaling of the studied plant is based on the nominal thermal solar field/ tower receiver capacity. In SAM, the PT system is simulated with the physical PT model, a performance analysis PT model which uses geometry and physical properties as input. The simulations results are used to calculate the approximation function for the total aperture reflective area, the thermal energy output of the SF and the auxiliary energy demand of the SF as function of the SF nominal thermal power. The surrogate models (approximation functions) for PT are mostly linearly correlating the aperture area with the nominal thermal solar field capacity. The surrogate model is further used to calculate the energy yield per timestep as well as the auxiliary energy demands based on the nominal solar field thermal capacity. For this a reference plant size is defined that should match with the expected average CSP field thermal capacity for the studied hybrid plant.

Central Receiver Tower System:

The CRT system is also modelled in SAM. The surrogate model is used to determine the central receiver thermal power, Tower height, Heliostat reflective area, and auxiliary energy demand. As for the CRT the relationship between field aperture area and thermal receiver capacity as well as tower height are not linear (because of atmospheric attenuation, cosine error, etc.), the initial evaluation for each project location requires the simulation of a wide range of nominal receiver capacities in SAM for the creation of a useful surrogate model. The resulting approximation functions are non-linear, mostly quadratic and should only be used for the optimisation of a similar range of thermal power capacities as used to generate the surrogate models. This should always be considered when setting up the HYPPO tool inputs for a new project location. The surrogate model is further used to calculate the energy yield per timestep as well as the auxiliary energy demands based on the nominal receiver thermal capacity. For this a reference plant size is defined that should match with the expected average CSP field thermal capacity for the studied hybrid plant.

Photovoltaic System:

A surrogate model of the PV production is created as function of nominal capacity. The boundaries of the PV subsystem are at the transfer points of electrical energy for SF, BESS, EH, and the grid. To simulate the electrical energy output of the reference PV system, PVSyst software is utilized. It is assumed for simplicity that PV output linearly increases with installed capacity in each timestep. The reference PV plant configuration used to create the surrogate model is optimized for the project location regarding DC/AC ratio, tilt angle, selection of technologies (module type, inverter type, mounting structure).

Power Block:

To model the Power Block, EBSILON Professional based on SIEMENS turbines is used. Here a characteristic diagram mapping the net efficiency of the PB as function of the load fraction of rated capacity and different ambient temperatures is used. In the net efficiency all losses and auxiliary power demands of the PB including the energy for pumping the HTF from the TES into the steam generator are included. To get net efficiency and heat requirement of a certain timestep, the values in the characteristic diagram are interpolated linearly. Further, the PB model contains a heat demand for turbine heat up. It is defined as fraction of the heat required at nominal load and for an average ambient temperature.

Electrical Heater, Thermal Energy Storage, Battery Storage:

The Electrical Heater (ERH) is modelled simply as the efficiency of the transformation of electrical into thermal energy. The electricity consumption is determined based on the HTF flow rate and the temperature change. A constant thermal capacity of the HTF is assumed.

The TES is not modelled as a two-tank storage system but simplified as an energy storage with a nominal thermal energy capacity and a state of charge (SOC) at a certain time (t). The TES thermal losses are assumed to be constant in every timestep per day. The thermal losses depend on the daily efficiency of the TES and the nominal thermal capacity of the TES. The daily efficiency indicates, how much thermal energy is left in the TES after one day and is calculated once for each day of evaluation.

For the model of the BESS a roundtrip efficiency is assumed. The roundtrip efficiency summarizes all losses which occur between charging and discharging. The total electrical energy transferred from the PV system to the BESS is the sum of energy flow in timestep t into the BESS and total losses.

3.2.2. 2nd level: Control Strategies

In the following the control strategy for the hybridized Parabolic Trough system is presented exemplarily. The control strategies are realized as a sequence of conditional statements. It is conducted for every timestep *t* and depends on the previous timestep *t−1*. As an example, the priorities in the PT-PV plant's control strategy are listed below.

- First the hybrid systems auxiliary energy demands are covered from the PV system outputs.
- In the second step, as much HTF as possible leaving the PT-SF is heated up in the EH to the temperature level of the hot tank of the TES and the steam generator. If the PV power is insufficient to heat up the complete flow of HTF, the flow rate is reduced, leading to curtailment of the (partial defocusing of the solar field). The HTF flow is simplified as the amount of thermal energy it carries. The thermal energy leaving the EH is stored in the TES for night-time usage. Night-time is defined same as the definition in the control strategy of the PV plant, depending on the PV output.
- The remaining PV output is used to charge the small BESS system that can cover some auxiliary energy demand during absence of solar radiation.
- All remaining electrical energy produced by the PV system is injected into the grid until the grid injection limit is reached.
- The PB is started to be available at full nominal power at the beginning of the night if the requirements for night generation are met. The electrical energy output of the PB is first used for fulfilling the hybrid systems auxiliary energy demands and the rest is injected into the grid. It runs until the TES is empty or daytime begins.
- If the plant cannot fulfil its auxiliary energy demands, electrical energy is purchased from the grid.

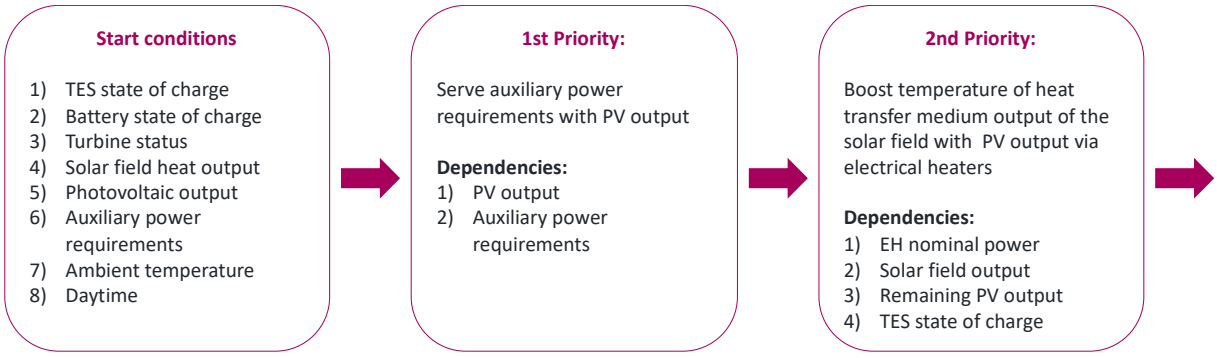

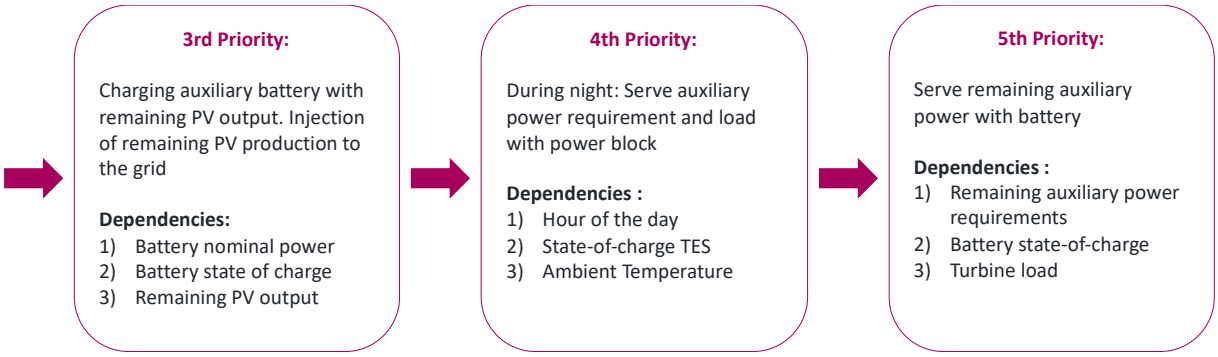

Figure 10: Control strategy and priorities in HYPPO

3.2.3. 3rd level: Optimization Algorithm

Particle Swarm Optimization (PSO):

Particle Swarm Optimization (PSO) is used in this work to optimize the sizing of the different subsystems of the studied plant topologies. PSO can be used for solving nonlinear multidimensional problems. The algorithm works in simple words as following: In a multi-dimensional solution space there is a swarm of particles. Each particle has a velocity $\vec{v}$ and a position $\vec{a}$. At the beginning both vectors are randomized. The solution space is spread out by abscissa and ordinate. Each particle is represented by an x mark. The velocity $\vec{v}$ of each particle is represented by the arrows, whereby the length of the arrows represents the magnitude of the particle's velocity. Each particle evaluates its position based on the objectives and keeps track of the best position it has achieved so far $\overrightarrow{p_{best}}$. Further the global best position that one particle of the swarm has found $\overrightarrow{g_{best}}$ is kept in track and known by all particles.

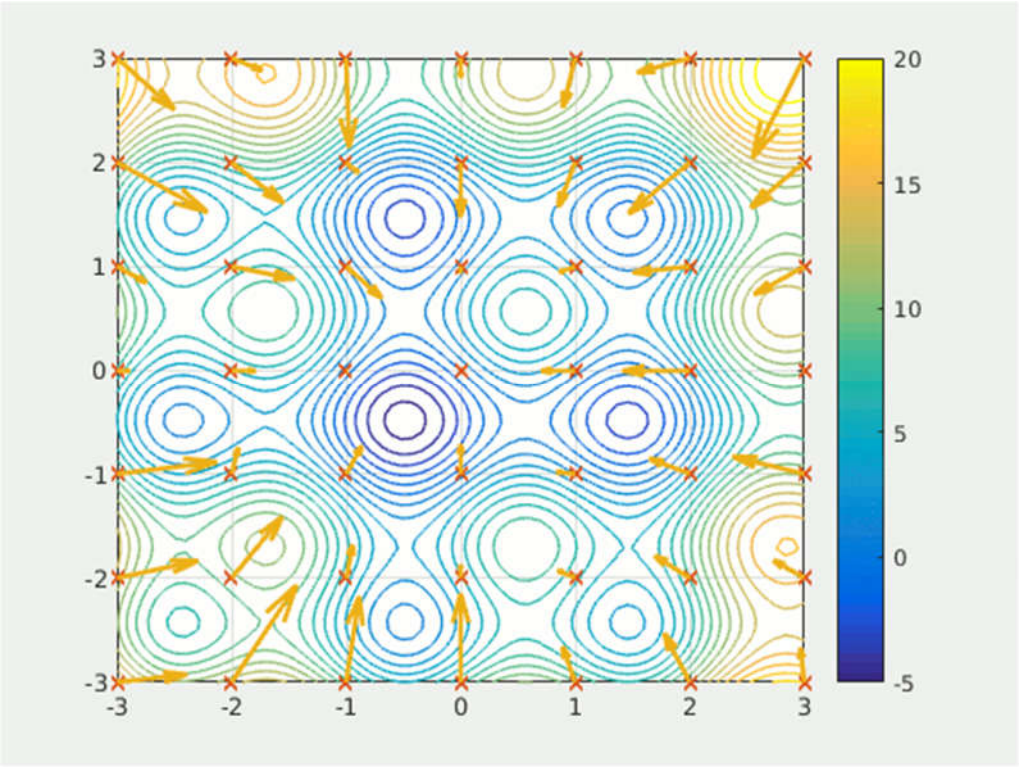

Figure 11: Graphical representation of the optimization scheme use in HYPPO

The velocity of each particle is changed towards $\overrightarrow{p_{best}}$ and $\overrightarrow{g_{best}}$ and the next iteration step begins. The optimization procedure finishes when the maximum number of iterations is reached. A solution consists of $\overrightarrow{g_{best}}$ and the evaluation of this position regarding the objective function.

Multi Objective Particle Swarm Optimization (MOPSO)

The optimization approach used in the HYPPO tool includes a multi-objective optimization with the two objective functions LCOE and capacity factor (CF). This optimization problem aims at simultaneously minimizing LCOE and maximizing CF. It results in a 2D-Pareto front, showing the best trade-off solutions between LCOE and CF. The sizes of the subsystems of the studied plants are getting optimized within defined borders. These borders form the solution space. The list mentioned below shows the parameters of the different plant topologies to be optimized. Furthermore, a maximum number of iterations is defined as stop criterion.

Technical Parameters that can be optimized:

- Solar field (SF) - Nominal Thermal Power of PT solar field or CRT tower receiver + solar field
- Photovoltaic (PV) – PV Nominal AC Power
- Thermal energy storage (TES) - Nominal Capacity
- Electrical resistance heater (ERH) - Nominal Thermal Power
- Battery energy storage (BESS) - Nominal Power and Energy Capacity
- Auxiliary Battery energy storage - Nominal power and Energy Capacity (only for auxiliary power provision)

4. Cost assumptions

Dornier Suntrace and DLR have jointly estimated the specific component costs used for the simulations based on previous projects, Dornier Suntrace project experience, market analysis and published information. Table 1 shows the assumed costs for all required components. A cost estimate for 2030 was made to analyse future projections for all systems. CSP costs were taken from [14]. According to an analysis conducted by DLR, the costs of the Parabolic Trough and Central Receiver Tower are expected to decrease by 12 percent between 2021 and 2030. The cost of BESS is based on the NREL ATB 2021 report [15] and the U.S Photovoltaic and Energy Storage Cost Benchmarks: Q1 2021 [16]. The BESS cost is expected to decrease by 20% for power and 23% for capacity until 2030 due to strong competition with the automotive sector, limited raw material availability, and high demand. Electrical resistance heater cost values were assumed from DLR projects, with a 10 percent cost reduction expected from 2021 to 2030. The cost of the PV system was determined by Dornier Suntrace project experience and current market scenarios, and it is expected to fall by only 23% between 2021 and 2030.

Storage costs for both thermal storage and battery storage refer to net capacity. The costs for electricity supply by the grid were adjusted for each site (prices from https://www.globalpetrolprices.com/electricity_prices/). The land costs were set to zero because of its negligible influence on the LCOE (assuming low cost desert sites). EPC surcharges were assumed differently for each subsystem because of the different maturity levels of the technologies. Increased

operation and maintenance costs for BESS are used to account for replacement or addition of batteries in order to enable the life time of 25 years assumed for all systems. For all systems a 5% debt interest rate have been assumed.

At the beginning of the project, the greatest uncertainty resided in the cost of the electric heater. Therefore, cost variations were carried out to determine the influence of this value. Finally, a value of 100 $/kW was assumed using as a reference, the value was determined from other projects DLR is involved in and is based on an indicative offer. However, a variation of this cost was performed to determine its final impact on the LCOE. Other cost sensitivity analyses including PV cost, BESS cost and combined PV+BESS costs were performed and are presented in section 9.3.

Table 1: Costs assumptions

		Values 2021	Values 2030	Unit
Parabolic trough	**Solar field**	202	178	$/m²
	Thermal storage	38	33	$/kWh$_{th}$
	Power block	930	860	$/kW$_{el}$
	EPC	0.2	0.2	of CAPEX
	O&M	0.015	0.015	of CAPEX
Central receiver tower	**Heliostat field**	127	112	$/m²
	Tower	88000	77440	$/m
	Receiver	122	107	$/kW$_{th}$
	Thermal storage	26	23	$/kWh$_{th}$
	Power block	966	863	$/kW$_{el}$
	EPC	0.2	0.2	of CAPEX
	O&M	0.015	0.015	of CAPEX
BESS	**Cost per power**	245	196	$/kW$_{el}$
	Cost per energy capacity	246	189	$/kWh$_{el}$
	EPC	0.235	0.235	of CAPEX
	O&M	0.045	0.045	of CAPEX
Electric resistance heater	**CAPEX**	100	90	$/kW
	EPC	0.2	0.2	of CAPEX
	O&M	0.01	0.01	of CAPEX
PV system	**Inverter**	53	41	$/kW$_{ac}$
	PV field	454	350	$/kW$_{dc}$
	EPC	0.1	0.1	of CAPEX
	O&M	0.005	0.005	of CAPEX

5. Technical assumptions

The following technical assumptions were agreed between project partners for each component. The estimations are based on previous project experiences, market research, and other publications.

- Parabolic trough:
  - Collector type: Ultimate Trough (Aperture width: 7.51 m, Collector length: 246.7 m, effective mirror area: 1716 m^2, HCE diameter: 8.9 cm, Nominal optical efficiency: 82.7 %). This collector has been used as a typical large aperture trough collector.
  - Distance between rows: 22.5 m; Distance between collectors: 0.5 m
  - HTF: Therminol VP-1
  - Nominal field outlet temperature: 395 °C
  - Nominal field inlet temperature: 310 °C
  - Mean mirror cleanliness: 97%
  - Degradation: 0.4 % per year
  - Auxiliary demand: Constant need: 1 W/m^2 SF aperture, power of field pump: 8.3 W/m^2 SF aperture

- Tower system:
  - Single heliostat area: 121.3 m^2
  - Clean mirror reflectivity heliostat: 94%
  - Average cleanliness heliostat: 95%
  - Heliostat field availability: 99%
  - 360°-type Receiver made of tube bundels
  - HTF: Solar Salt (60% NaNO3, 40% KNO3)
  - Nominal outlet temperature: 565°C
  - Nominal inlet temperature: 300°C
  - Degradation: 0.4% per year
  - Other parameters: Heat loss piping (at dT = 408 K): 0.5 % of nominal receiver output, nominal friction pressure drop piping and pressure drop receiver: 10 bar, efficiency HTF pump: 80%, operating auxiliary consumption: 1100 kW, permanent auxiliary consumption: 400 kW, maximum start-up power fraction: 50% of the nominal energy delivered per hour, minimum start-up time: 2 hours (for cold start).

- Thermal energy storage:
  - Storage Medium: Solar Salt (60% NaNO3, 40% KNO3)
  - Nominal Hot Temperature: 565°C (380°C for PT without booster)
  - Nominal Cold Temperature: 300°C (287°C for PT without booster)
  - Relative losses in 24h: 1% of nominal storage capacity
  - Pumping parasitics: 0.003 W_{el}/W_{th}

- Power block:
  - Live Steam Temperature: 553°C (367.5°C for PT without booster)
  - Turbine Inlet Pressure: 170 bar (100 bar for PT without booster)
  - Steam turbine with 7 preheaters plus feed water storage
  - Dry cooling with air-cooled condenser

- Power block efficiency: nominal Cycle Efficiency: 46.5%, (38.3% for PT without booster)
- Startup losses: Maximum startup power: 50% of nominal value, minimum startup time: 2h (for cold start), cool-down half-life: 12h.

- PV
  - Bifacial-monocrystalline PV modules (best suited for sandy ground = high albedo)
    - Name: Longi LR4-72-HBD425M
    - Nominal MPP power: 425 Wp
    - Dimensions: Length: 2.131m, width: 1.052m, weight: 29.5 kg
  - Single-Axis Tracking Systems (best economics in sunny regions)
  - Inverters
    - Name: SMA MVPS 2500
    - Nominal DC power: 2535.5 kW
    - Nominal AC power: 2500 kVA
  - Ground Cover Ratio (GCR): 34% (low land cost in desert environments)
  - DC/AC ratio: 1.3
  - Assumption: flat, homogenous site, rectangular area
  - Main Assumption: Optimised stand-alone PV configuration will lead to highest benefits in integrated hybrid plants as well. A representative system with one inverter was designed and in the hybrid plants many of these systems were used to reach the required nominal power.
  - Degradation: 0.4% per year
  - Availability: 98%
  - Cleanliness module: 97%
  - Shadowing factor module: 91%

- Power2Heat technology: Electrical resistance heater
  - HTF: molten salt
  - Conversion efficiency: 99%

- Battery energy storage system
  - Technology: Lithium-Ion NMC (most typical)
  - Round-trip efficiency: 85% related to HVAC, self-discharge, BMS, PCS efficiency, etc.
  - Definition of Net capacity: available Energy (MWh) when discharging from maxSOC to minSOC at BOL
  - C-Rate: flexible, depends on selected storage duration (C-rate is the ratio of battery power and energy, a C-rate of 2 defines a storage with a discharge duration at nominal power of 0.5 hours)
  - Lifetime (Warranty duration): 15 years (BESS has to be completely replaced after 15 years, O&M cost assumption includes a share to build up an O&M budget for the replacement)
  - Degradation: ≈2% of nominal capacity per year (Lost BESS capacity has to be restored by adding additional batteries on a regular basis to keep up BESS functionality, O&M cost includes a share to compensate degradation)

- O&M cost: 4.5% (0.5% of CAPEX for general annual O&M activities + 2% for degradation compensation + 2% for Battery replacement after 15 years)

6. Boundary conditions

6.1. Fixed Project Boundary Conditions / Assumptions

Several boundary conditions were defined for the simulations. Different locations with different climatic conditions were also considered for a wider range of results.

The grid injection limit was fixed at 150 MW_{el} for all the systems (power block and battery system net power) to allow the comparability of all concepts. In this way it was also possible to avoid difficulties in the design of the PV plant. This limit might be caused by an upper limit of the grid connection of the solar power plant as well. Nominal gross output of the CSP power block was necessary to be set to 160 MW_{el} because this plant should be able to deliver the required net power of 150 MW_{el} to the grid and to cover the auxiliary demand of the plant even under hot ambient conditions.

A constant load curve for the whole day ("baseload") was assumed. That means that the required load at night was also 150 MW for each system. Additionally, a peak-load curve was studied for the PSA site using the Spanish electric demand data of 2019. For most cases, the size of the storage tanks was varied in the simulations between 3 hours and 12 hours capacity, providing different nightly electricity demand coverage ratios.

Power block and CSP solar field auxiliary requirements were modelled as temperature dependent. Stand-by auxiliaries (Solar fields, PV, BESS) were considered with fixed values.

Grid connection, substations and transmission lines were not included in the project scope to allow the comparison of plants independently of their location.

6.2. Sites used for the simulations

The techno-economic evaluation was performed for different locations to consider different boundary conditions (e.g. DNI and GHI values) and latitudes. The widest possible variety of locations was sought. Depending on the characteristic values of the sites, some locations are more suitable for CSP plants or for PV plants. In the first step, three sites were used for which high-quality meteorological datasets were available (Table 2). Unfortunately, it was not possible to find sites with almost identical parameters but differing only in one parameter.

Table 2 and Table 3 show the main parameters of the selected sites.

Table 2: Main parameters of the first evaluated sites

Site	Riyadh (Saudi Arabia)	De Aar (South Africa)	PSA (Spain)	Unit
Annual DNI (TMY)	2275	2712	2207	kWh/m²
Annual GHI (TMY)	2236	2040	1860	kWh/m²
Average temperature	26	17.5	16.6	°C
Latitude	24.91	-30.67	37.09	°N
Altitude	650	1285	492	m
Electricity price from the grid	68	77	124	$/MWh

Later four additional sites were considered (Table 3) in order to analyse the impact of a wider range of site parameters.

Table 3: Main parameters of the additional evaluated sites

Site	Diego de Almagro (Chile)	Ouarzazate (Morocco)	Daggett (USA)	Dunhuang (China)	Unit
Annual DNI (TMY)	3477	2518	2723	2158	kWh/m²
Annual GHI (TMY)	2449	2123	2090	1755	kWh/m²
Average temperature	15.8	18.8	19.7	10.6	°C
Latitude	-26.3	30.9	34.9	40.2	°N
Altitude	1014	1140	586	1140	m
Electricity price from the grid	125	116	120	98	$/MWh

The standard site in this document for the simulations was Riyadh although certain specific calculations were only done for other locations and generally all technologies were compared for each site. The same technical and cost assumptions were used for all locations.

6.3. Definition of day and night-time

It was also necessary to define the night hours for each month and location separately. An hour was considered as night-time if the PV output on a sunny day in the middle of the month did not reach 25% of its nominal value for that hour. Table 4 shows the defined night hours for the simulation of the systems in all sites. So, night begins for Riyadh in January at 17:01, as shown in Table 4 but at 19:01 for De Aar and at 18:01 for PSA.

Due to the hourly timesteps used in the simulations the definition of day and night time is rather coarse but comparisons to 1-minute timestep simulations showed that this does not affect the annual results considerably.

Table 4: Night hours for the simulation in greenius

	Night hours greenius													
	Riyadh		De Aar		PSA		D. Almagro		Ouarzazate		Daggett		Dunhuang	
Month	Start	End	Start	End	Start	End	Start	End	Start	End	Start	End	Start	End
Jan	17:01	07:00	19:01	06:00	18:01	09:00	19:01	06:00	17:01	08:00	16:01	07:00	18:01	10:00
Feb	17:01	07:00	19:01	06:00	19:01	08:00	19:01	07:00	18:01	08:00	17:01	07:00	19:01	09:00
Mar	18:01	06:00	18:01	07:00	19:01	07:00	19:01	07:00	18:01	07:00	18:01	06:00	19:01	08:00
Apr	18:01	06:00	18:01	07:00	19:01	07:00	18:01	07:00	18:01	07:00	18:01	06:00	20:01	08:00
May	18:01	06:00	17:01	07:00	19:01	06:00	18:01	08:00	19:01	06:00	18:01	05:00	20:01	07:00
Jun	18:01	06:00	17:01	08:00	20:01	06:00	18:01	08:00	19:01	06:00	19:01	05:00	21:01	07:00
Jul	18:01	06:00	17:01	08:00	20:01	06:00	18:01	08:00	19:01	06:00	19:01	05:00	21:01	07:00
Aug	18:01	06:00	18:01	07:00	19:01	07:00	18:01	08:00	19:01	06:00	18:01	05:00	20:01	07:00
Sep	18:01	06:00	18:01	07:00	19:01	07:00	18:01	07:00	18:01	07:00	18:01	06:00	19:01	08:00
Oct	17:01	06:00	18:01	06:00	18:01	07:00	19:01	06:00	17:01	07:00	17:01	06:00	18:01	08:00
Nov	17:01	07:00	18:01	06:00	18:01	08:00	19:01	06:00	17:01	07:00	16:01	07:00	18:01	09:00
Dec	17:01	07:00	19:01	06:00	18:01	08:00	19:01	06:00	17:01	08:00	16:01	07:00	18:01	09:00

7. Methodology – Simulations in greenius

7.1. Introduction

Simulations of all systems were performed using greenius [12] in different steps. For the evaluation of the results, the LCOE and the night-time fraction of electricity was used. The Levelized cost of electricity (LCOE) is a simple metric widely used in other projects for techno-economic analysis. However, it is not sufficient to evaluate and compare such hybrid power plants. If the LCOE is the only criteria, a standalone PV plant would be the least-cost solution, but it would just provide electricity during sunshine hours without any dispatchability. Hybrid solar power plants instead are capable of providing solar electricity even after sunset, often at elevated costs and the aim of this project was to find cost optimized combinations. Therefore at least a second parameter must be fixed, to compare the systems on a fair basis.

This second parameter could be the capacity factor (CF) relating the delivered electricity of a system to the theoretical maximum electricity this system could produce, if it provided the required nominal net output during every hour of the year. For the simulations with greenius it was decided rather to use the night-time electricity fraction, defined as amount of electricity produced during night-time divided by the total produced. Night-time electricity fraction has the advantage that this is what an owner of such a hybrid plant is looking for. The CF does not explicitly account for the production after sunset and identical CF may be reached with different night-time production rates. However, as in all hybrid systems analyzed, a PV system will inject directly to the electricity grid, it can be assumed that CF and night fraction are proportional to a certain extent. A system showing a high CF (> 0.75) will necessarily have a high night time fraction.

7.2. LCOE and night-time calculation

LCOE and night-time electricity fraction were used for the characterization of the systems. Equation 1) shows how night-time fraction is calculated.

$$Night\ time\ electricity\ fraction = \frac{annual\ electricity\ production\ during\ night\ hours}{total\ annual\ electricity\ production} \quad 1)$$

LCOE can be calculated in different ways. The lowest costs appear when producing solar electricity and delivering it to the grid directly. In grids with high penetration of solar electricity this will lead to a mismatch of demand and production. Storage solutions are needed to balance the system. The addition of storage requires an increased investment which leads to higher electricity costs. Published tariffs for PV-CSP and for PV-BESS power plants are often a kind of "blended tariff" made of the tariff for direct feed-in and the tariff for electricity generated from the storage. If the stored energy is more expensive than the energy which is fed to the grid directly, the blended LCOE grows for increasing storage fractions.

This blended LCOE was used for the evaluation of the results. One reason for the utilization of blended LCOE values is the difficulty to assign all subsystem costs to day- or night-time electricity production exclusively in hybrid power plants. This allocation of component costs is not straight forward:

- Storage → Night-time electricity production (provided that the storage is only discharged during night-time).
- Power block → Night-time electricity production (provided that it only runs during night-time).
- PV field → used for daytime production but also to charge the storage. The PV field is over dimensioned, and this increases also the annual daytime production during several time periods.
- Inverter → may be used during day and night-time.
- Battery → may be used during daytime to bridge short irradiation gaps since this will be the most economical solution.

Night LCOE can be calculated theoretically. If the overall (blended) costs, the costs of daytime electricity production and their fractions are known, we can calculate the night-time costs. This is however not the full truth since in hybrid systems the daytime costs will be different from that of a standalone PV system without storage.

Equation 2 shows the formula used for the calculation of blended LCOE.

$$LCOE = \frac{Total\ Investment\ Costs + \sum_{t=1}^{t_{ges}} \frac{Annual\ Running\ Costs_t}{(1+r)^t}}{\sum_{t=1}^{t_{ges}} \frac{Annual\ Electricity\ Solar_t \times (1-d)^{t-1}}{(1+r)^t}} \quad 2)$$

LCOE: levelized cost of electricity [€/kWh$_{el}$]

r: interest rate

t: year within the period of use (1, 2, … t_{ges})

t_{ges}: period of use (system life time in years) [a]

Total Investment Costs [€]: Major Equipment Costs (EPC cost of all components) + Other Costs (Land Costs, Infrastructure Cost, Project Development, Insurance during Construction, Supervision and Startup) + Contingencies

Annual Running Costs [€]: O&M Costs, Replacement Costs, Insurance Costs, Electricity Costs

Annual Electricity Solar: solar energy yield in the year t [kWh_{th}]

d: degradation rate per year

7.3. Simulations with greenius

After adaptation of greenius for the simulation of hybrid power plants, these were performed in two steps.

In a first step, the simulation of a single PV system without storage was done (1 Inverter with dedicated PV modules and nominal AC power of 2.5 MW). This first simulation run delivers the AC-power of the system for each timestep. The output of this system was not limited by feed-in restrictions but there might by some clipping due to the DC/AC ratio of 1.3. The resulting time series of electricity generated by the PV system were used in a second step as input for the hybrid PV-CSP plant. The output of the 2.5 MW PV was multiplied by the number of units to reach the desired nominal PV power. This kind of linear scaling was possible since large PV plants are built of many identical units made of one inverter and a number of modules connected to this inverter. In the hybrid plant the power fed to the grid is limited, which may cause curtailment.

Parameter variation and simulation of many configurations was used to find the system configurations with least LCOE. For the variation of the parameters, it was necessary to take certain limits and steps for all of them, which are shown in Table 5. The parameter variation was done for: CSP field nominal output, PV system nominal output (AC), ERH nominal power and storage net capacity to find the optimized configurations and compare the technologies.

Table 5: Steps and limits of the parameter variation

	PV field size [MW]	Storage net capacity [h]	CSP field nominal power [MW]	Electric heater nominal power [MW]
Tower	-	3h - 12h (3h step)	400 - 1150 (50 MW step)	-
Parabolic trough	-	3h - 12h (3h step)	652 - 1847 (109 MW step)	-
Tower hybrid w/o electric heater	150 - 300 (25 MW step)	3h - 12h (3h step)	200 - 700 (50 MW step)	-
Tower hybrid with electric heater	150 - 300 (25 MW step)	3h - 12h (3h step)	200 - 600 (50 MW step)	0 - 400 (variable step)
Trough hybrid	150 - 650 (50 MW step)	3h - 12h (3h step)	22 - 196 (22 MW step)	45 - 405 (variable step)
PV with battery	150 - 525 (25 MW step)	3h - 12h (3h step)	-	-
PV with EH and power block	150 - 750 (50 MW step)	3h - 12h (3h step)	-	5 - 600 (variable step)

Once the simulations were performed, numerous results were available. Figure 12 shows a point cloud representing each of the simulated configurations in the parameter variation. All of them have their corresponding LCOE and night-time electricity fraction. For a clear and visual representation of the results only those configurations with the lowest LCOE for each storage size were selected as shown in Figure 13. This type of representation was used for most diagrams of this report. Normally, the variation of the storage size was 3h, 6h, 9h and 12 hours but for obtaining higher capacity factors, it was necessary to simulate also greater storage sizes.

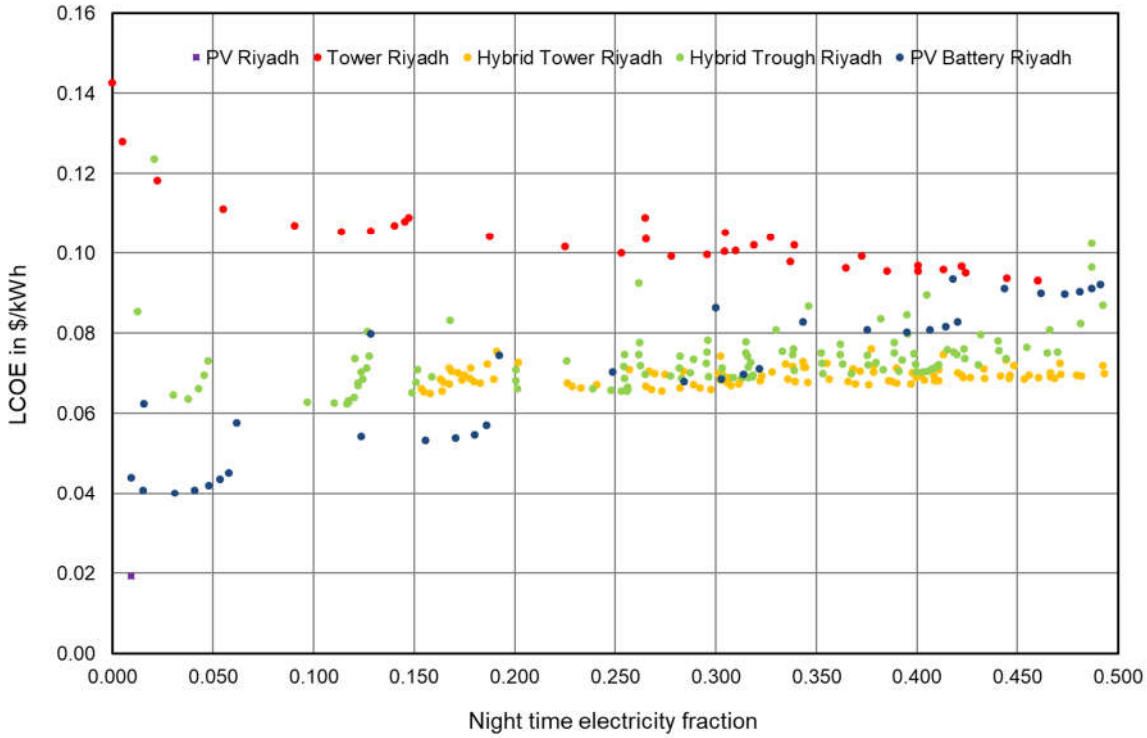

Figure 12: Complete parameter variation results for Riyadh

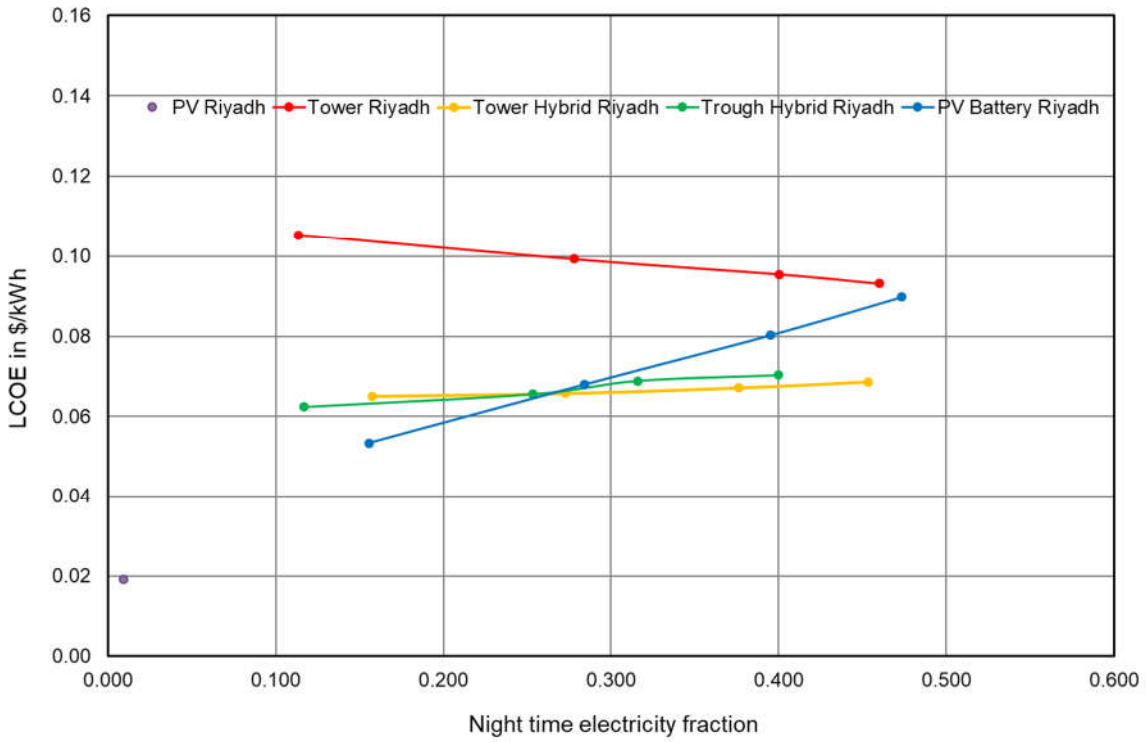

Figure 13: LCOE optimized configuration selection

Explanation for the CSP-field minimum and maximum size in greenius:

In greenius the solar tower simulation is based on a set of lookup tables which have been precalculated using the special software tool HFLCAL (reference?). HFLCAL allows for optimization of the heliostat field layout of solar tower plants which must be done in principle for each site (latitude), nominal thermal power, heliostat and receiver type. In order to provide a fast first estimation, greenius contains the results of several HFLCAL runs as lookup tables assuming a common heliostat type, a reasonable receiver type and tower height. Independent variables are design thermal output and latitude. Once these 2 are fixed, greenius calculates the solar field performance for each sun position by multi-dimensional interpolation in these lookup tables. This is not as exact as a detailed heliostat field layout for each specific site but gives a good first approximation as long as no further details are known about the site, the actual heliostat type, etc. The lookup tables delivered with greenius are of course limited to a lower and an upper design thermal power and extrapolation is not foreseen.

8. Methodology and Simulations in HYPPO

Please note: The Dornier Suntrace GmbH as the industry partner in the IntegSolar project developed the HYPPO tool as an independent simulation and optimisation tool. The development of this tool was one of the objectives of the IntegSolar project. Most analyses presented in this report were conducted using both tools, greenius and HYPPO. However, to reduce double content and increase the quality of this report, the greenius results are presented here and HYPPO results are shown additionally, only in cases when both models show relevant deviations or when the HYPPO results provide additional information and allow a deeper understanding of the underlying technical and economic mechanisms.

8.1. Introduction Optimisation Methodology HYPPO

The python-based tool is used to simulate and optimize the various components for each topology. It is able to provide single case simulations, batch simulations, single topology optimisation and also multiple topology optimisations. Variations of project site, meteo data, cost assumptions, etc. require multiple simulation runs, but can easily be done.

The sizes of different components are optimized using a multi-objective optimization used for the optimization of multiple input parameters considering more than one competing objective function. The hybrid plants in this work are optimized considering the levelized costs of electricity (LCOE) and the capacity factor (CF), which are the competing objective functions. Simplified schemes of the different plant topologies as mentioned in the section 3.2 are created and the different main components are modelled accordingly with the help of various tools as an input for the final optimization algorithm.

The simulation is done based on a typical meteorological year type 3 (TMY3). The used meteorological data as well as the results are regarding one year with a timestep size Δt of one hour. The control strategies are realized as a sequence of conditional statements. To make the different power plants comparable, a constant grid injection limit similar to the rated net power of the PB is assumed. Without

grid injection limit, the annual injection of electricity produced by the PV system would just increase linearly with increasing PV capacity. Therefore, a constant grid injection limit which can be interpreted as baseload provision, was used.

The sizes of the subsystems of the studied plants are getting optimized within defined borders. These borders form the solution space. Various technical parameters as stated in the 3.2.4 of the different plant topologies are optimized. Furthermore, a maximum of 10000 evaluations are set as a stop criterion in the optimization process, with 150 best solutions displayed in the pareto front diagram.

8.2. LCOE and Capacity Factor Calculation

The LCOE as one of the objective functions is calculated with the below mentioned equation. Thereby $CAPEX_{tot}$ is the total capital expenditure of one plant at year zero. $OPEX_{tot}$ are the total operational expenditures of a plant of one year. Hereby it is assumed that OPEX are an average value over the lifetime of the project. Including a degradation rate into the LCOE calculation is a simplified approach for considering degradation, without changing the model and the dispatch strategy of the plant for every year of the plants lifetime. The disadvantage is that different degradation rates of different components are not considered in detail. This simplification is considered acceptable, as the PT and the PV system have a similar degradation and the OPEX of the BESS include costs for replacing batteries. The total electrical energy injected into the grid $E_{grid,tot}$ is calculated according to the control strategy mentioned in the section 3.2.3. It is also important to note that the LCOE function considers the zero degradation for the first year.

$$LCOE = \frac{\left(CAPEX_{tot}(t=0) + \sum_{t=1}^{n} \frac{OPEX_{tot}}{(1+i)^t}\right)}{\sum_{t=1}^{n} \frac{E_{grid,tot} \cdot (1-d)^{(t-1)}}{(1+i)^t}} \quad 3)$$

$LCOE$**:** Levelized costs of energy

n: Plant lifetime

t: Year of plant lifetime (1, 2…n)

i: Interest rate

d: Degradation rate

The Capacity Factor (CF) was selected as objective function for the HYPPO analyses as it allows easy comparison to other types of power plants, even in different contexts. Compared to the night-time fraction, the CF does not directly give information about the timely distribution of plant availability. However, as in most topologies the PV system injects to the grid as first priority, it can be assumed that for higher CF values, the daytime is saturated, and the CF allows a good estimate for the night electricity generation as well. The HYPPO tool is able to provide the night-time fraction as an output parameter.

The CF as second objective function is calculated using the below mentioned equation. Therefore, the total grid injection $E_{grid,tot}(t)$ of every hour of one year is summed up and divided by the sum of the

grid injection limit $P_{grid,lim}$ multiplied with the timestep size Δt of every hour of one year. It is only calculated for the first year of the lifetime of the plant. The degradation is not considered for the CF.

$$CF = \frac{\sum_a E_{grid,tot}(t)}{\sum_a P_{grid,lim} \cdot \Delta t} \quad 4)$$

CF: Capacity factor

$E_{grid,tot}(t)$: Total grid injection in timestep t

$P_{grid,lim}$: Grid injection limit

Δt: Step size of timestep t

8.3. Additional Boundary conditions of HYPPO Simulations

The boundaries of the different parameters that are optimized with the PSO are shown below. The parameters can take values between the lower and the upper limit. The upper limits are set depending on the results of pre-optimizations, preliminary estimations or simply experience. Therefore, an optimization was conducted, and it was determined for which sizes of the plant components namely the LCOE start growing exponentially with increasing CF. Subsequently, the limits are set so that the part of the pareto front between LCOE and CF without exponential growth is completely included, and further a relatively small part of the pareto front with exponential growth. This is done to reduce simulation time and avoid getting too many results in less interesting ranges of the CF (as very high CFs will lead to extreme system capacities and, thus, LCOEs).

The minimum values for the nominal thermal power of the PT plant and the nominal thermal storage capacity is 1 MW_{th} and 1 MWh_{th}, respectively. The table shows the upper limits for the nominal thermal power $\dot{Q}_{PT,nom}$ and the nominal capacity of the TES $Q_{TES,nom}$ for the PT plants for all sites.

Table 6: Upper limits of the solution space for the PT plant for all sites analysed with HYPPO

Site	$\dot{Q}_{PT,nom}$ **[MW_{th}]**	$Q_{TES,nom}$ **[MWh_{th}]**
PSA	2650	9500
De Aar	2600	12000
Diego de Almagro	1800	6000
Riyadh	2800	12000

For the PV plant the lower limit of the nominal PV capacity $P_{PV,AC,nom}$ is 1 MW_{AC}, the lower limit of the nominal usable energy capacity of the BESS $E_{BESS,nom}$ is 1 MWh, and the lower limit of the nominal power of the BESS $P_{BESS,nom}$ is 150 MW. The lower limit of the nominal power of the BESS $P_{BESS,nom}$ is 150 MW as the BESS must be able to reach the grid injection limit to be comparable to the other two plant types. A higher nominal power of the BESS can be necessary for charging the BESS with PV excess energy.

Table 7: Upper limits of the solution space for the PV plant for all sites analysed with HYPPO

	$P_{PV,AC,nom}$ [MW$_{AC}$]	$E_{BESS,nom}$ [MWh]	$P_{BESS,nom}$ [MW]
PSA	1500	2400	500
De Aar	1200	2600	500
Diego de Almagro	650	2150	350
Riyadh	1300	2500	500

As reference-case, a PT-system with an installed nominal thermal power $\dot{Q}_{PT,nom,ref}$ of 90 MW$_{th}$ is simulated for each site. The total aperture reflective area $A_{PT,ref}$ of a 90 MW$_{th}$ PT-system amounts to 137,600 m^2. For the CRT topology a reference-system with an installed thermal receiver power of 438.92 MW$_{th}$ and with a corresponding heliostat field with an aperture area of 906,225 m^2 is modelled. As a reference case for each site, a PV plant with an installed capacity of 100 MW$_{AC}$ is simulated. PBs with a rated net power of around 150 MW$_{el}$ are chosen for the PT plant, the PT-PV hybrid plant as well as the CRT hybrid plant. These reference plants are used to generate the expected plant power outputs for each timesteps and scale it according to the simulated capacities.

The ERH capacity can also be reduced to 0, leaving that component away completely. For the PT hybrid plants, an auxiliary BESS will always be required, so the minimum capacities are set to 7.5 MW and 15 MWh to provide for the solar fields auxiliary power demand during the night with roundtrip efficiency of 85%.

8.4. Evaluation of HYPPO Simulations

If all topologies are optimised using the MOPSO algorithm in HYPPO the pareto fronts of all topologies are generated as per Figure 14 below. Only the LCOE of the most economic configurations leading to the same CF are displayed for each topology. If different configurations lead to the same CF, only the configuration with the lower LCOE is displayed. This allows to directly compare the different plant topologies to each other, as for each point over the CF each case can be considered as the optimised configuration for that topology.

Further, the kind of display as used in HYPPO allows the analysis of boundary effects. These effects are explained here briefly for the Riyadh reference case, specifically highlighting the peculiarities of HYPPO. A detailed interpretation of results for all sites and cases is provided in section 0 of this report based on the results from greenius.

It can be seen below that for higher CF values the LCOEs grow exponentially, which can be expected as it would be required to significantly increase storage and solar capacities to provide power also during series of multiple days without direct sunlight. One main difference between the BESS and the TES is the marginal cost, which results in a different gradient of the LCOE over CF for the PV-BESS topology. In order to provider more energy annually, the BESS and PV capacities have to be linearly increased, which nearly leads to linearly increased CAPEX for the complete hybrid system. For the hybridized CSP systems, increasing the storage capacity, only a low marginal cost is required, while the increase of PV and CSP capacities corresponds with an increased energy yield. This leads to rather flat LCOE curves over the dominant range of CF values for these topologies. In other words: The additional investment for increasing the CF of plants using a thermal energy storage is directly

leading to an increased overall energy output, while for the BESS a significant share of the additional investment is related to the storage itself, which does not generate additional energy.

However, the TES requires a huge initial investment related to the power block. This is the reason why the PV-BESS pareto front crosses the others at a CF value of approximately 55…60% corresponding to approximately 3…4 hours of storage discharge during the night. This means that TES used in hybridized solar plant can break even with BESS if peak loads need to be covered regularly for 4 hours or more. Not surprisingly, this break-even point is very sensitive to the BESS investment cost, which is further evaluated in 9.3 of this report.

For CF values below 40% in this diagram, the results can be misleading. In these cases, the storage capacity is reduced to 0 or the minimum limit as the PV systems are able to cover CFs up to 40% without additional storage. Due to the structure of the HYPPO tool and especially the nature of the MOPSO optimisation algorithm, the fixed PB cost is still considered, even if this component is not used at all. This shears the results, and it can be expected that for CF values below 40% PV plants without any storage will be significantly cheaper. Only for the PV-BESS system the LCOE in this range can be considered as realistic, as no fixed cost component is included for that system. This behaviour of the model can be considered as a bug and may be corrected in later versions of the HYPPO tool. However, the main purpose of the tool is the optimisation of plants with higher CFs and including storage, so the error is acceptable for the purpose of this study.

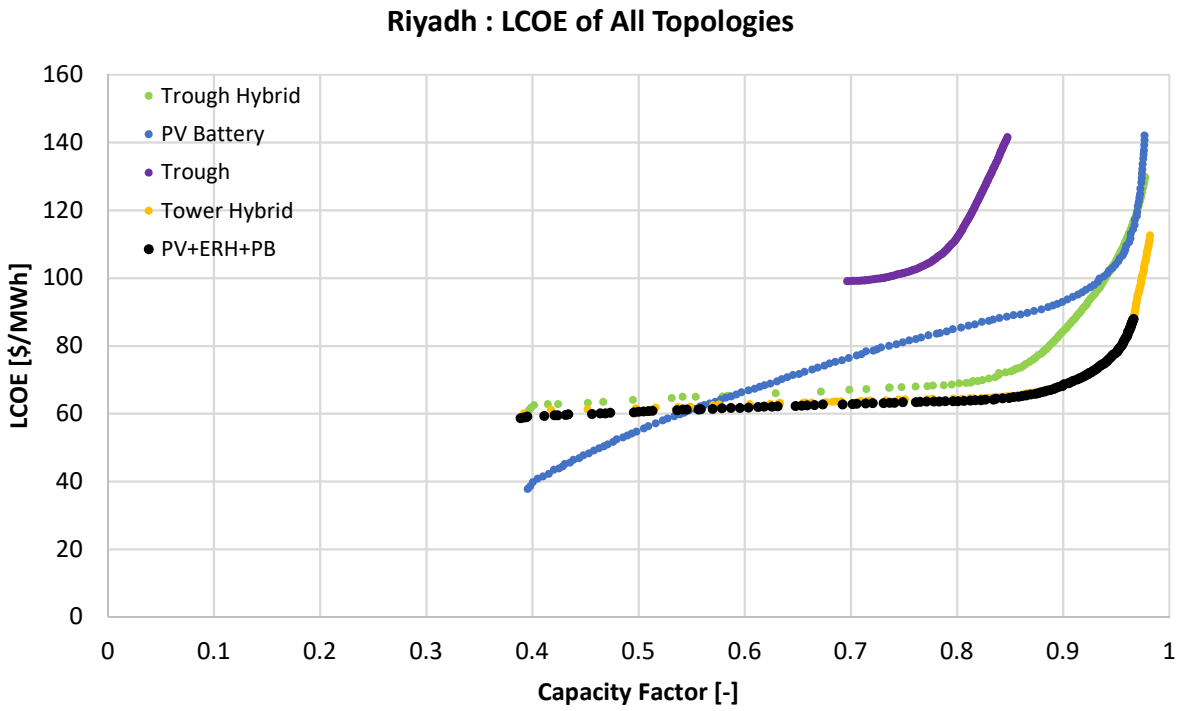

Figure 14: HYPPO Optimisation Results for all topologies for Riyadh

Comparing the different topologies for the reference location in Riyadh, it is clear that a stand-alone PT plant that only injects electricity during the night cannot compete with the other topologies. Hybridised CRT plants as well as PV plants using P2H technology with thermal energy storages show the lowest LCOEs for capacity factors higher than 55%. Hybridised PT plants generate electricity at

slightly higher LCOEs but show generally the same behaviour. Depending on cost developments in the CSP market the differences between CSP cases could further reduce, leading to very similar LCOE results. For very high CF values (above 80%) the PT hybrids cannot compete with CRT or PV+P2H. Battery storages according to current market prices and developments only seem the right choice for peaker systems with CF values between 40 and 60%, which could easily change if BESS costs are reduced in the future. Below 40% pure PV seems to be the best choice. High C-rate BESS could play a role in these systems to further optimise the LCOE for CF values above 35%.

The above interpretation is not only based on the figure above, but also other output diagrams that are automatically generated by HYPPO giving additional information about the component capacities for each case and of course simulation result parameters such as annual energy yield, curtailment, etc. These diagrams are not shown in this report for the sake of readability.

9. Results

In this chapter the results for all different analyses are presented. The results are shown for the greenius simulations as it mostly matches the simulation results from HYPPO. For the sake of readability, the HYPPO result diagrams have been added to the Annex.

9.1. Results Riyadh (Base Case)

We started the investigation with Riyadh since it is the site with a DNI resource lying between PSA (Spain) and De Aar (South Africa), the 3 sites we originally selected at the beginning of the project. In this chapter the results will be analysed for each technology at this site.

Figure 15 shows the LCOE values versus the night-time electricity fraction for the optimal configurations for different storage sizes of different topologies. Each point stands for an LCOE-optimised configuration for a certain storage capacity (3, 6, 9, 12 hours duration of discharge at full power block output). Cases without any storage are not displayed, with one exception which is the standalone PV system as a reference.

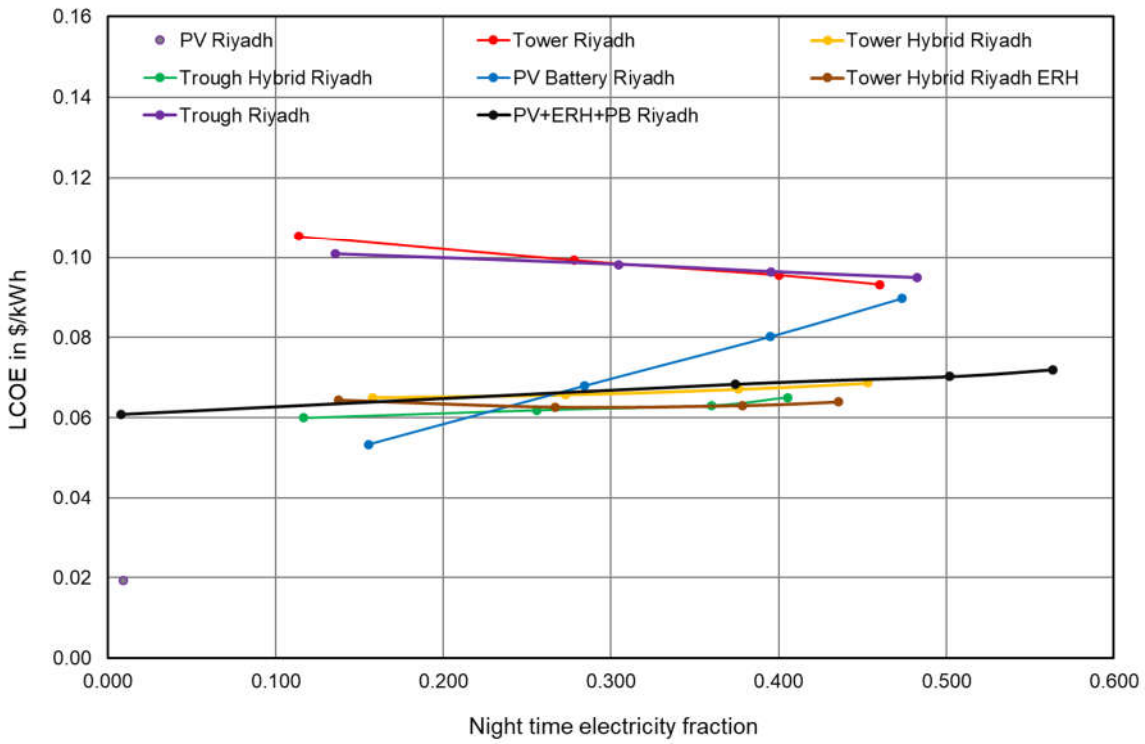

Figure 15: Best LCOE configuration Riyadh

The top lines show the results for pure CSP systems. These plants have the highest LCOE since they do not benefit from the low electricity cost of PV. They are shown as reference and their LCOE is higher than that of the hybrid systems. The LCOE decreases with increasing night-time electricity fraction which is caused by the cheap thermal storage and better utilization of the power block (which is kept at constant nominal power but reaches more operating hours with increasing thermal storage size).

The higher storage costs of battery systems compared to thermal storage results in a different dependency of LCOE with increasing night-time electricity fraction. PV with battery is the technology

that provides the lowest LCOE for night-time fractions below 20-25% (approximately 4-5 hours of storage capacity). However, from 20-25% night-time fraction upwards, the costs start to be higher and this difference grows linearly as the storage size increases. For a storage size of 12 hours the LCOE is similar to standalone CSP plants. Hybrid PV-CSP systems in contrast, show less dependency of LCOE on the night-time electricity fraction and they are almost constant in this figure.

Hybrid plants show a significant decrease in costs compared to standalone CSP plants. LCOE remains relatively constant regardless of the night-time fraction (storage capacity). There is better utilization of the thermal storage as it increases in size, but there is also an increase in dumping and component costs. Hybrid parabolic plant and the hybrid tower plant with electric heater show almost the same LCOE with a small advantage of parabolic trough hybrid system for low storage capacity and a small advantage for hybrid tower systems for higher storage capacity. There is a slight cost increase when the tower does not incorporate an electric heater because of the lower heat production costs of PV with electric heater in comparison to the tower system as well as other synergies that will be analysed separately. Therefore, an improvement of the system is achieved by incorporating an electric heater.

It can be seen that the night-time fraction of electricity from the tower plant with heater is lower than the one without heater, if one compares plant configurations with identical storage size. The night fraction of parabolic hybrid is even slightly lower. This is due to the greater weight of the PV field in the optimal design of the plant. This increases the electricity production during the day but reduces it at night.

Another interesting question is whether a system using PV, ERH, thermal storage and PB could be cheaper than a hybrid PV-CSP plant and how much night time electricity it can offer. Figure 15 shows that the LCOE values and night fractions of the PV+ERH+PB system are higher than those in hybrid plants. Note that operating strategy 1 of this kind of system is used here, so thermal storage charging has priority [see also subsection 2.3 Summary PV power operating strategies]. This operating strategy was used for direct comparison since, as in the case of hybrid systems, storage charging is prioritized. A separate comparison with operating strategy 2 is shown in subsection 9.1.1. Analysing the results, it can be seen that for a 3-hour storage, the night share leans towards zero because the small storage capacity does not justify the cost of the electric heater. The optimum 3 h system would have a storage that would not be used at all. This changes for higher storage capacities where the electric heater and the storage tank would be used. Although the LCOE is higher than that for hybrid systems, the nightly fractions are much higher for large storage capacities. This is also of great importance since not only reducing costs is one of the objectives of the plant, but also, being able to provide a greater amount of electricity during the night.

Plotting the results over capacity factor on the x-axis gives us more information. We can see in Figure 16 how the hybrid power plants maintain their cost of electricity up to about 80% capacity factor and from that point on the LCOE rises significantly due to the enormous costs required to achieve these factors. Electricity costs in the case of PV with battery rise more steadily, although from 90% capacity factor there is also a significant increase. This steep and exponential increase starts approximately at the point, where the storage capacity exceeds 12 hours. These plants may bridge time periods when the solar irradiation is low for whole days but are over-dimensioned for the typical day-night cycle which is the prevailing operation scheme for solar power plants with storage. The break-even point between all technologies is approximately 55% capacity factor. LCOE values of just over 6 cents per

kWh for 80% and 10 cents for 95% CF for these hybrid plants are interesting results and are significantly lower than for pure CSP plants which show increasing LCOE at much lower CFs. The same results could be achieved using HYPPO as displayed in Figure 14.

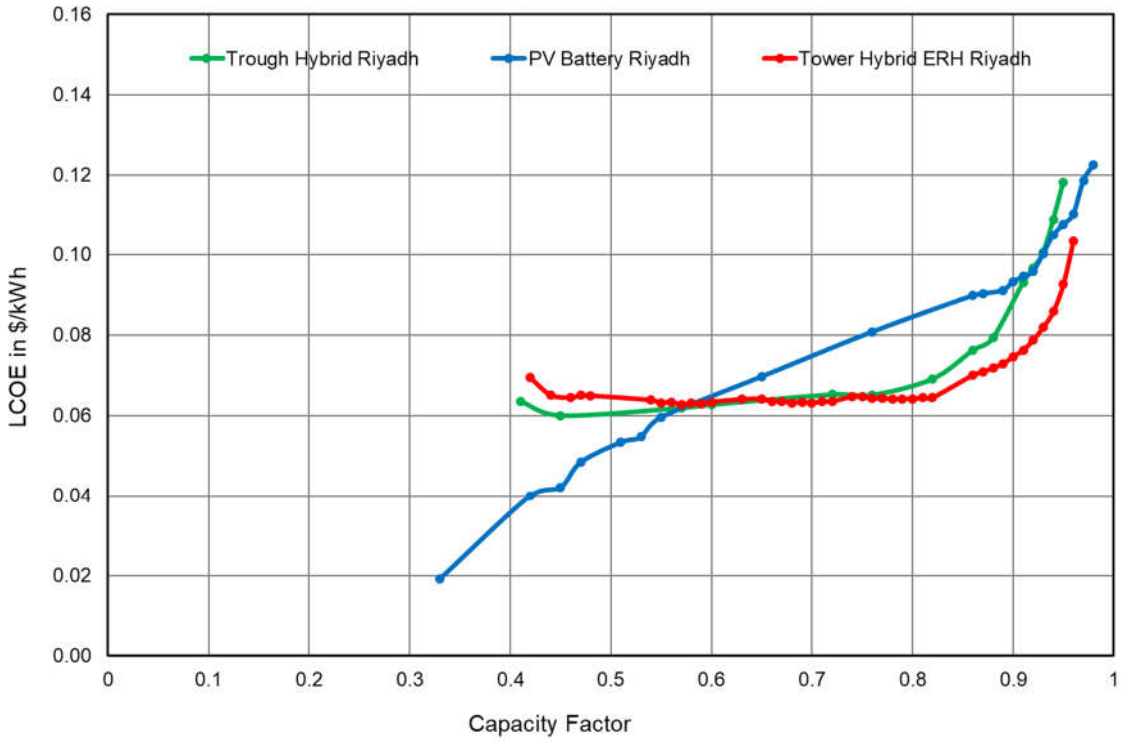

Figure 16: Capacity factor representation for Riyadh

9.1.1. Comparison of the operating strategies of the PV+ERH+PB system

Two different operating strategies were compared for the PV+ERH+PB system [see also subsection 2.3 Summary PV power operating strategies]). The first one prioritizes charging the thermal storage while the second prioritizes the direct grid supply. Some interesting observations can be made by comparing their results as shown in Figure 17. Operating strategy 1 shows higher LCOE values and night shares than operating strategy 2. Direct grid supply reduces PV dumping and increases the amount of electricity delivered. The optimized PV field is smaller but less electricity is converted into thermal energy. This results in the reduction of electricity costs. On the contrary, the cost-optimized design cannot charge the thermal storage to the same extent as operating strategy 2. So, it is not possible to reach the night shares of the first strategy. The difference in night time electricity between both strategies is not only percentage but also absolute. Strategy 1 supplies 557677 MWh at night during a year while the second strategy provides 464744 MWh. The notable differences in LCOE and night fractions shown for each strategy prove how sensitive the results are to these boundary conditions.

Unlike in Figure 15, assuming operating strategy 2, LCOE values are slightly lower than those for hybrid plants. The differences are very small and strongly sensitive to cost assumptions. Night shares are similar to hybrid plants in that case as well.

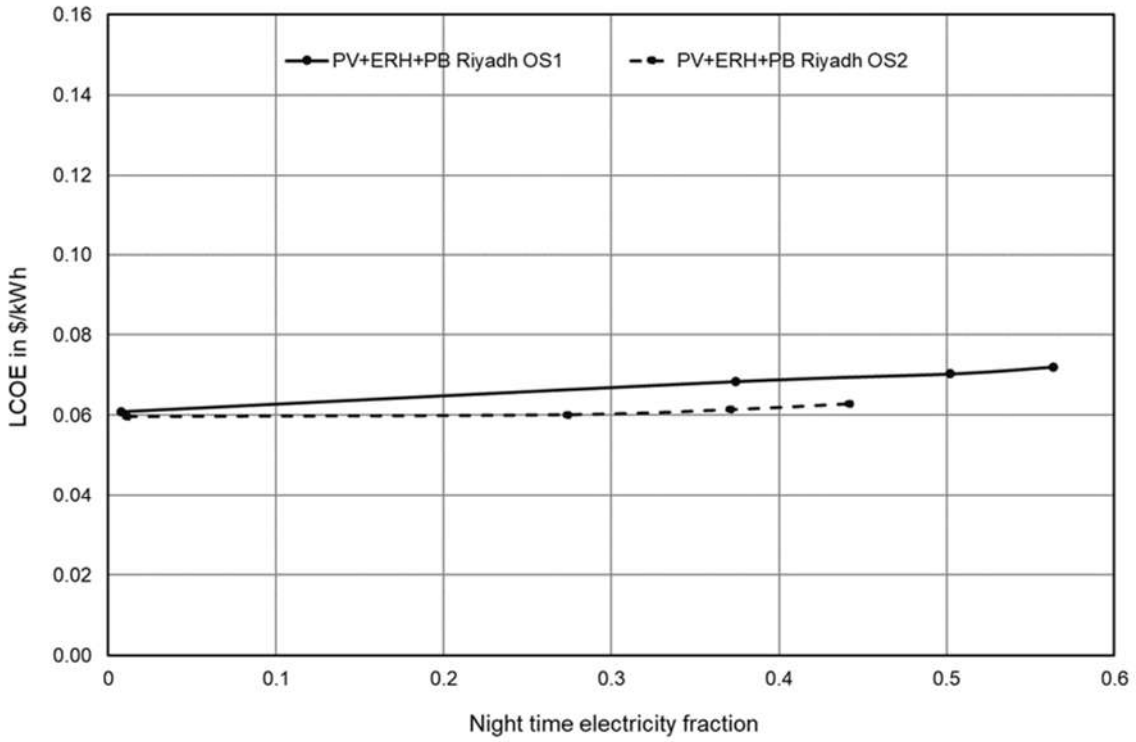

Figure 17: Impact of operation strategy on LCOE and Night Fractions

9.1.2. Comparison of the LCOE optimized configurations

The main design parameters of all optimized systems for each storage size are presented below. The analysis presents additional information to that obtained from the diagrams.

Table 8 shows the parameters of the optimized systems with a storage of 3 hours, the lowest capacity considered. The parabolic hybrid plant has the smallest CSP field. This is due to the greater flexibility in the design of this plant. The hybrid tower plant has a minimum CSP field design size of 200 MW. Towers smaller than this size were not considered in the optimization. For smaller storages, the daytime electricity cost is more important in the LCOE. Therefore, a larger PV field is advantageous. For this reason, in the parabolic trough hybrid power plant there is a significant difference in size between the aperture area of the PV and CSP fields. On the other hand, when the storage size is small, there is hardly any improvement in implementing an electric heater in hybrid tower power plants. There is no significant use of surplus electricity so there is almost no difference in the optimal design of the plant with or without a heater. The heater has a nominal power of only 30 MW which is quite small compared to the CSP field with 200 MW.

The PV field of the PV-BESS system is only slightly larger than the PV field of the hybrid power plants due to the low capacity of the storage. In the case of the PV+EH+PB system the optimization even leans towards minimizing the nominal power of the electric heater since it seems to be more economic to leave the storage and the power block almost unused in this scenario. Tower plants have a larger total land area, especially the pure CSP plant. The thermal capacity of the storage tank is higher for the standalone parabolic power plant since the power block has a lower efficiency due to the lower temperature level and therefore requires more energy to deliver 150 MW_e.

Table 8: 3h best configurations parameters

Technology	Trough	Solar Tower	Hybrid Trough	Hybrid Tower	Hybrid Tower EH	PV-BESS	PV+ERH+PB OS1	PV+ERH+PB OS2	Unit
Storage duration	3	3	3	3	3	3	3	3	h
Thermal storage capacity	1248	1033	1033	1033	1033	-	1033	1033	MWhth
Battery storage capacity	-	-	-	-	-	450	-	-	MWe
CSP field aperture	1.2	1.2	0.07	0.3	0.3	-	-	-	km²
CSP field nominal output	760	650	43	200	200	-	-	-	MWth
PV system nominal output	-	-	250	200	200	250	200	200	MWAC
PV system module area	-	-	1.7	1.4	1.4	1.7	1.4	1.4	km²
ERH nominal power	-	-	80	-	30	-	5	5	MWe
Power block nominal output	160	160	160	160	160	-	160	160	MWe
Total land area	4.5	7.4	5.2	5.5	5.5	4.9	3.9	3.9	km²

Table 9 presents the main design parameters for the optimized 6-hour storage systems. Interesting is the difference that arises in the optimization of the hybrid tower plant with or without electric heater and that can also be observed for larger storage sizes. In the case of a plant without heater, the size of the PV field is kept constant, since an increase in its size would have no use, as the excess of electricity cannot be used. However, in the case of a power plant with a heater, the opposite is true. The optimization prioritizes an increase of the PV field because heat production costs are lower with PV and electric heater. In the case of parabolic trough hybrid plants, there is a greater increase in the CSP field for higher storage capacities because the booster system requires an increase of both technologies (PV and CSP). Therefore, an increase of the PV size can also be observed. The non-hybrid plants correspondingly increase the size of their main components to make use of the new storage capacity. There is a big difference in the land area for the tower and parabolic trough plant, but this does not occur for hybrid plants. PV+ERH+PB with operating strategy 1 leans towards larger PV fields and smaller electric heaters than operating strategy 2. This happens for all storage capacities. This makes sense because there is more excess electricity available for supplying the grid directly with the reduction of electricity costs that this operating strategy implies.

Table 9: 6h best configurations parameters

Technology	Trough	Solar Tower	Hybrid Trough	Hybrid Tower	Hybrid Tower EH	PV-BESS	PV+ERH+PB OS1	PV+ERH+PB OS2	Unit
Storage duration	6	6	6	6	6	6	6	6	h
Thermal storage capacity	2494	2066	2066	2066	2066	-	2066	2066	MWhth
Battery storage capacity	-	-	-	-	-	900	-	-	MWe
CSP field aperture	1.5	1.6	0.14	0.5	0.3	-	-	-	km²
CSP field nominal output	978	850	87	300	200	-	-	-	MWth
PV system nominal output	-	-	350	200	275	300	450	400	MWAC
PV system module area	-	-	2.4	1.4	1.9	2.1	3.1	2.8	km²
ERH nominal power	-	-	160	-	100	-	200	250	MWe
Power block nominal output	160	160	160	160	160	-	160	160	MWe
Total land area	5.8	11.0	7.4	6.6	7.0	5.9	8.9	8.9	km²

Table 10 shows the parameters of the optimized systems with 9 hours of storage. The trend seen for the 6 hours of storage continues. For hybrid parabolic power plants, the size of both fields (PV and CSP) increases again due to the synergies and dependence established. So, the sizes of the CSP and PV are considerably increased to cover more night-time demand allowing at the same time a higher supply during the day. The larger storage size in turn reduces the dumping that a larger PV field would entail. This synergy is one of the most interesting features of hybridization. It is also interesting to observe the effects on the land area. The land area factor is different for each

technology. For the PV field 2.86 was assumed while for the parabolic field 3.73. For the tower field it is higher and varies between 4.67 and 8.5 depending on the system size. Solar tower plants instead have a larger specific land demand, and it grows with increasing system size. Heliostats far away from the central tower require a larger distance to their neighbours to limit shading and blocking between each other. This shows how the total land area of the tower plant is increasing significantly for bigger storage sizes. The combination of effects makes the total area for the hybrid power plants more or less similar. PV has a lower land cover ratio but requires a larger area per power. PV system with battery requires a smaller land area than hybrid power plants because of the higher round trip efficiency of the battery that leads to smaller PV fields.

Table 10: 9h best configurations parameters

Technology	Trough	Solar Tower	Hybrid Trough	Hybrid Tower	Hybrid Tower EH	PV-BESS	PV+ERH+PB OS1	PV+ERH+PB OS2	Unit
Storage duration	9	9	9	9	9	9	9	9	h
Thermal storage capacity	3742	3099	3099	3099	3099	-	3099	3099	MWhth
Battery storage capacity	-	-	-	-	-	1350	-	-	MWe
CSP field aperture	1.7	2.0	0.21	0.8	0.3	-	-	-	km²
CSP field nominal output	1087	1050	130	450	200	-	-	-	MWth
PV system nominal output	-	-	400	200	400	375	550	500	MWAC
PV system module area	-	-	2.8	1.4	2.8	2.6	3.8	3.4	km²
ERH nominal power	-	-	230	-	225	-	300	350	MWe
Power block nominal output	160	160	160	160	160	-	160	160	MWe
Total land area	6.4	16.5	8.6	8.4	9.4	7.4	10.8	9.8	km²

The same general trend is observed for 12-hour storage in Table 11. One of the most surprising parameters is the size of the electric heater for hybrid power plants. It reaches 290 - 300 MW for a 12-hour storage. The nominal power of the tower reaches 1150 MW, which is the maximum available system size in greenius for the simulation. In the case of hybrid tower power plant with electric heater the CSP field remains at its minimum size because of the higher heat productions costs in comparison to the electric heater.

Table 11: 12h best configurations parameters

Technology	Trough	Solar Tower	Hybrid Trough	Hybrid Tower	Hybrid Tower EH	PV-BESS	PV+ERH+PB OS1	PV+ERH+PB OS2	Unit
Storage duration	12	12	12	12	12	12	12	12	h
Thermal storage capacity	4989	4132	4132	4132	4132	-	4132	4132	MWhth
Battery storage capacity	-	-	-	-	-	1800	-	-	MWe
CSP field aperture	2.1	2.2	0.24	1.1	0.3	-	-	-	km²
CSP field nominal output	1304	1150	152	600	200	-	-	-	MWth
PV system nominal output	-	-	450	200	475	450	700	600	MWAC
PV system module area	-	-	3.1	1.4	3.3	3.1	4.8	4.1	km²
ERH nominal power	-	-	290	-	300	-	400	450	MWe
Power block nominal output	160	160	160	160	160	-	160	160	MWe
Total land area	7.7	19.1	9.7	10.6	10.9	8.9	13.8	11.8	km²

9.1.3. Additional Synergies of PV and CSP technologies

Synergies between both kinds of plants are one of the most interesting aspects of hybridization. The difference between LCOEs of the hybrid tower plants with and without electric heater cannot be explained solely by lower heat production costs with ERH. Some additional synergies can be observed. For example, it can be seen in Figure 18, especially in December, that the electric heater provides power earlier in the morning than the CSP field (we do not consider any heating up time or

start up energy for the ERH). In addition, the PV system provides higher power some hours in the morning (10 am) and in the afternoon (2-3 pm) compared to its power at 12 pm and can thus complement the CSP field quite well. This is especially true in winter but also in fall and spring. This causes an increase in the capacity factor and leads to a reduction of the LCOE.

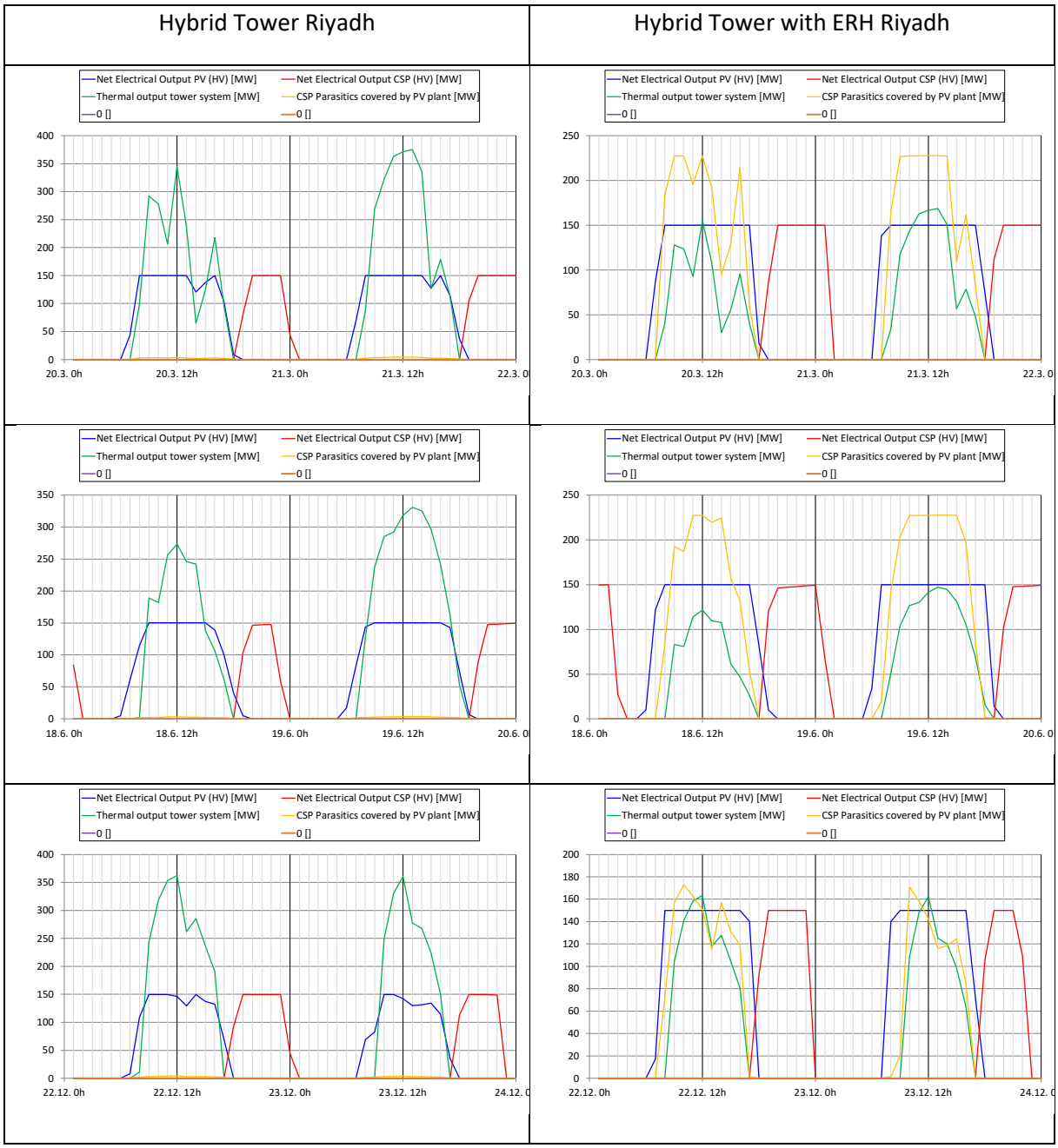

Figure 18: Outputs comparison of tower hybrid power plants with and without electric heater for two days in March, June and December

Figure 19 shows the relative power difference for CSP and PV fields and that the peaks for the PV fields are broader. This also leads to an increase of the capacity factor for the tower hybrid power plant with electric heater.

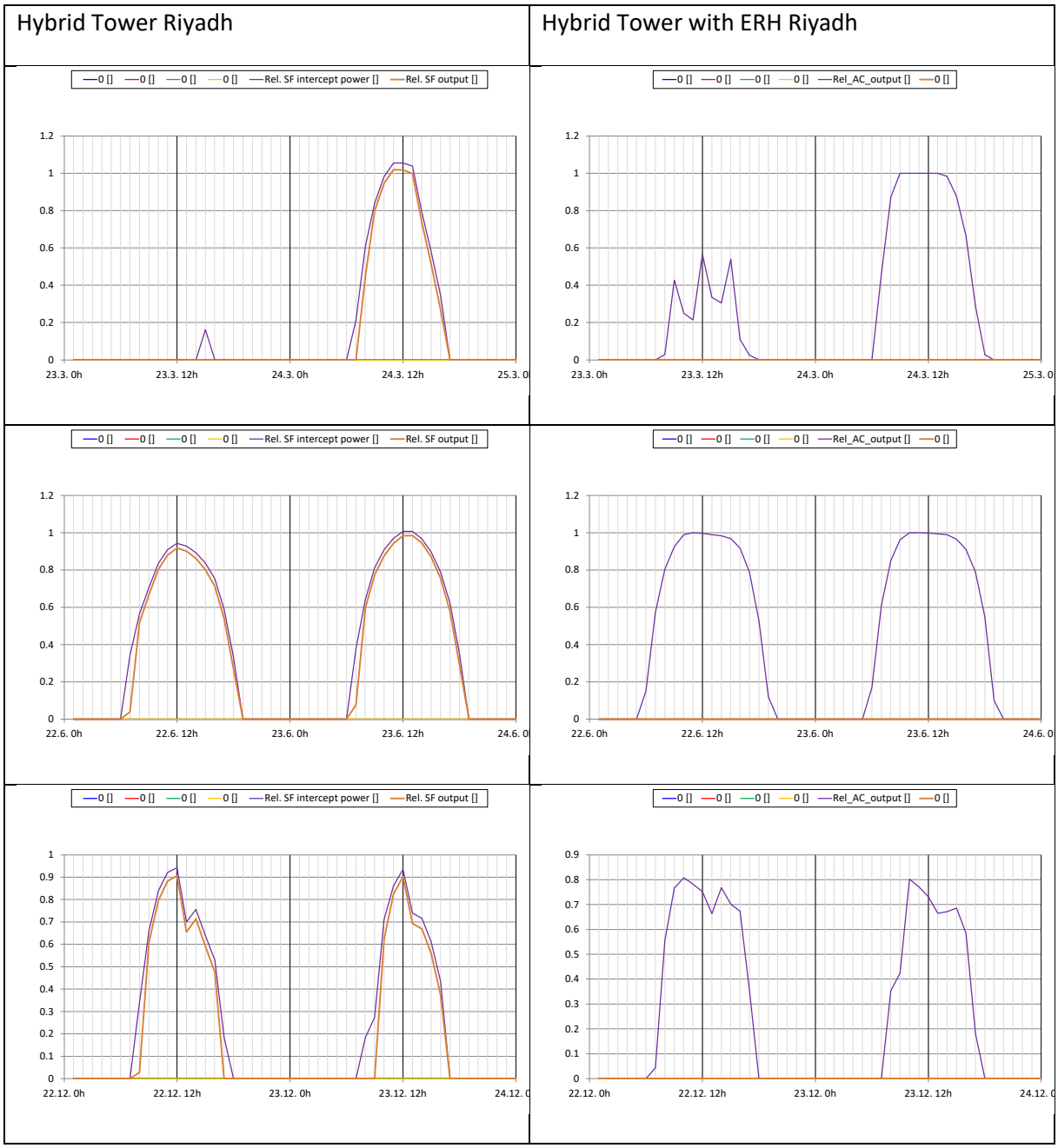

Figure 19: Relative powers comparison of tower hybrid power plants with and without electric heater for two days in March, June and December

Figure 20 compares the storage levels of both systems and shows that these are higher with an electric heater, mainly in spring and autumn. Also, PV dumping decreases even though the PV field is larger with an electric heater. The monthly distribution of the two figures below shows that the performance is better throughout the year when the system has a heater. All these synergies in combination with the lower heat production costs of PV with ERH help reducing the LCOE.

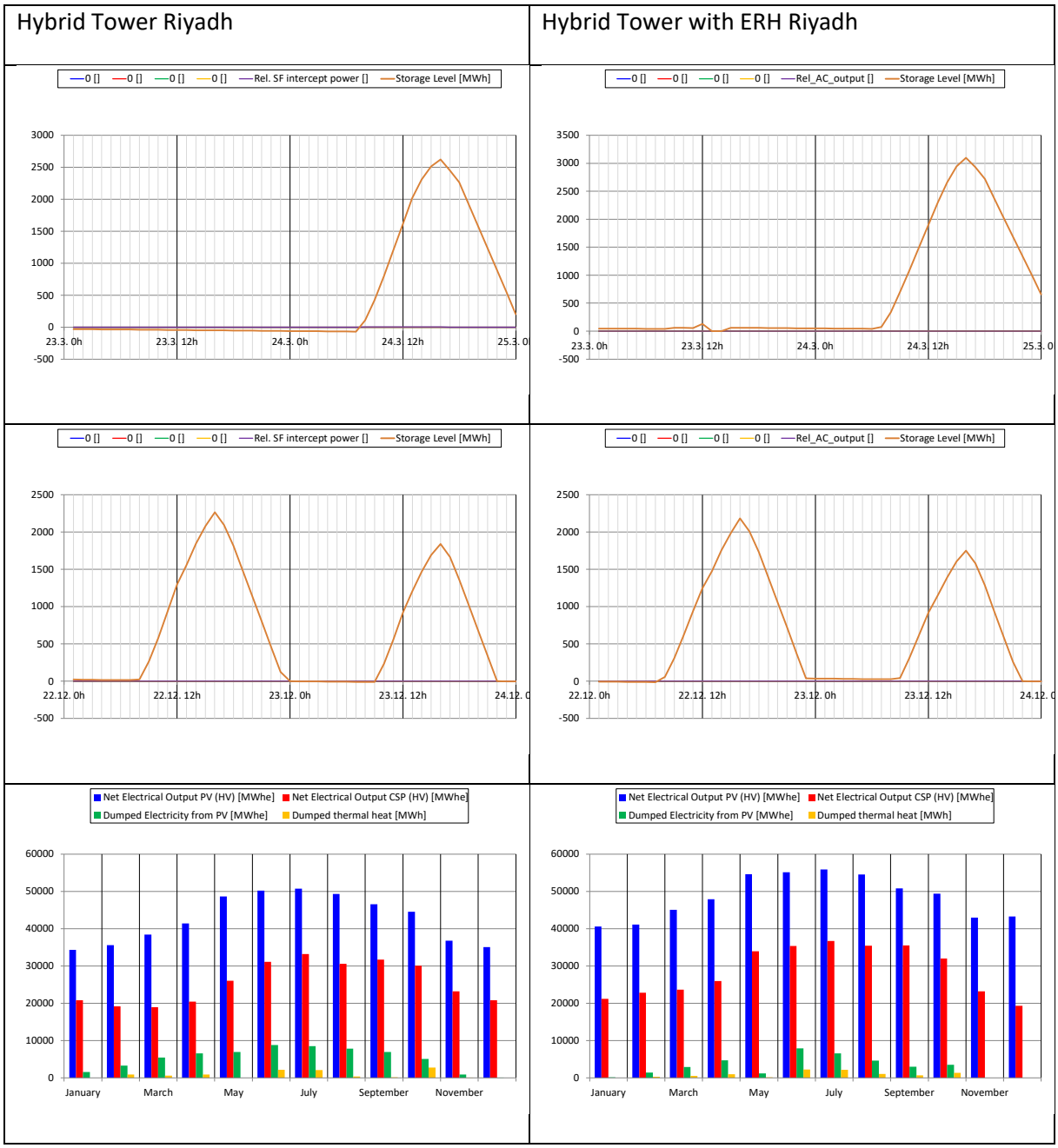

Figure 20: Storage level comparison of tower hybrid power plants with and without electric heater for two days in March and December. Monthly output comparison of both systems.

9.2. Results for all sites (Comparison of Plant Locations)

This section shows the results obtained for the remaining sites. First of all, it is interesting to compare the radiation values for each location and time of the year. Figure 21 shows the average value of DNI per hour for each month and location. Figure 22 shows the average GHI per hour. Figure 23 shows the monthly relative share of annual DNI sum and Figure 24 does the same with the GHI. Figure 25 and Figure 26 respectively show the DNI and the GHI for each hour of the year ordered descending according to their value. All these diagrams help to explain some of the differences observed between sites in the results. Please note that the southern hemisphere sites radiation values are displaced 6 months.

Figure 18 shows how Diego de Almagro's DNI values are higher throughout the year. In winter they are even similar to the summer values of Riyadh. Daggett, Ouarzazate and De Aar present similar maximum and minimum values but with different distribution throughout the year. DNI in Dunhuang hardly changes during the year. Figure 19 shows again that the GHI values are higher during the year in Diego de Almagro, although the relative difference is reduced. Dunhuang again presents a lower irradiation, mainly due to the lower values during the summer.

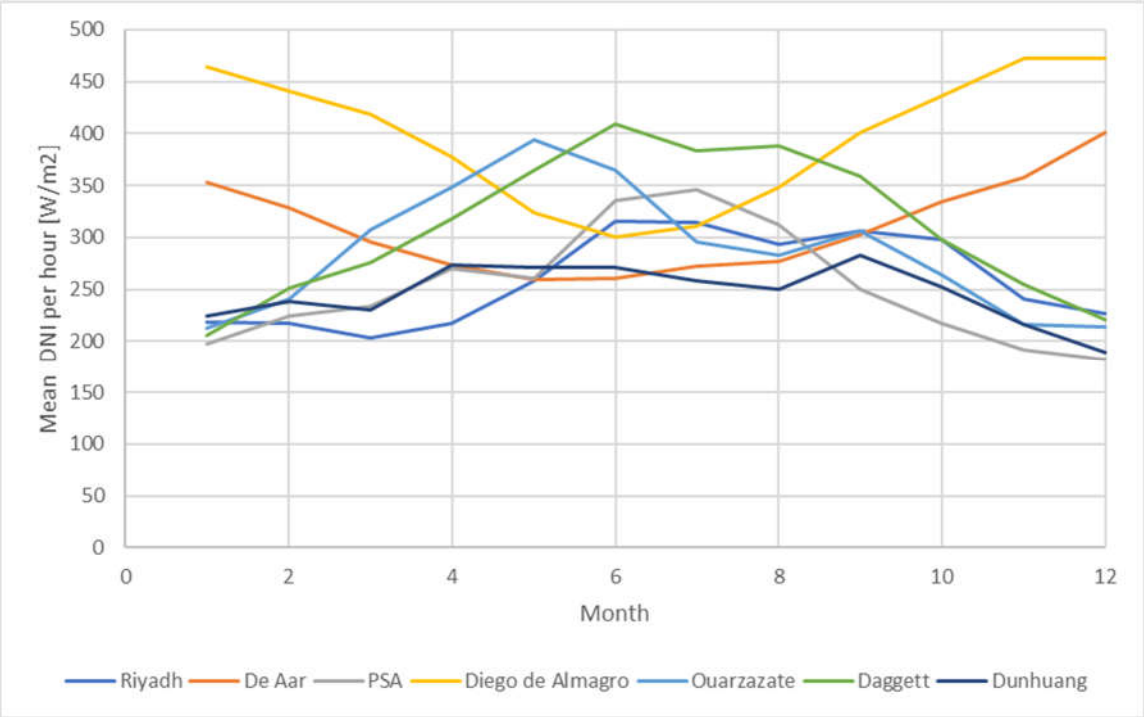

Figure 21: Mean DNI per hour for each site

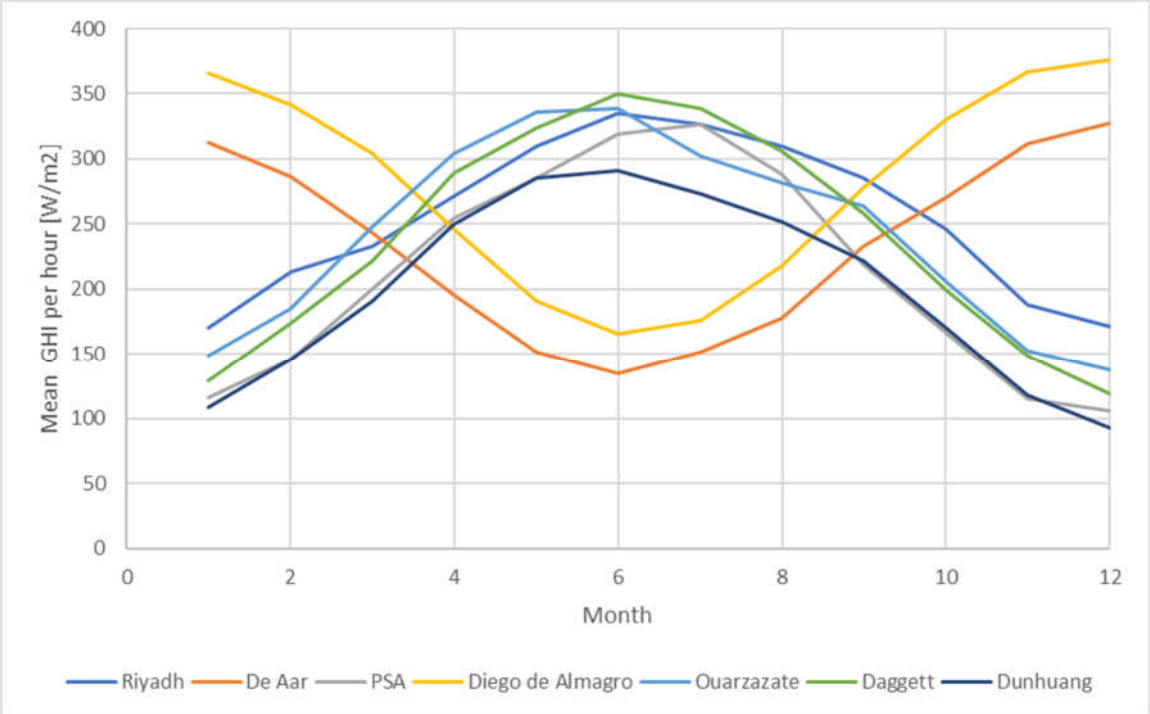

Figure 22: Mean GHI per hour for each site

Figure 23 shows a greater range of percentage variation between winter and summer for higher latitude sites such as PSA and Daggett. However, this does not occur for Dunhuang where local meteorological effects cause a very constant DNI throughout the year. For the rest of sites, both Figure 21 and Figure 24 show values expected from those described in Table 2 and Table 3.

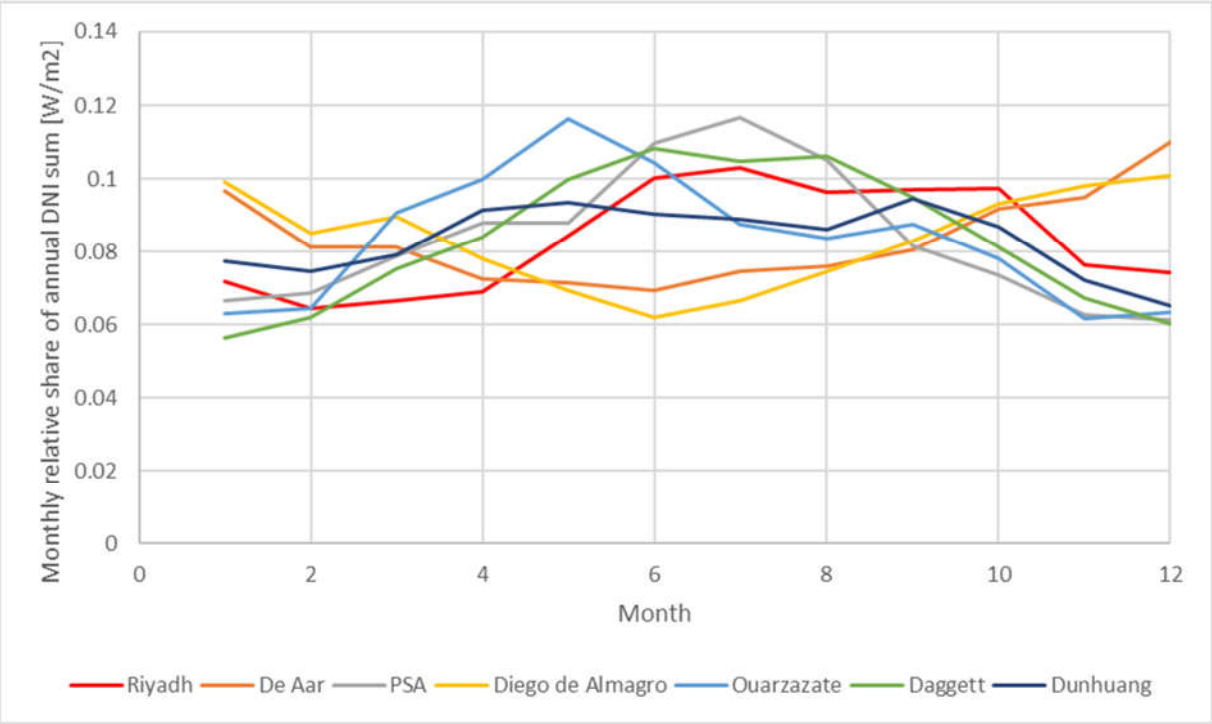

Figure 23: Monthly relative share of annual DNI sum for each site

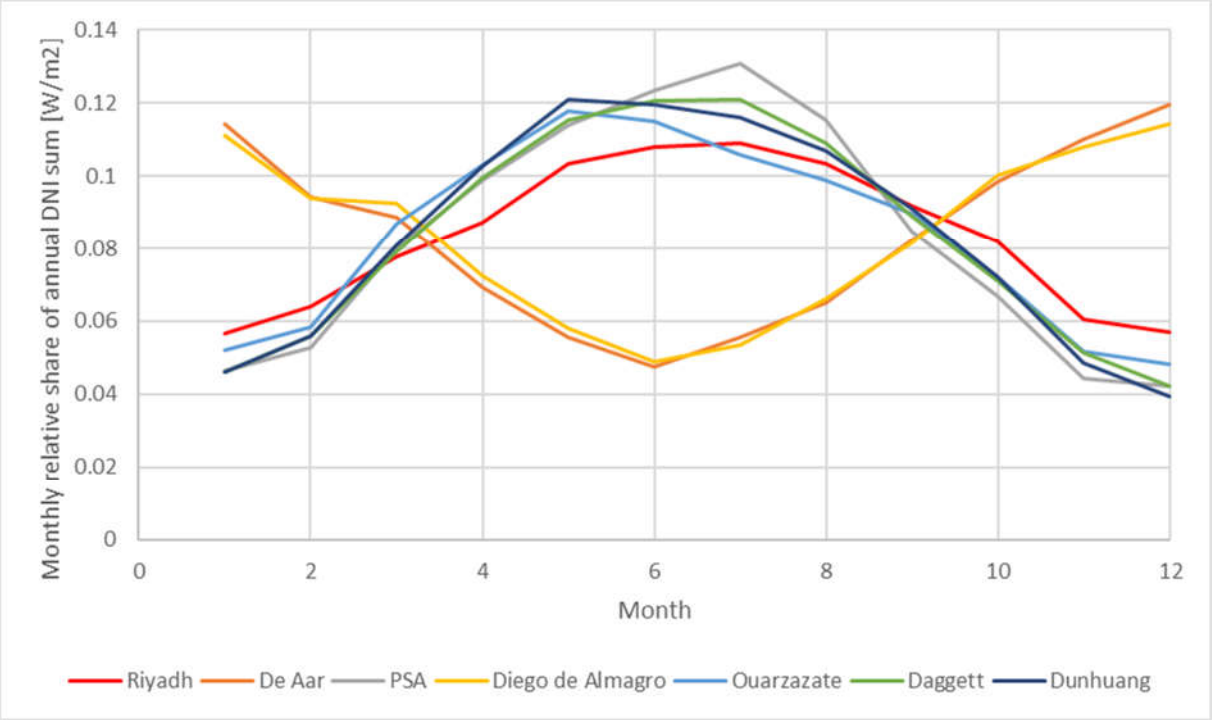

Figure 24: Monthly relative share of annual GHI sum for each site

Figure 25 and Figure 26 give additional information for the classification of sites. The DNI is greater than 1000 W/m2 in De Aar and Diego de Almagro for a significant number of hours. These sites are optimal for CSP plants. Diego de Almagro shows a very flat duration curve indicating very stable DNI conditions with low cloud coverage and low atmospheric impacts. A faster descent of the curve indicating a greater variability of the irradiation conditions occurs for PSA and De Aar.

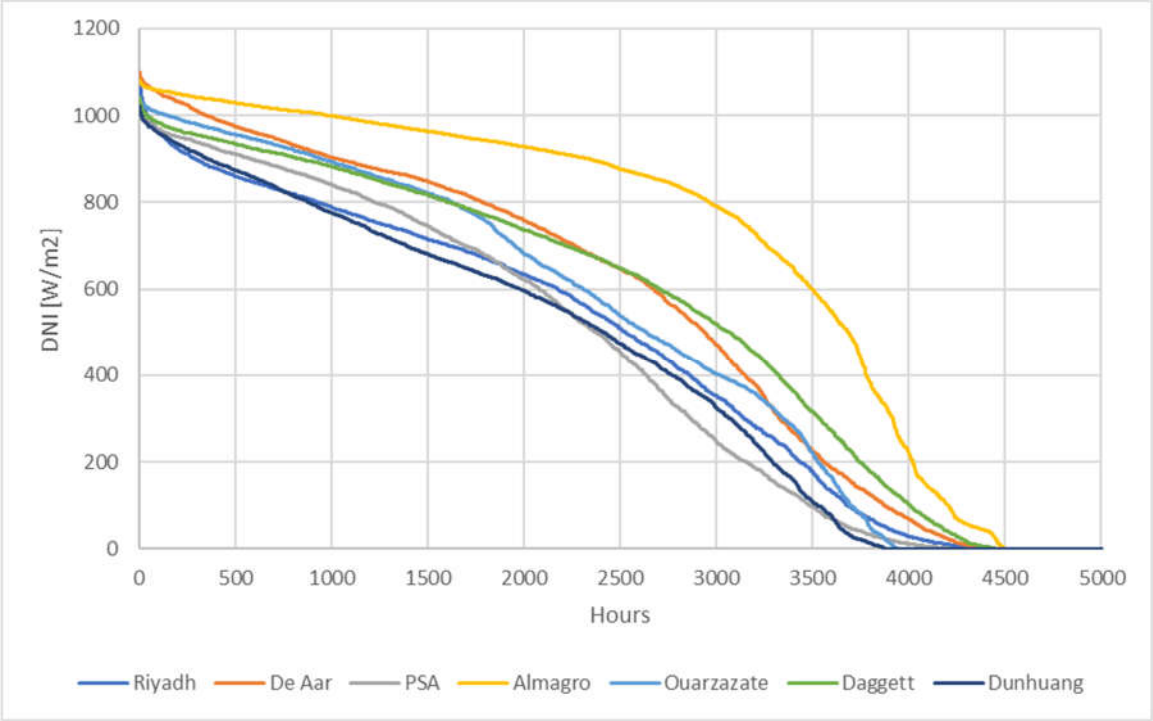

Figure 25: Hourly descendent DNI distribution

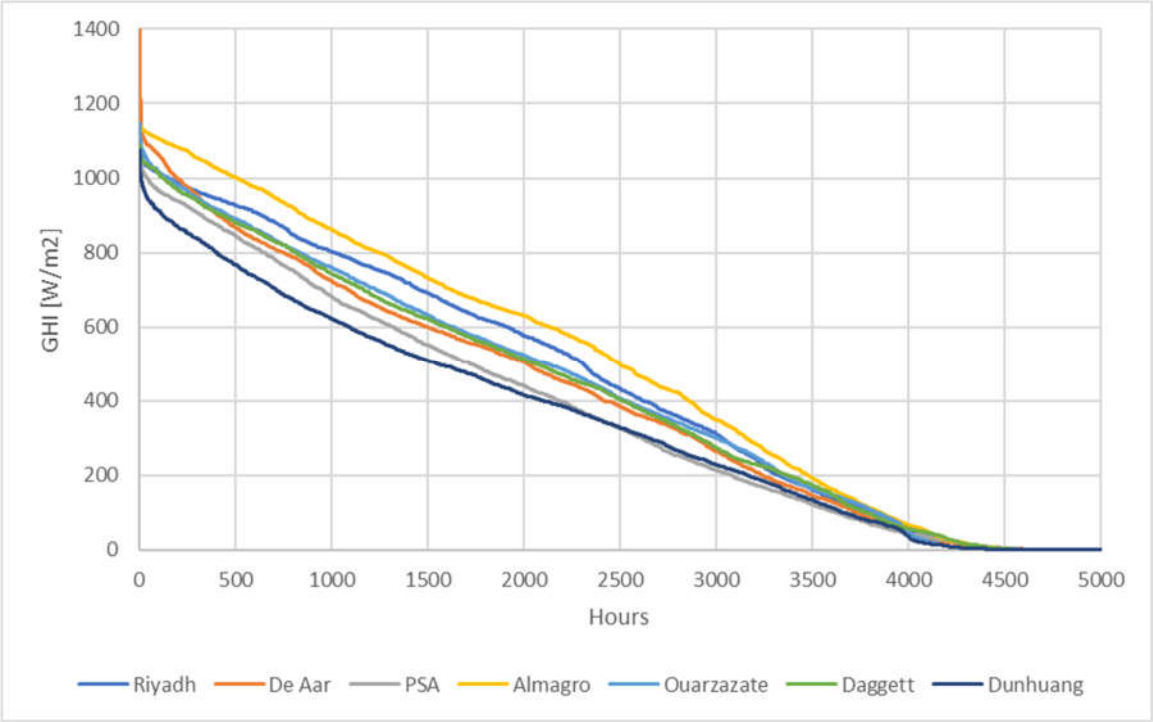

Figure 26: Hourly descendent GHI distribution

Figure 27 shows the results for De Aar, South Africa. It can be seen how the higher value of DNI compared to Riyadh lead to lower costs for pure CSP technologies. PV with battery technology suffers a slight increase and hybrid plants maintain similar costs because of the synergies of PV and CSP. Note that the PV+ERH system refers again to the first operating strategy (thermal storage charging has priority).

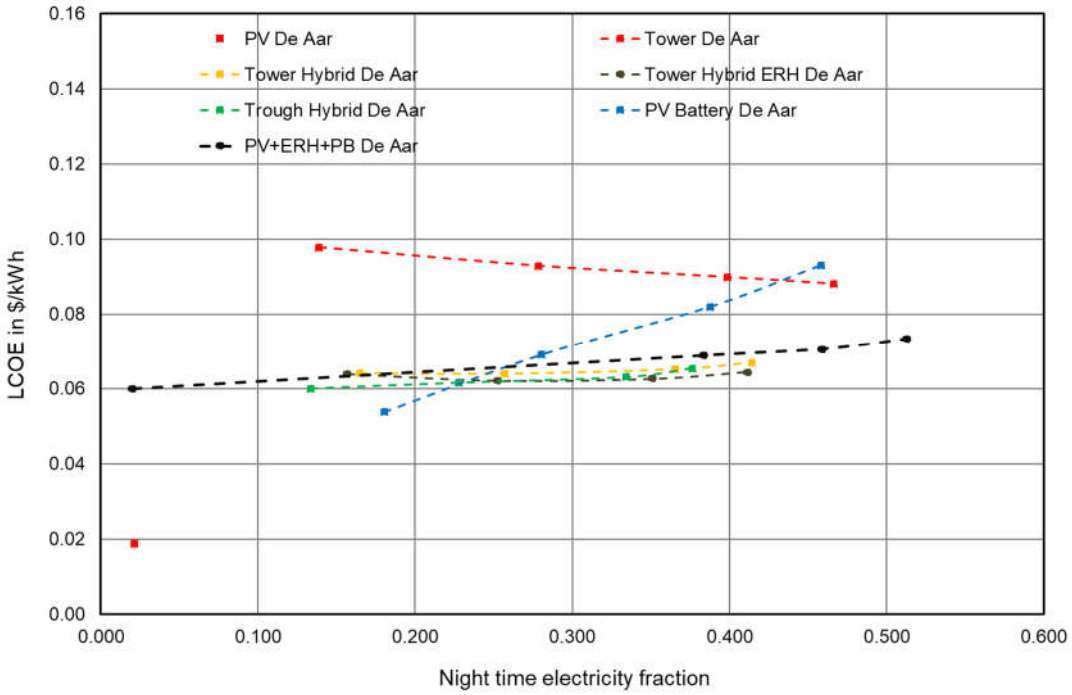

Figure 27: LCOE for optimized plants for De Aar

Figure 28 shows the results for PSA in Spain. We can see a general increase in costs mainly due to lower overall radiation. Standalone tower plant exceeds 10 cents for all storage sizes and the hybrid plants exceed 7 cents. There is also a general decrease in electricity delivered at night.

The outstanding high radiation values at Diego de Almagro, in Chile, lead to impressive results for all technologies being the site with the lowest costs for all of them, as shown in Figure 29. This is especially noticeable for technologies incorporating CSP due to the extremely high DNI values. This is the only site where costs are below 6 cents for hybrid systems and below 8 cents for the standalone tower.

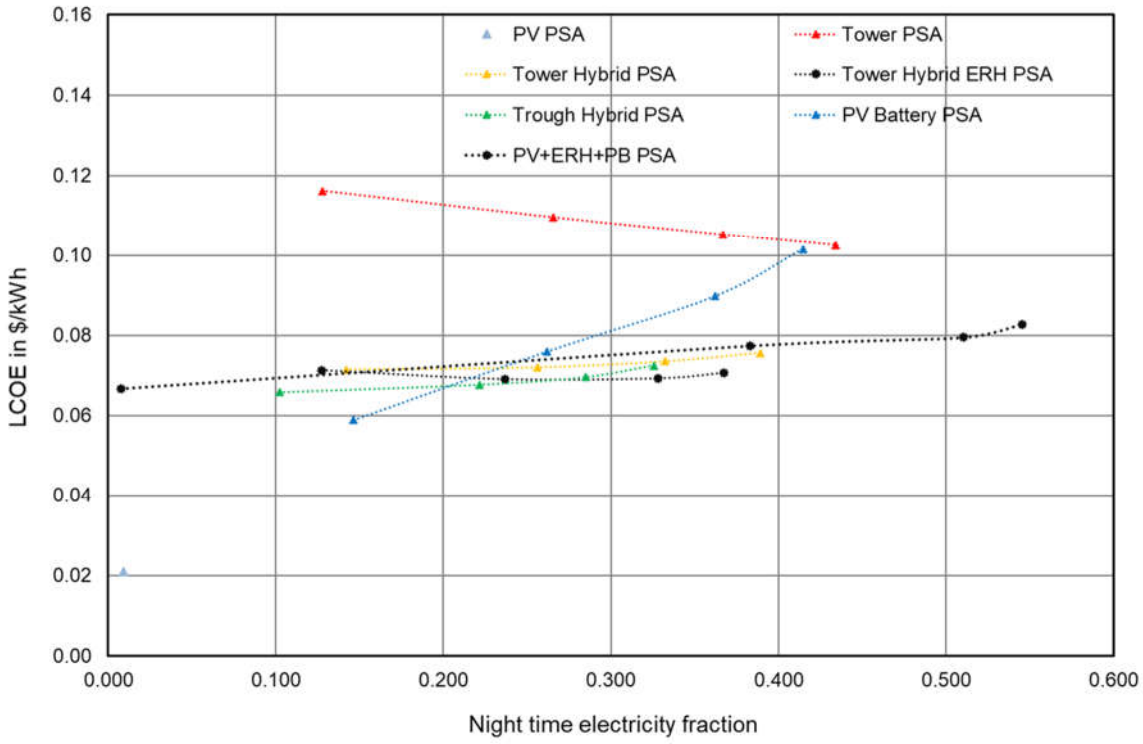

Figure 28: LCOE for optimized plants for PSA

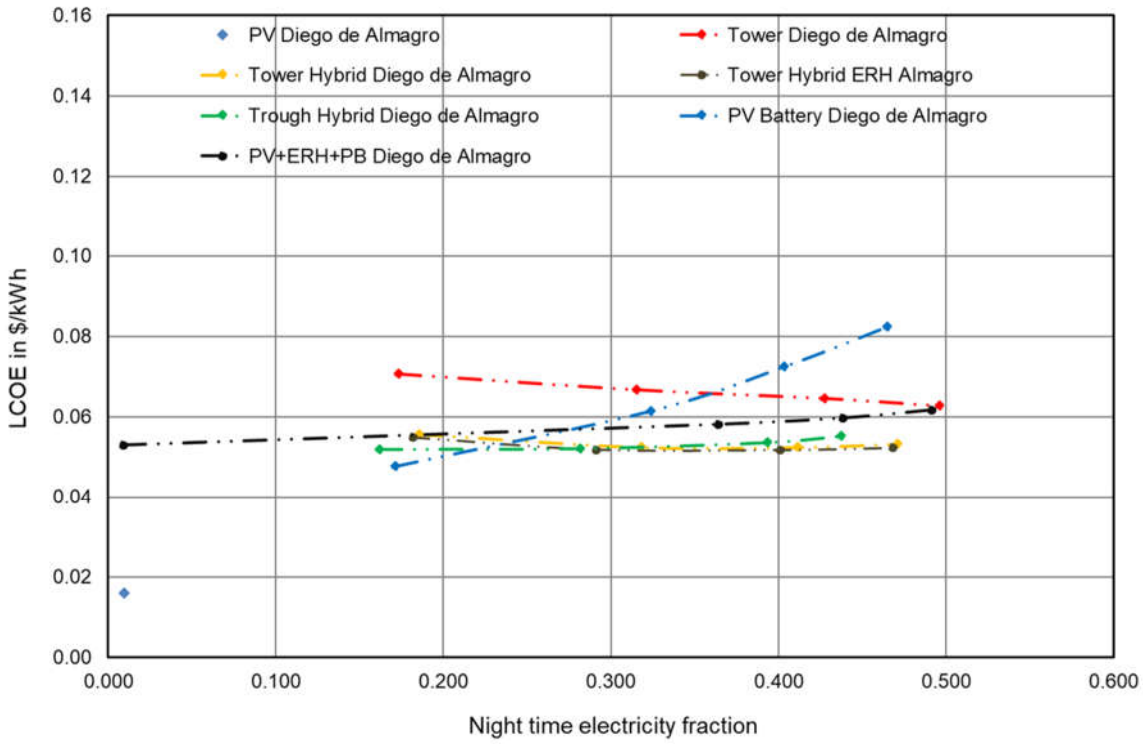

Figure 29: LCOE for optimized plants for Diego de Almagro

A similar trend to the other sites can be observed in Daggett, USA, in Figure 30.

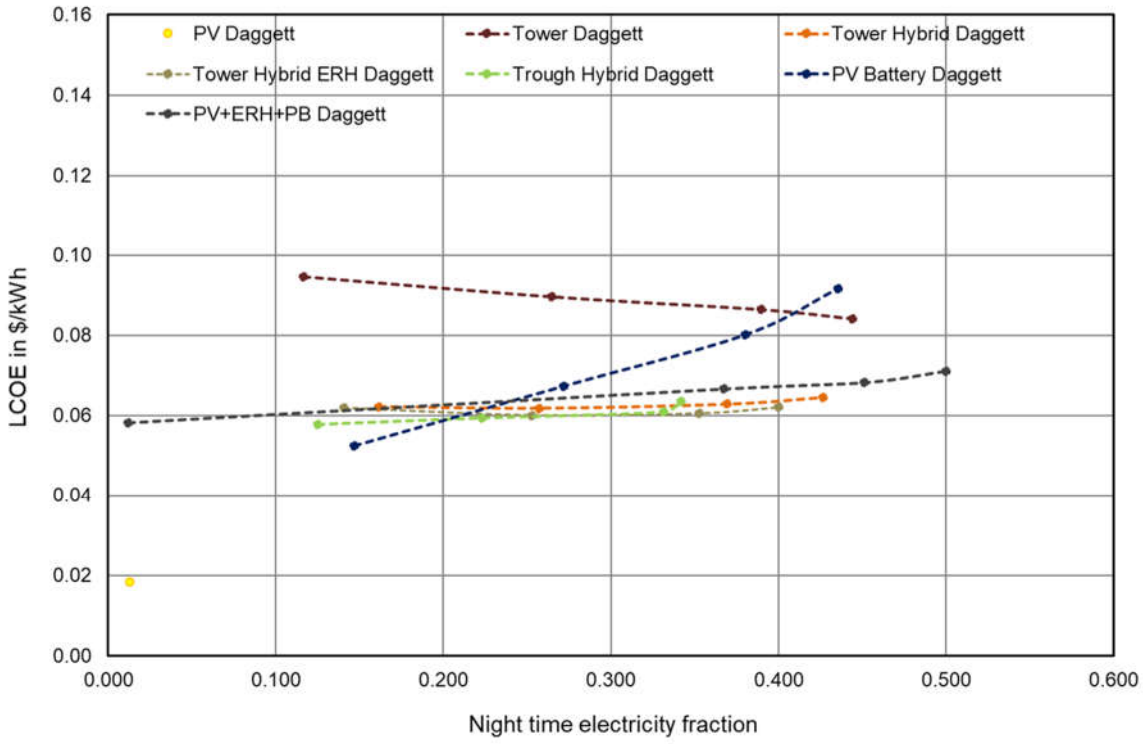

Figure 30: LCOE for optimized plants for Daggett

This trend is repeated for Ouarzazate, Morocco, in Figure 31.

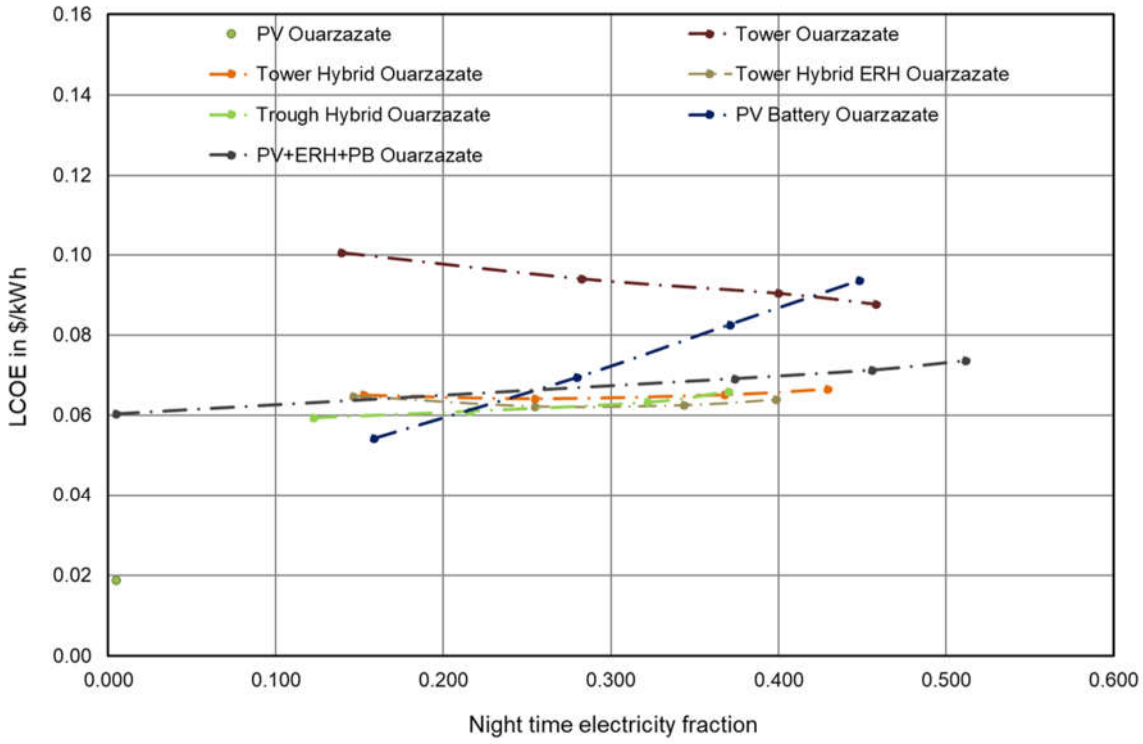

Figure 31: LCOE for optimized plants for Ouarzazate

Figure 32 shows the results for Dunhuang, in China, the site with the lowest radiation values investigated in this study. This causes higher LCOEs for all technologies. Hybrid parabolic trough plants show particularly low night fraction fractions. It only reaches 5% for a 3h storage and 26% for a 12h storage. This is because the optimization results in a very small CSP field due to the low DNI. In the case of the hybrid tower system, such a small field is not reached in the optimization but this is caused primarily by the minimum CSP size of 200 MW defined for this technology.

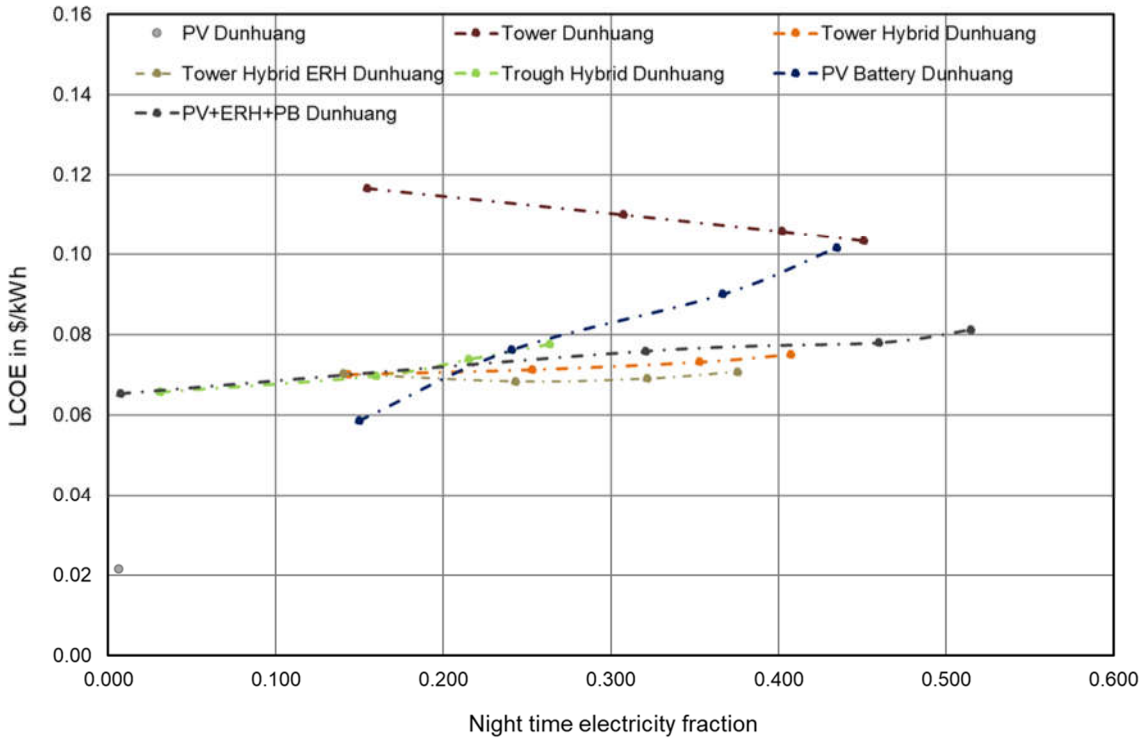

Figure 32: LCOE for optimized plants for Dunhuang

9.2.1. Comparison for each technology

All technologies were compared for all sites to properly assess the impact of the location. Figure 21, Figure 22, Figure 25 and Figure 26 are useful for this analysis.

Figure 33 shows the tower LCOEs for each site. The order in which the curves are placed corresponds to the magnitude of the DNI values. The site with the lowest DNI is represented by the upper line and the site with the highest radiation by the lower line. PSA has a worse LCOE than expected considering its DNI value. This is due to the higher latitude of this site, which limits its performance in winter to a greater extent (Table 2). Even having an annual DNI similar to Riyadh, the more pronounced seasonal differences imply a higher LCOE due to the lower efficiency of the CSP field. There is also a slightly higher LCOE than expected for De Aar with CSP technologies. This is mainly due to the intercept heat which must be dumped to protect the receiver. As shown in Figure 25, DNI exceeds 1000 W/m^2 several hours, which causes greater dumping, increasing the LCOE. This explains why, despite having an annual DNI similar to Daggett, the LCOE is higher. The results at Diego de Almagro are outstanding despite the dumping for exceeding the maximum absorbable radiation during many hours, while the LCOEs at Dunhuang and PSA exceed those from the other sites by almost two cents. Most sites have

values between 8 and 10 cents per kWh. This is a big difference with respect to hybrid power plants. There are no significant differences in the night-time fraction.

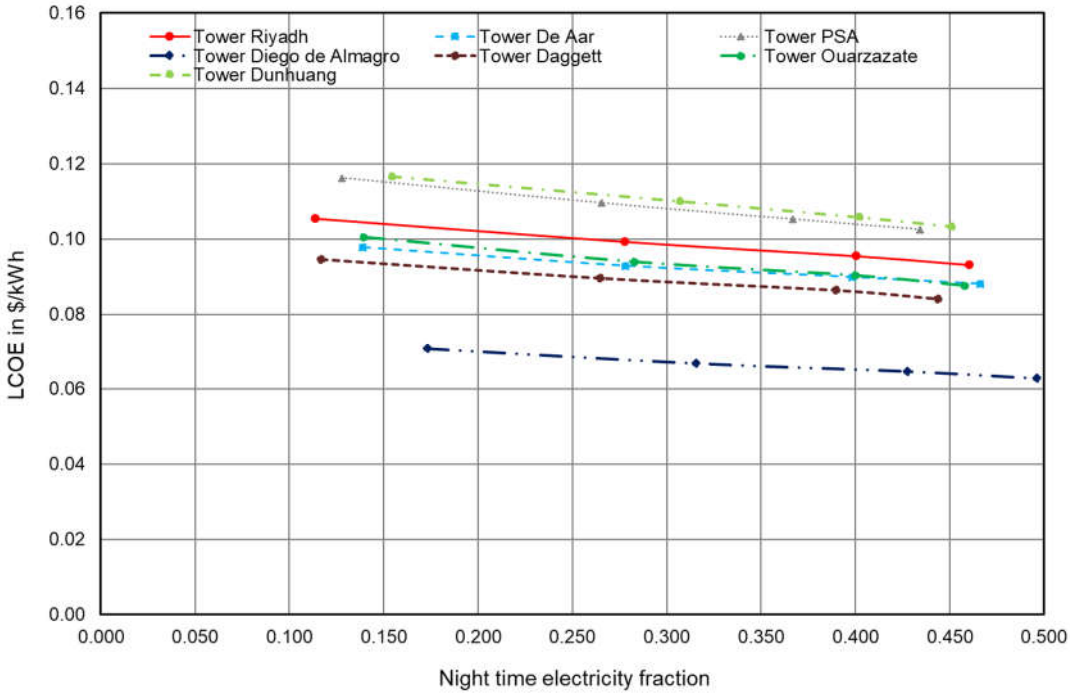

Figure 33: Comparison of Locations – Central Receiver Tower standalone

The positions in which the hybrid tower curves are arranged can be explained with the irradiance values. For larger storage capacities there is a greater dependency on DNI due to the larger size of the CSP field in comparison to the PV field size as can be seen in Table 11. The synergies between the two types of technologies also have an important impact on the arrangement. The LCOE advantage for Diego de Almagro is not as big as for the standalone tower (it is no longer two cents) but still significant. The hybridization causes a significant overall decrease in costs compared to the standalone CSP systems.

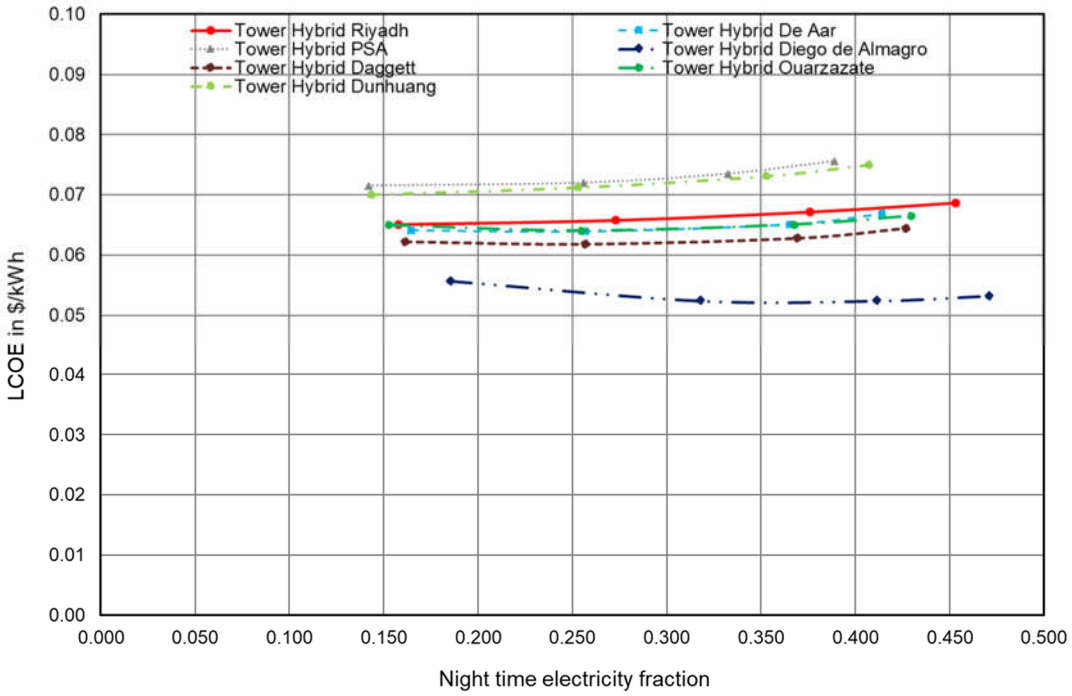

Figure 34: *Comparison of Locations* – Tower hybrid without EH

With the incorporation of an electric heater, as shown in Figure 35, there is similar dependency on the solar resource as without electric heater. It is interesting to observe how the DNI continues to have more weight than the GHI in the arrangement of the curves, even though the PV field is larger than the CSP field for greater storage capacities.

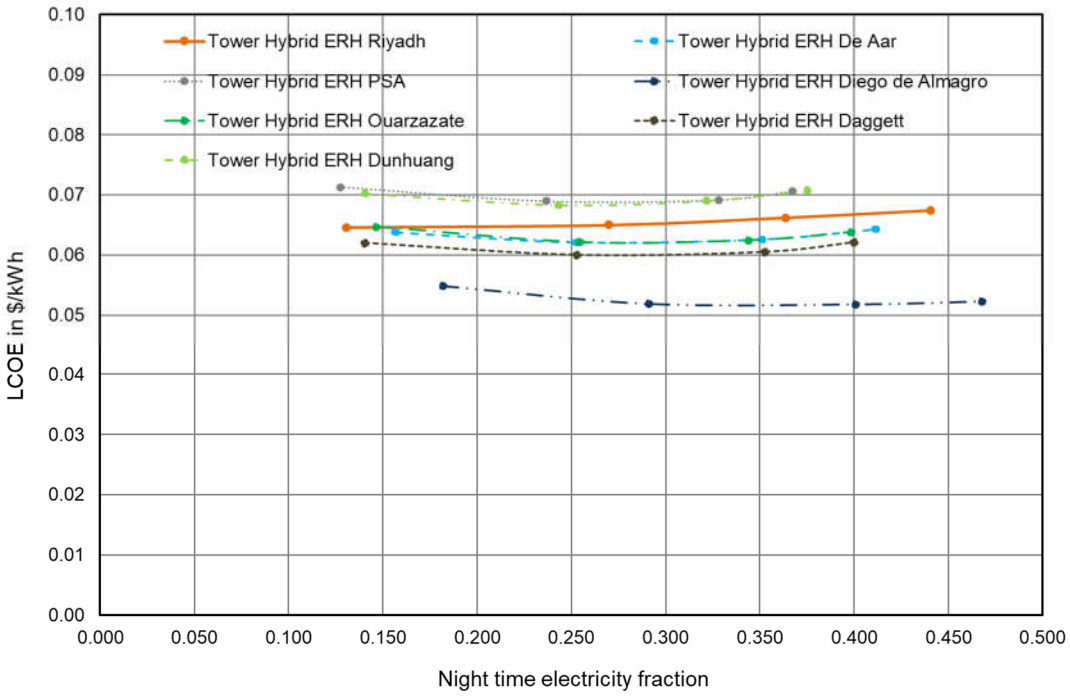

Figure 35: Comparison of Locations – Tower hybrid with EH

The same dependence on solar resource can be observed for trough hybrid plants in Figure 36. There is a slight increase in costs as the storage capacity increases because of the higher component costs and dumping. Also note that the night-time fraction is higher for Riyadh and Diego de Almagro due to the greater proximity to the equator. Parabolic troughs suffer from low sun angles and sites close to the equator show less differences in sun angles between summer and winter. Furthermore, day length is also rather constant compared to sites with higher latitudes. This is an advantage for storage charging and discharging which is less perfect for sites with more pronounced seasons and short days in winter. For all sites, LCOE is below 8 cents per kwh. Due to the larger PV field, GHI increases its influence compared to the DNI. PSA clearly shows lower LCOE values than Dunhuang because of the higher GHI. Riyadh, the site with the second highest GHI, also displays a clear improvement with this technology showing lower LCOE than Ouarzazate and De Aar for large storages.

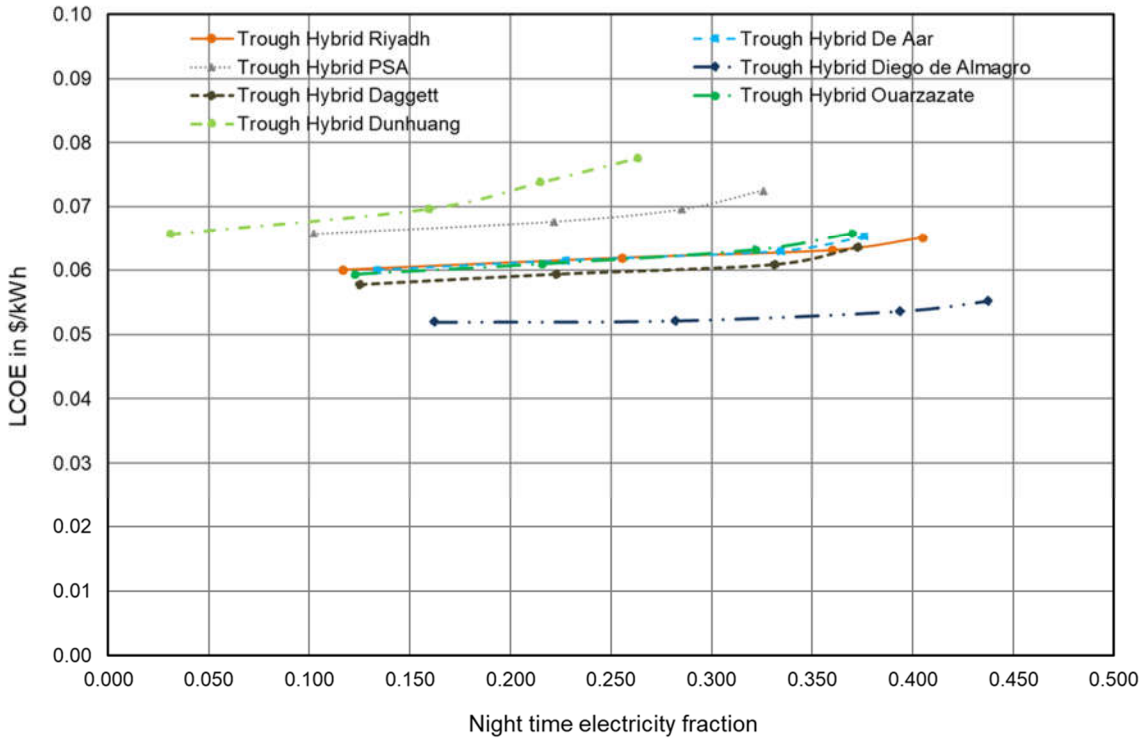

Figure 36: Comparison of Locations – *Trough Hybrid*

Figure 37 shows again the dependence on solar radiation, in this case for the PV system with battery. Very similar values for the De Aar, Riyadh, Ouarzazate and Daggett sites. Similar upward trend for all locations because of the battery costs.

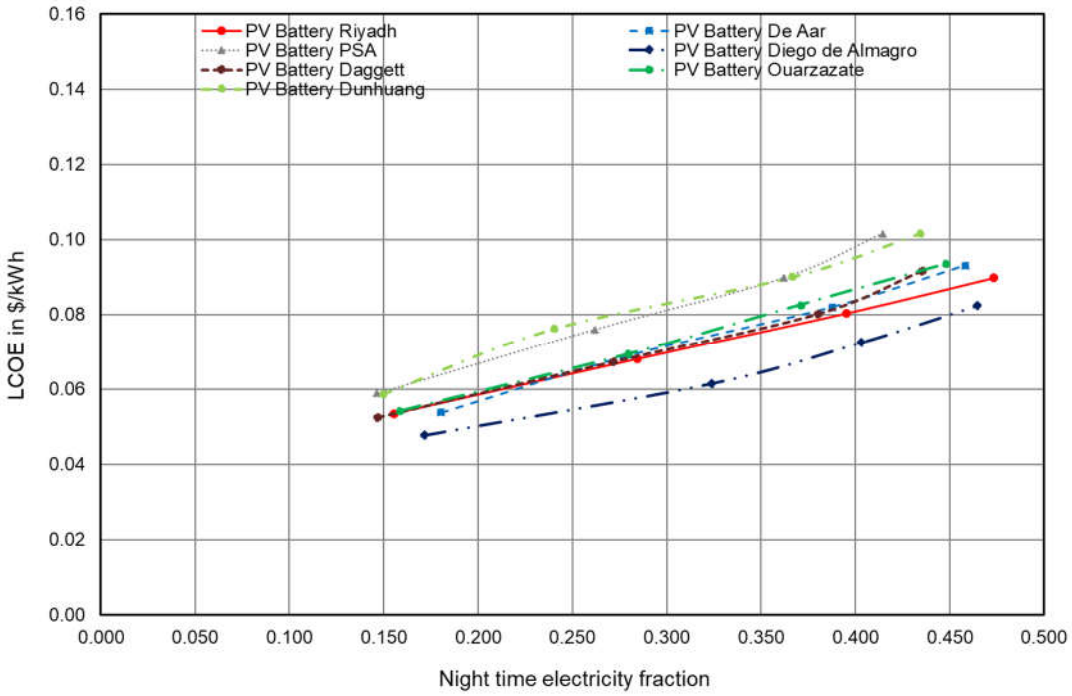

Figure 37: Comparison of Locations – PV Battery

The PV+ERH+PB systems shows some similar effects as PV-BESS system. The higher impact of the GHI causes a lower LCOE and higher night fraction in Riyadh in comparison to other technologies. The meteorological effects in Daggett reduce the LCOE even though the lower GHI values. Diego de Almagro remains the most economic site and the difference between PSA and Dunhuang is very small despite the higher radiation in the Spanish location.

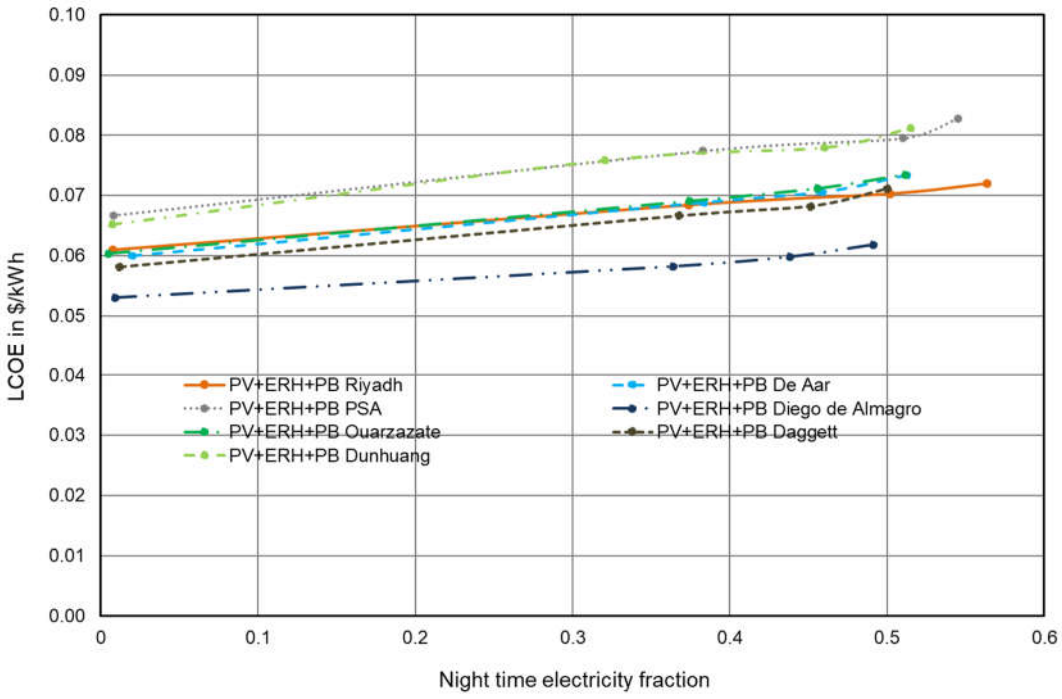

Figure 38: Comparison of Locations – PV+ERH+PB

9.3. Financial Sensitivity Analysis

9.3.1. Variation electric heater costs

Due to the uncertainty at the beginning of the project regarding the costs of the electric heater, a cost variation was performed to reliably determine its impact on the LCOE. It was proven that this cost had a significant influence on the final techno-economic analysis. The price of the heater greatly determines the final design of the hybrid power plants.

Figure 39 shows the results of varying the price of the heater from 278 $/kW (solid line) to 140 $/kW (dashed line), 100 $/kW (dash-dotted line) and 70 $/kW (dotted line). This cost reduction implies a drop in LCOE in the order of one cent per kW in the PV+EH+PB system with OS1. For tower power plants, it makes the difference between an electric heater being worth the investment or not. For a cost of 278 $/kW there is no difference whether a heater is introduced or not, but if the cost is 70 $/kW the difference reaches one cent per kW. A similar order of magnitude is observed for the hybrid parabolic power plant. This cost reduction would also mean a significant shift to the left of the cut-off point with the battery PV system.

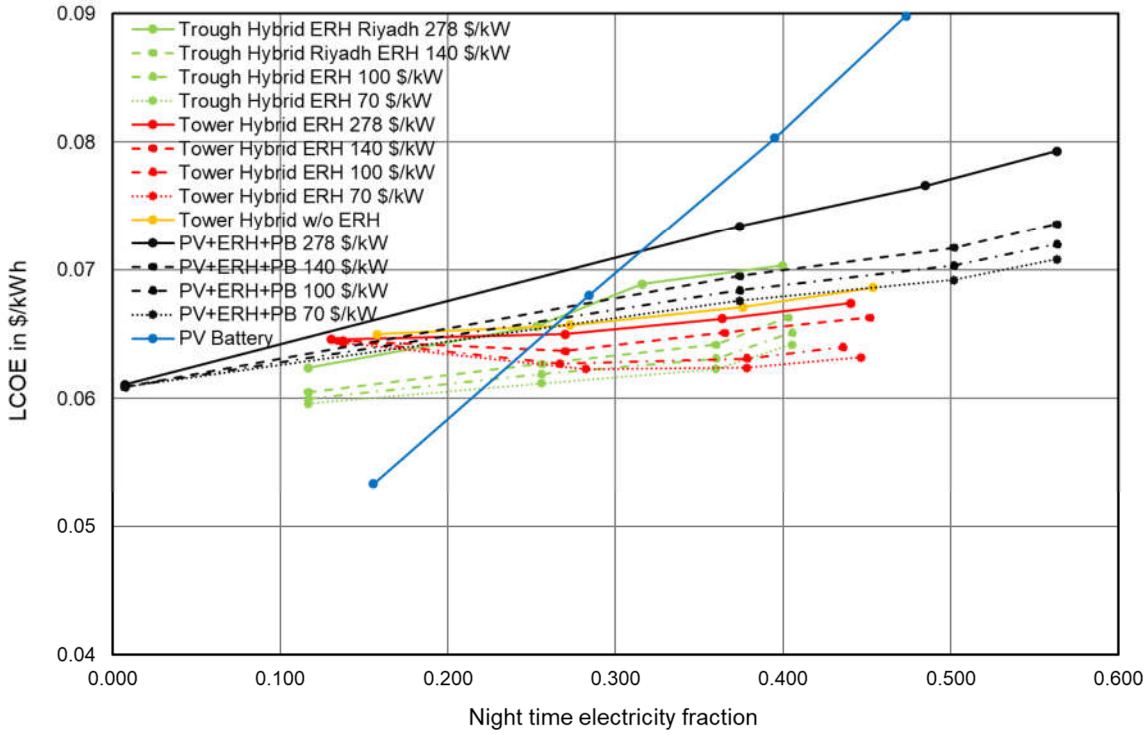

Figure 39: Variation ERH costs Riyadh alt

9.3.2. Variation of PV cost

The figure below shows the impact of increased and reduced cost assumptions for the PV component. A range from +20% until -40% of cost assumption related to the base assumptions as presented in section 4 was selected. This range reflects long term market expectations from the PV and BESS sector (before 2020) as well as current observations from the raw material and energy crisis currently negatively affecting the PV and BESS industry (in 2021 and 2022). All other cost assumptions are kept constant. Only the central topologies (PT hybrid, CRT hybrid, PV-P2H and PV-

BESS) are considered for the sensitivity analysis. The diagram shows clearly that the PV cost strongly affects the LCOE but does not change the proportion of the pareto fronts. This can easily be explained: all presented topologies depend strongly on PV for the direct electricity generation and all cases require PV energy to fill up their energy storages. Changing the PV cost therefore does not change the overall observations on suitability of topologies for specific use cases.

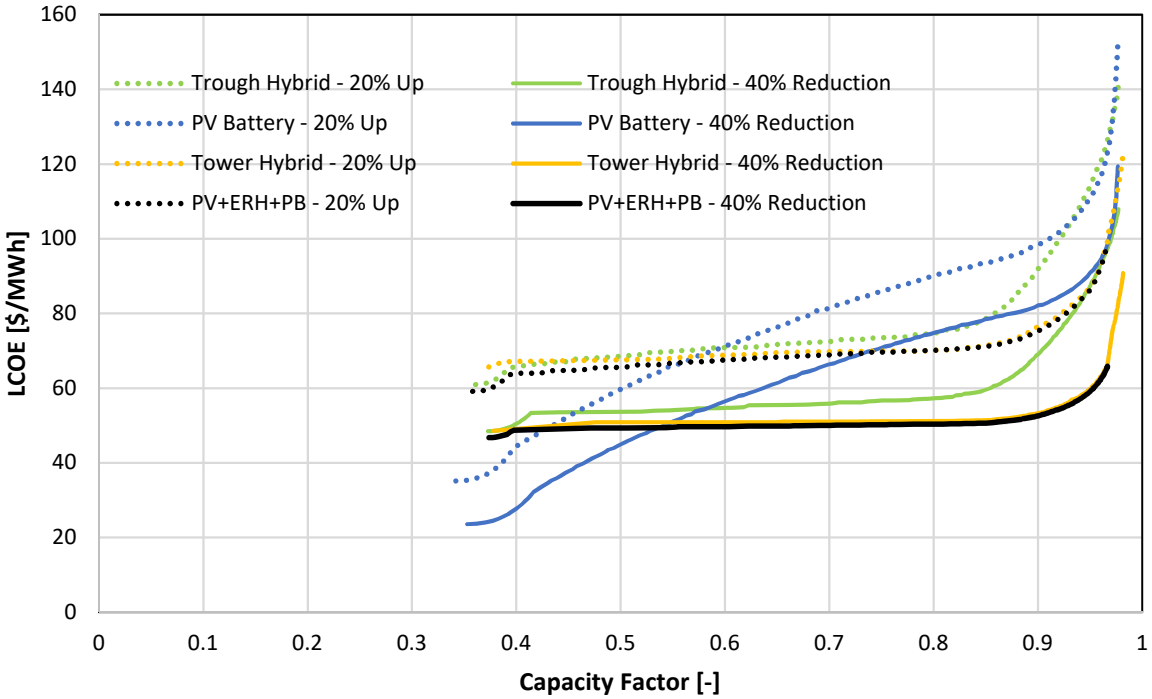

Figure 40: Sensitivity Analysis - Variation of PV cost (Riyadh HYPPO results)

9.3.3. Variation of BESS cost

The same cases are observed as before, but this time only the BESS cost assumptions are changed. It is clear that topologies using thermal energy storages are not affected. For the PV-BESS topology the BESS cost sensitivity has an impact on the pareto front's gradient: increased BESS cost lead to a steeper LCOE curve making BESS as energy storage practically useless for longer storage durations. Significantly reducing the BESS cost, however, could make BESS the only reasonable choice even for extreme capacity factors. BESS has very high storage efficiencies compared to thermal energy storages. This leads to a high sensitivity to the BESS investment cost. As long as BESS cost projections are unstable, choosing a TES in combination with CSP direct heat generation or P2H applications could be a more reliable choice.

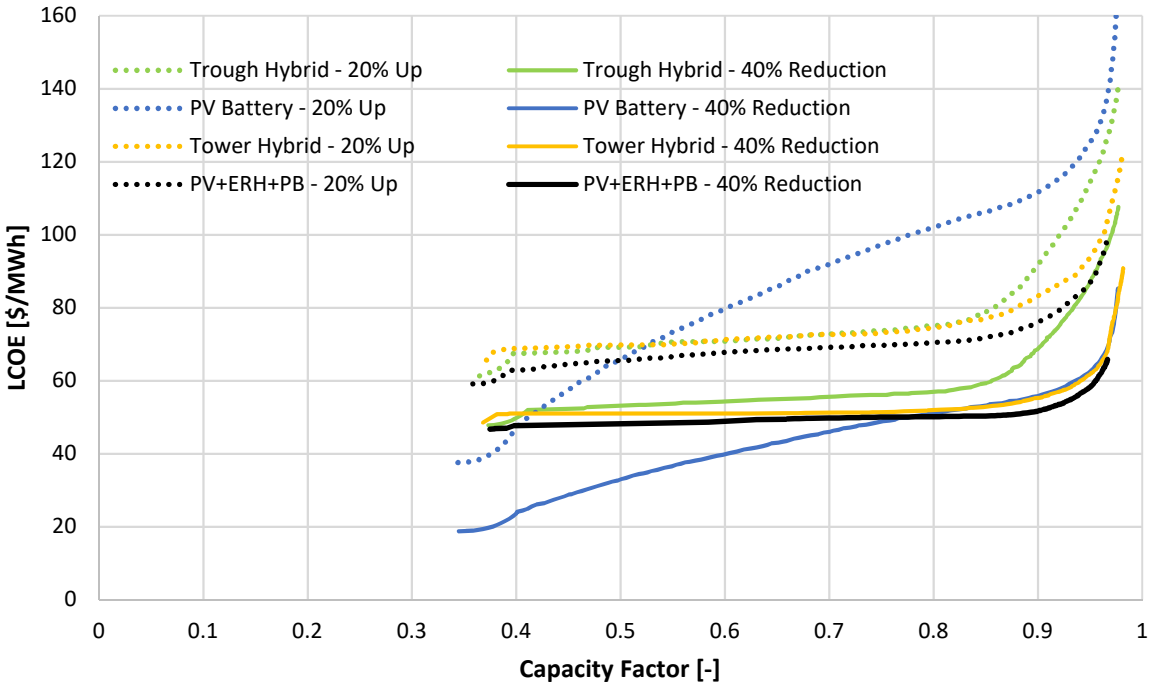

Figure 41: Sensitivity Analysis - Variation of BESS cost (Riyadh HYPPO results)

9.3.4. Variation of combined PV and BESS cost

If both cost assumptions – for PV and BESS – are varied in the same ranges as before, the full potential of cost reductions and at the same time the full sensitivity of results becomes visible. All topologies could reach LCOE values of below 55$/MWh over the whole (reasonable) range of capacity factors. PV-BESS systems could lead to even lower LCOEs between 20 and 50 $/MWh for CF-values between 35 and 80% respectively. At the same time PV-BESS systems are affected strongest by price increases limiting their feasibility easily for CFs higher than 50% for cost increase scenarios.

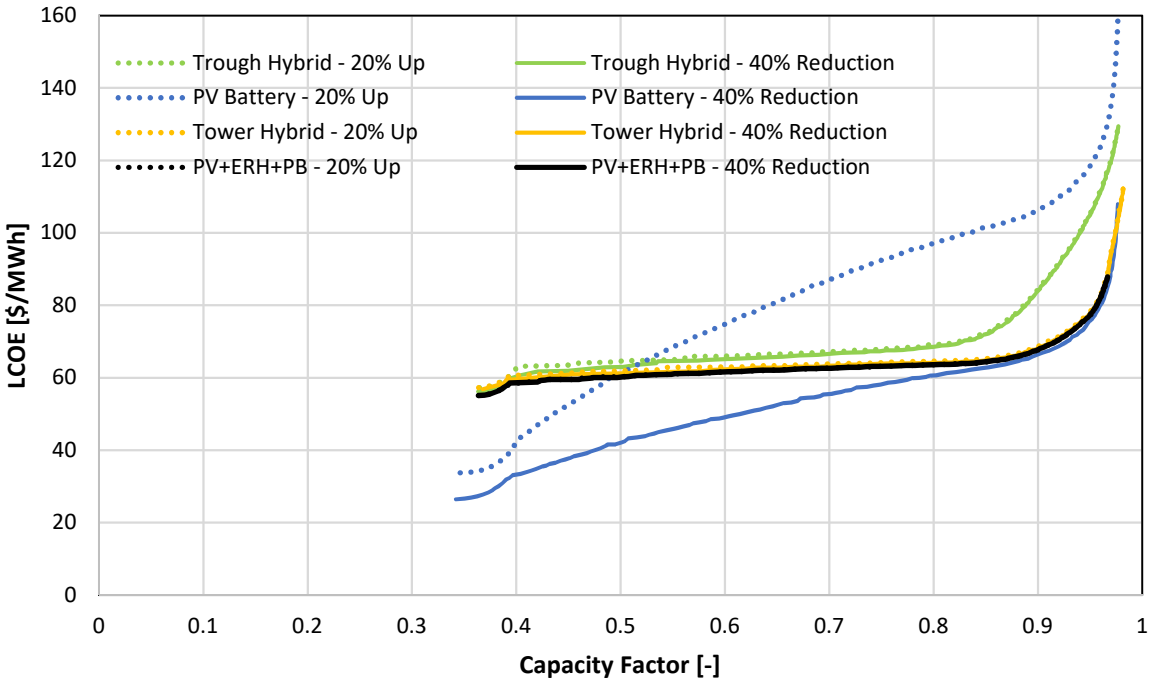

Figure 42: Sensitivity Analysis - Variation of combined PV and BESS cost (Riyadh HYPPO results)

9.3.5. Variation of tower cost

The specific costs per meter of the tower were varied from 88000 $/m to 68400 $/m for the standalone tower and the hybrid tower systems. The LCOE values showed little difference with the new assumed cost. Hence, it is not one of the most relevant costs in the economic evaluation.

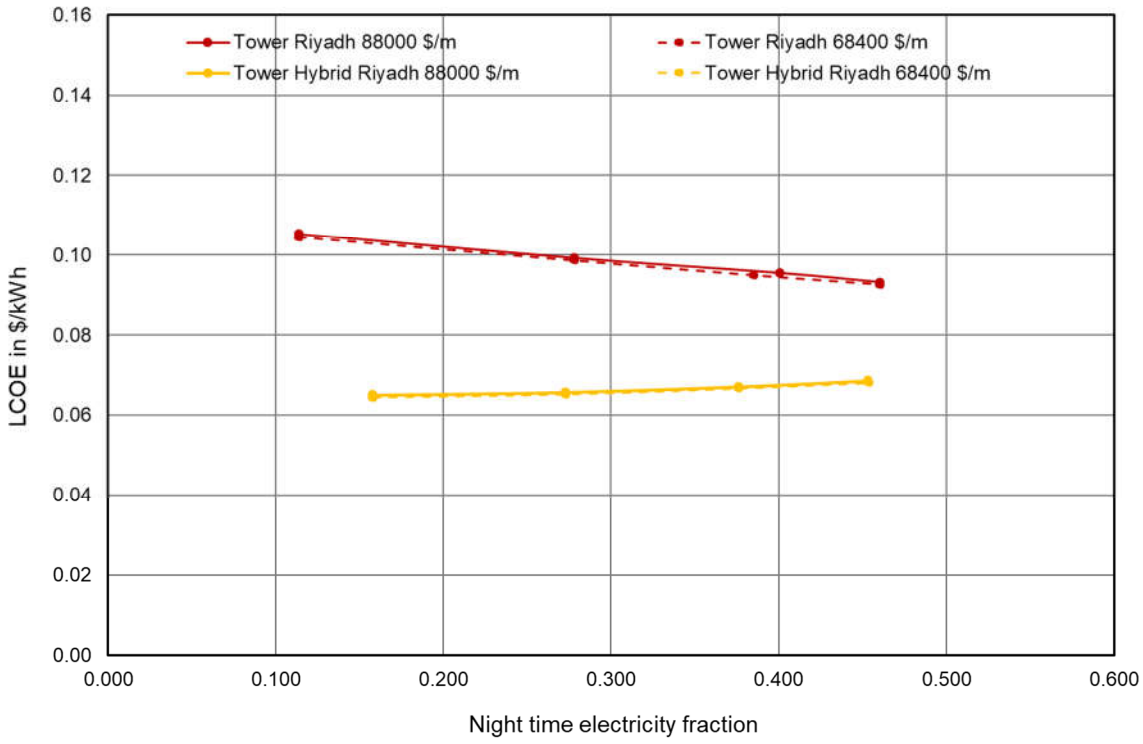

Figure 43: Sensitivity Analysis - Variation of tower cost (Riyadh greenius results)

9.3.6. Variation of project lifetime

The following sensitivity analysis is done based on the hypothesis that CSP plants could have a significantly longer operational lifetime than PV and BESS plants. This is based on the experience of first generation CSP plants already under operation for 30 years and the assumption that lifetime can be further extended with today's market standards for CSP. The power block could, with proper maintenance be operated for 40 years, the CSP solar fields could be maintained with proper O&M measures for 40 years, allowing some additional degradation (reduced reflectivity of mirrors, lost vacuum in receiver tubes). PV modules can be operated for 30 years and eventually longer (double-glass monofacial modules), but BESS have to be replaced after 12 to 15 years.

For this analysis it was assumed that the hybrid CSP plants will be operated for 40 years before decommissioning and the PV-BESS topology will be decommissioned after only 25 years. As a reference case the stand-alone PT plant is displayed in order to show the effect of extending the lifetime on the LCOE for a single topology. This extension of lifetime can lead to a 15% reduction in LCOE.

The main impact of this hypothesis analysed here is the change in break-even points between PV-BESS and the CSP hybrids, going down from 55 and 58% CF to 47 and 50% CF respectively. This means

there could be a certain additional potential for the CSP systems using some technological benefits to improve their electricity costs compared to PV and BESS technologies.

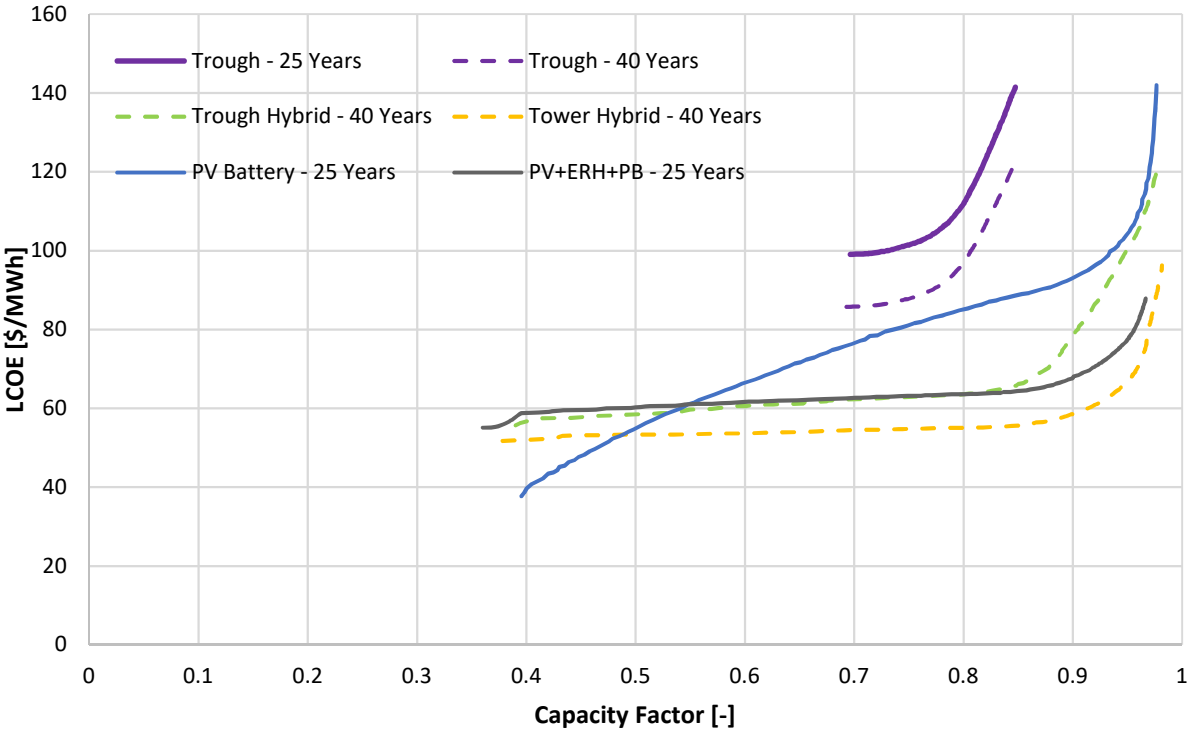

Figure 44: Operational Lifetime Sensitivity - longer CSP life hypothesis (Riyadh HYPPO results)

9.3.7. Variation of electricity from grid price

The influence of the grid electricity price on LCOE was determined for 3 different technologies comparing the costs with a price of 0.15 $/kWh and free electricity. It was observed that the LCOE sensitivity on this cost is very small. The synergies produced in the hybrid plants make the purchase of external electricity practically unnecessary. In the case of the standalone tower, it is necessary to cover the auxiliary demand, but even so, it does not modify the LCOE beyond 1.23%. The hybrid tower needs more electricity from the grid than the hybrid trough. This is due to the constant need of the tower throughout the day. The parabolic trough field has almost no need during the night and the freeze protection is seldom active. Thus, the influence of the grid electricity price on the LCOE is practically negligible.

Table 12: Grid electricity priceSensitivity - Hybrid trough

HYBRID TROUGH						
PV field size [MW]	Electric heater nom. power [MW]	CSP field nom. power [MW]	Storage net capacity [h]	LCOE [$/kWhe]	LCOE [$/kWhe]	Difference [%]
Electricity from the grid				**0.15 $/kWhe**	**0 $/kWhe**	
250	80	43	3	0.0600	0.0600	0.00
350	160	87	6	0.0619	0.0619	0.00
400	230	130	9	0.0631	0.0631	0.00
450	290	152	12	0.0651	0.0651	0.00

Table 13: Grid electricity price Sensitivity - Hybrid tower

HYBRID TOWER					
PV field size [MW]	CSP field nom. power [MW]	Storage net capacity [h]	LCOE [$/kWhe]	LCOE [$/kWhe]	Difference [%]
Electricity from the grid			**0.15 $/kWhe**	**0 $/kWhe**	
200	200	3	0.0652	0.0648	0.61
200	300	6	0.0658	0.0656	0.30
200	450	9	0.0672	0.0671	0.15
200	600	12	0.0686	0.0685	0.15

Table 14: Grid electricity price Sensitivity - Tower standalone

TOWER STANDALONE				
CSP field nom. power [MW]	Storage net capacity [h]	LCOE [$/kWhe]	LCOE [$/kWhe]	Difference [%]
Electricity from the grid		**0.15 $/kWhe**	**0 $/kWhe**	
650	3	0.1061	0.1048	1.23
850	6	0.0998	0.0989	0.90
1050	9	0.0958	0.0952	0.63
1150	12	0.0934	0.0929	0.54

9.4. Analysis of different technical aspects

9.4.1. Direct Calculation of the Heat Generation Cost

Although heat production is not the final target, it is an interesting parameter to compare the systems. Furthermore, the question whether the heat production by a CSP field or a PV field and a electric heater will be cheaper arises when dealing with these systems. Levelized cost of heat (LCOH) was calculated for this comparison of technologies. Note that these costs are only approximate values due to the problem of allocating component costs to either day or night production.

The optimized size of the 6h storage systems was used for this calculation (except for PV). The systems are a 150 MW_{AC} PV field (optimized PV system without battery), a 978 MW parabolic trough system (optimized standalone trough) and a 300 MW central receiver (optimized size of the tower of a hybrid system without electric heater). Note that the tower heat production costs can still be reduced a bit with a larger system, but we are mainly interested in comparing hybrid systems heat production costs with those from PV with an electric heater. The calculations presented in Table 15 to Table 17 are solely based on design parameters and component cost assumptions, except for the annual heat output, which is taken from greenius simulations for Riyadh. Therefore, this input value is marked by a green background.

Table 15: Calculation of heat production costs for 150 MWAC PV system with electric heater

Component	**PV field**	**Inverter**	**Electrical heater**	**Overall plant**	Unit
Nominal power	195636	150000	150000		kW
Spec. costs	454	53	100		$/kW
Spec. O&M costs	0.5	0.5	0.5		%/a
Surcharge EPC	10	10	20		%
Total costs	97,700,618	8,745,000	18,000,000	124,445,618	$
Annual O&M costs	488,503	43,725	90,000	622,228	$/a
Interest rate				0.05	
Lifetime				25	a
Annual heat output				438410	MWh/a
Annuity				0.0710	
LCOH PV & E-Heater				**0.0216**	**$/kWh**

Table 16: Calculation of heat production costs for 300 MW tower system

Component	**Molten salt tower plant**			**Overall plant**	
Nom. Receiver power	304170.4			304170.4	kW
Spec. Costs receiver	122			122	$/kW
Aperture area	514,836			514836	m²
Spec. Costs SF	127			127	$/m²
Total costs tower	14,080,000			14080000	
Spec. O&M costs	1.5			1.5	%/a
Surcharge EPC	20			20	%
Total costs	139,887,553			139,887,553	$
Annual O&M costs	2,098,313			2,098,313	$/a
Interest rate				0.05	
Lifetime				25	a
Annual heat output				540007	MWh/a
Annuity				0.0710	
LCOH Tower system				**0.0223**	**$/kWh_th**

Table 17. Calculation of heat production cost for 978 MW parabolic trough system

Component	**Parabolic trough field**			**Overall plant**	
Nominal power	978029			978029	kW
Aperture area	1544400			1544400	m²
Spec. costs	202			202	$/m²
Spec. O&M costs	1.5			1.5	%/a
Surcharge EPC	20			20	%
Total costs	374,362,560			374,362,560	$
Annual O&M costs	5,615,438			5,615,438	$/a
Interest rate				0.05	
Lifetime				25	a
Annual heat output				2032247	MWh_th/a
Annuity				0.0710	
LCOH Parabolic trough field				**0.0158**	**$/kWh_th**

Table 15 and Table 16 indicate that central receiver plants (LCOH 0.0223 $/kWh) present higher heat production costs than PV with the electric heater (LCOH 0.0216 $/kWh). However, the differences are small and very sensitive to the costs assumed. Depending on the storage capacity this difference can be increased, reduced, or even reversed. Nevertheless, this finding is of great importance and influences the results shown in other chapters in which the LCOE is compared.

Although the parabolic trough system can generate the cheapest heat, as shown in Table 17, it does it at a lower temperature level and consequently has disadvantages in terms of storage costs and conversion efficiency to electricity. Depending on the general characteristics of the plant, the costs can be above or below other systems.

In any case, it can be seen how the 3 technologies present very similar heat generation costs. There is however a strong dependence on the assumed costs. In this approximate calculation, the PV system with electric heater shows slightly lower costs. As shown in the results sections 9.1 and 9.2, the lower heat generation costs also mean lower electricity generation costs for the different technologies and are an essential factor for the comparison of technologies.

9.4.2. Projections 2030

An interesting aspect to consider (though hard to determine) are cost projections for the future. There was active discussion about the cost values to be taken in the simulations for 2030. The costs of the components are continuously evolving depending on numerous factors and there are uncertainties in estimating their future values. Nevertheless, the values shown in Table 1 were assumed and the simulation of the different systems for Riyadh was performed.

The PV and BESS markets are currently (2022) in a crisis that has multiple causes with a general raw material shortage, high demands for renewable energy technologies, shortages in logistic capacities being only a few examples. The projection of costs for 2030 therefore has to be balanced between conservative cost assumptions reflecting the current crisis, while allowing some optimism for market growth and potential cost reduction that can be expected as a result. The presented results are based on cost assumptions that are balanced between both extremes considering cost development forecasts from before the crisis as well as current medium-term price increases specifically for PV and BESS components.

A general decrease in LCOE can be seen in Figure 38 for all technologies by 2030. It is interesting to note how the cut-off point of PV-BESS plants with hybrid plants shifts from the 4.5 - 5 hours of storage expected in 2021 to approximately 6 hours or more observed for 2030. PV+ERH+PB system slightly reduces its difference with hybrid plants due to the overall greater costs decrease by PV than by CSP components.

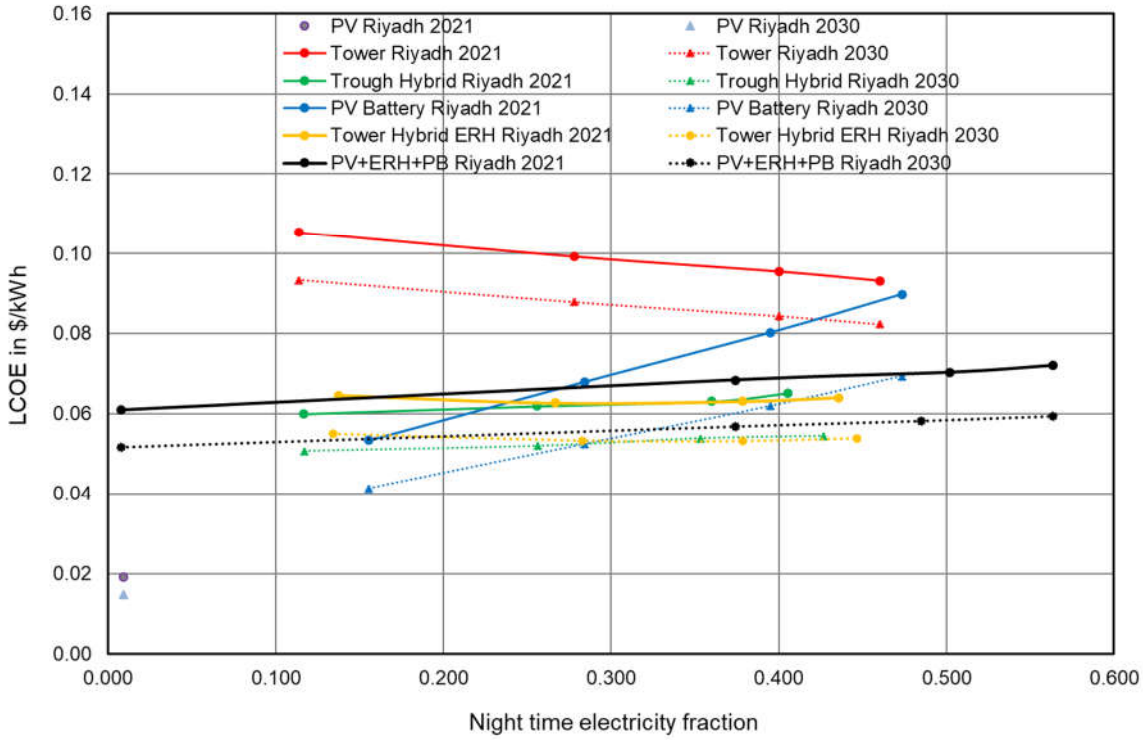

Figure 45: Results for 2021 component costs in comparison to 2030 cost projections for Riyadh

9.4.3. Seasonal analysis

A monthly analysis was conducted for the optimized systems with a storage capacity of 9 hours to see how seasonality affects different locations and technologies. The evaluation was carried out for two sites: PSA and Diego de Almagro.

Figure 46 and Figure 47 show the relative output for each technology in relation to the yearly output. Note that the site in Diego de Almagro is in the southern hemisphere, so it is summer there when it is winter in PSA.

There are no significant differences in the curves between locations. A slightly broader spectrum of results appears for PSA, aided by its greater latitude. The relative outputs are slightly higher in summer and lower in winter. With respect to the technologies, the differences are not significant too. In conclusion, the seasonal analysis shows a similar variability for all sites and technologies and explainable by site characteristics like irradiation, latitude and meteorological effects.

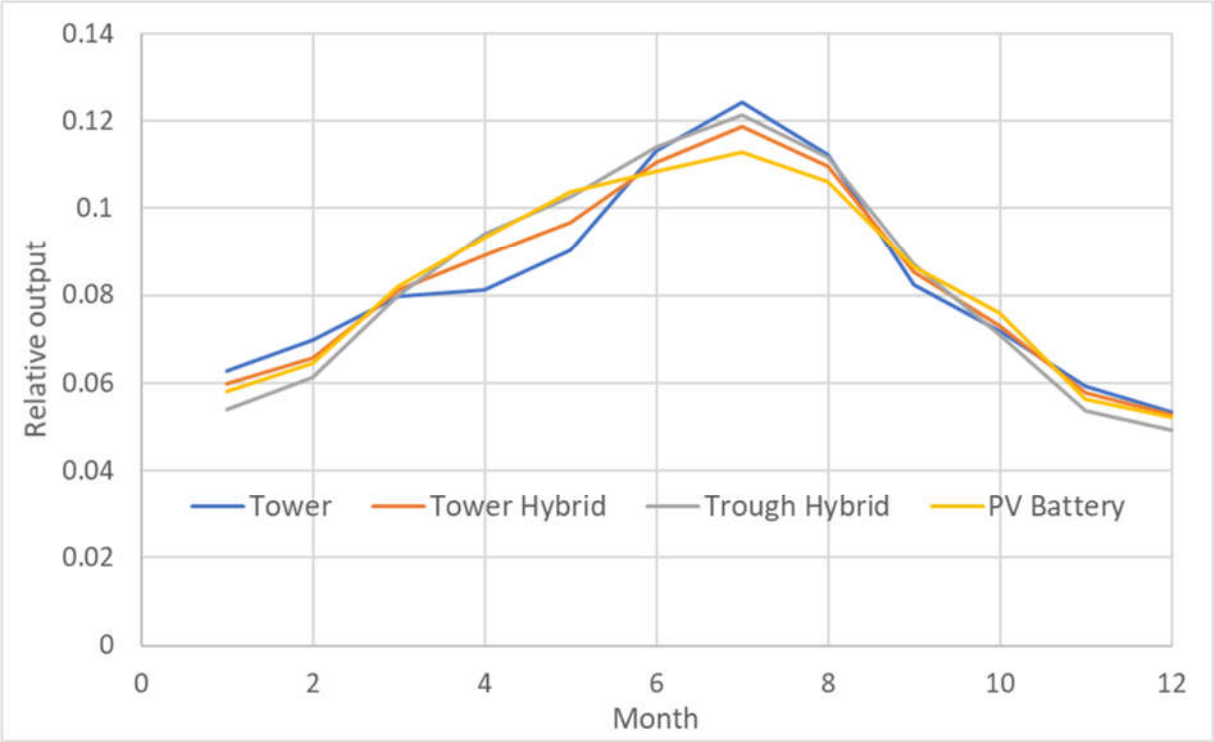

Figure 46: Seasonal analysis PSA

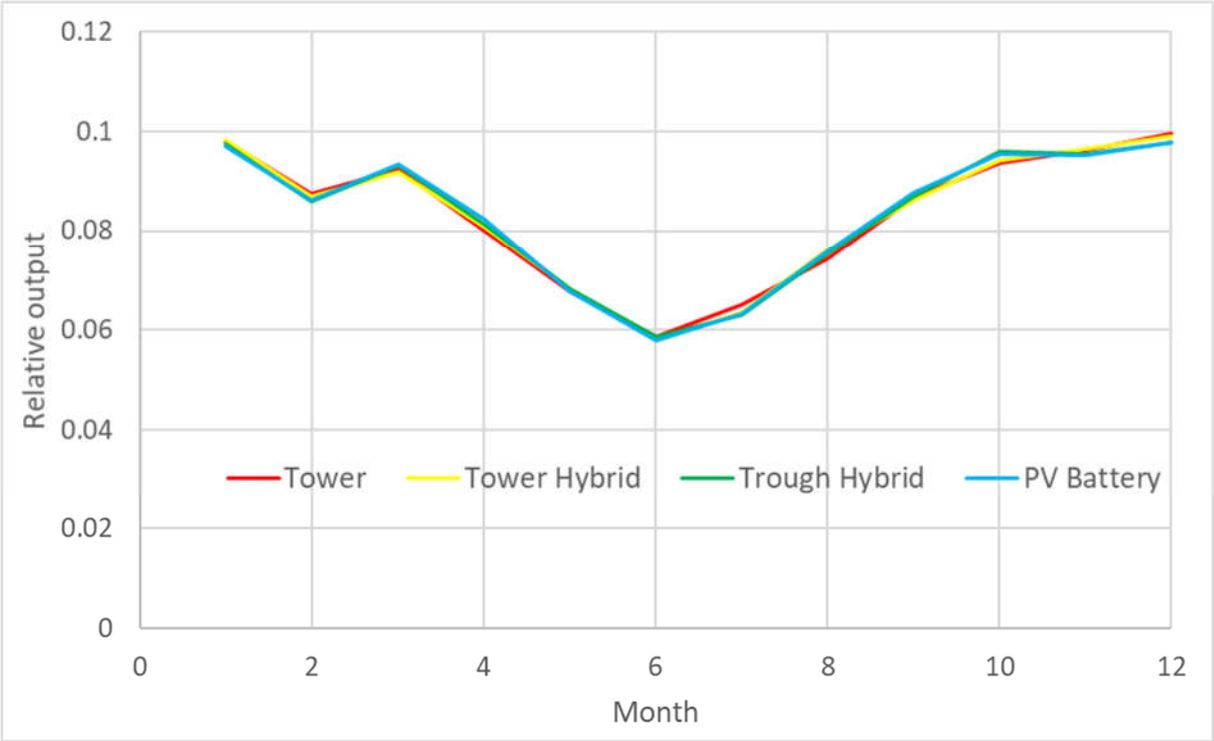

Figure 47: Seasonal analysis Diego de Almagro

9.4.4. Load-following Operation (Spain 2019)

A flat electricity demand curve might not be realistic for all sites and application cases. On the other hand, we do not want to base this study on a specific load curve, which might also be not representative for many sites. Therefore, we took the 2019 Spanish demand curve and simulated hybrid tower without electric heater and PV battery system for the PSA site. For each month, the average electricity demand was calculated for each hour. Taking 8:00 p.m. in January as the point of greatest demand, a load of 150 MW was assumed for this hour. For the rest of the hours, the load is proportional to the demand, scaled to 150 MW (equal to 100%).

This analysis is done as it can be expected for future developments that RE shares in national (or international) grids will reach values where RE generation will largely drive out dispatchable fossil generation. In that situation the RE generation will have to follow the load demand requiring dispatchable power generation especially during the night. To model such a situation, the solar hybrid plants must follow the general load demand, if all connected generators will follow the load in equal parts.

Table 18: Load curve Spain 2019 Monday - Friday

Working days (Mon-Fri) - normalized with the average maximum electricity demand of the working days																									
		Hour	Electricity demand																						
	Month	0	1	2	3	4	5	6	7	8	9	10	11	12	13	14	15	16	17	18	19	20	21	22	23	All
January	1	80%	74%	70%	67%	66%	65%	68%	74%	84%	91%	94%	97%	98%	98%	97%	95%	94%	93%	94%	98%	100%	98%	94%	89%	87%
February	2	75%	69%	65%	62%	61%	61%	62%	69%	78%	83%	87%	88%	89%	88%	87%	85%	84%	83%	82%	82%	84%	89%	87%	82%	78%
March	3	69%	64%	61%	59%	58%	58%	59%	64%	69%	74%	78%	80%	81%	81%	81%	80%	79%	78%	77%	76%	79%	82%	80%	75%	73%
April	4	68%	63%	60%	58%	57%	56%	57%	61%	68%	73%	76%	78%	79%	80%	79%	78%	77%	77%	76%	75%	74%	75%	77%	73%	71%
May	5	67%	63%	61%	59%	58%	57%	57%	61%	66%	71%	74%	77%	78%	79%	80%	79%	78%	77%	77%	76%	75%	75%	74%	72%	70%
June	6	71%	67%	64%	62%	61%	61%	61%	64%	69%	74%	79%	82%	83%	85%	86%	85%	84%	84%	84%	83%	81%	79%	77%	76%	75%
July	7	78%	74%	71%	68%	67%	66%	66%	69%	73%	78%	84%	89%	91%	93%	94%	94%	94%	93%	92%	91%	89%	87%	85%	84%	82%
August	8	75%	70%	67%	64%	63%	62%	62%	66%	68%	73%	79%	84%	87%	89%	89%	89%	88%	88%	87%	86%	84%	82%	82%	80%	78%
September	9	71%	67%	65%	62%	61%	61%	62%	67%	74%	76%	80%	84%	86%	88%	88%	87%	87%	87%	87%	86%	84%	84%	82%	78%	77%
October	10	68%	63%	61%	59%	58%	58%	59%	64%	70%	74%	77%	80%	82%	83%	83%	82%	82%	81%	81%	80%	79%	80%	77%	73%	73%
November	11	80%	76%	70%	68%	65%	64%	64%	66%	72%	80%	85%	88%	90%	91%	92%	92%	90%	89%	88%	87%	89%	89%	88%	85%	81%
December	12	77%	73%	68%	65%	62%	60%	60%	61%	66%	73%	78%	81%	83%	85%	86%	85%	84%	83%	82%	81%	83%	83%	83%	81%	76%
	All	73%	69%	65%	63%	61%	61%	61%	66%	72%	77%	81%	84%	86%	87%	87%	86%	85%	84%	84%	83%	83%	84%	82%	79%	77%

Table 19: Load curve Spain 2019 weekend

Weekends (Sat-Sun) - normalized with the average maximum electricity demand of the working days																									
		Hour	Electricity demand																						
	Monat	0	1	2	3	4	5	6	7	8	9	10	11	12	13	14	15	16	17	18	19	20	21	22	23	All
January	1	79%	73%	68%	64%	61%	60%	61%	62%	65%	67%	74%	78%	82%	82%	81%	80%	78%	77%	77%	81%	84%	84%	84%	82%	74%
February	2	76%	70%	65%	62%	61%	60%	60%	61%	63%	66%	72%	76%	78%	78%	78%	76%	73%	71%	71%	73%	79%	82%	81%	78%	71%
March	3	67%	63%	59%	57%	55%	54%	54%	55%	56%	58%	63%	67%	69%	70%	70%	69%	67%	65%	64%	64%	67%	72%	72%	69%	64%
April	4	66%	62%	59%	57%	55%	55%	54%	55%	56%	58%	62%	66%	68%	68%	68%	68%	66%	64%	63%	63%	63%	64%	68%	66%	62%
May	5	67%	64%	61%	59%	57%	56%	56%	56%	56%	60%	64%	68%	70%	70%	71%	70%	68%	67%	67%	68%	68%	67%	68%	68%	64%
June	6	70%	66%	64%	61%	59%	58%	57%	57%	58%	61%	66%	71%	73%	75%	76%	75%	74%	72%	71%	70%	70%	70%	71%	71%	67%
July	7	76%	73%	70%	67%	65%	64%	63%	63%	63%	65%	70%	75%	78%	80%	81%	81%	80%	79%	79%	78%	77%	76%	76%	77%	73%
August	8	73%	69%	67%	64%	62%	60%	59%	60%	60%	62%	67%	73%	76%	79%	80%	80%	79%	78%	77%	76%	75%	74%	75%	74%	71%
September	9	70%	66%	63%	61%	59%	58%	58%	59%	59%	61%	64%	69%	71%	73%	74%	74%	72%	70%	70%	70%	69%	71%	71%	70%	67%
October	10	65%	61%	59%	56%	55%	54%	54%	55%	56%	58%	62%	66%	69%	70%	72%	71%	69%	67%	66%	66%	67%	68%	68%	66%	63%
November	11	78%	74%	67%	66%	63%	61%	60%	61%	63%	65%	68%	73%	76%	79%	80%	80%	79%	78%	76%	75%	77%	78%	77%	76%	72%
December	12	74%	70%	66%	62%	60%	58%	56%	55%	57%	59%	61%	66%	70%	72%	73%	72%	72%	70%	68%	69%	71%	72%	73%	72%	67%
	All	72%	68%	64%	61%	59%	58%	58%	58%	59%	62%	66%	71%	73%	75%	75%	75%	73%	71%	71%	71%	72%	73%	74%	72%	68%

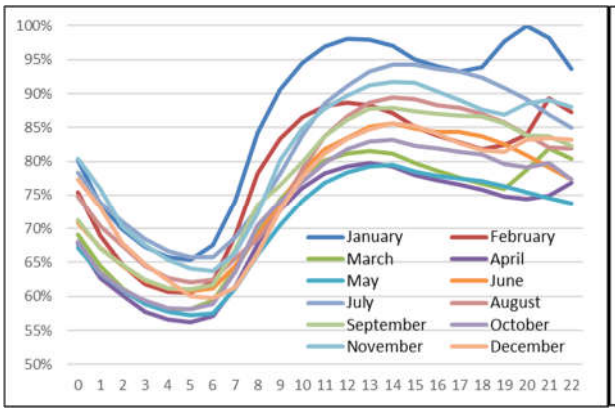

Figure 48: Load curve Spain Monday - Friday

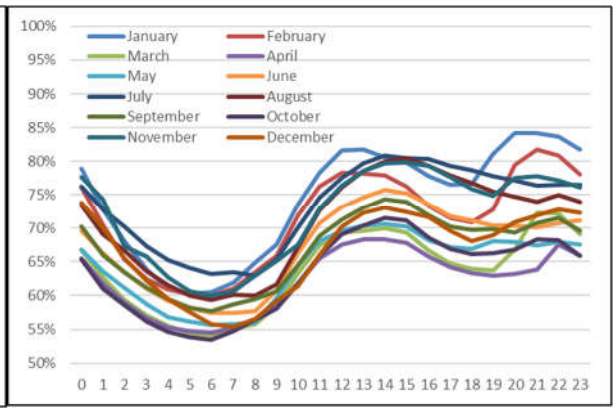

Figure 49: Load curve Spain 2019 weekend

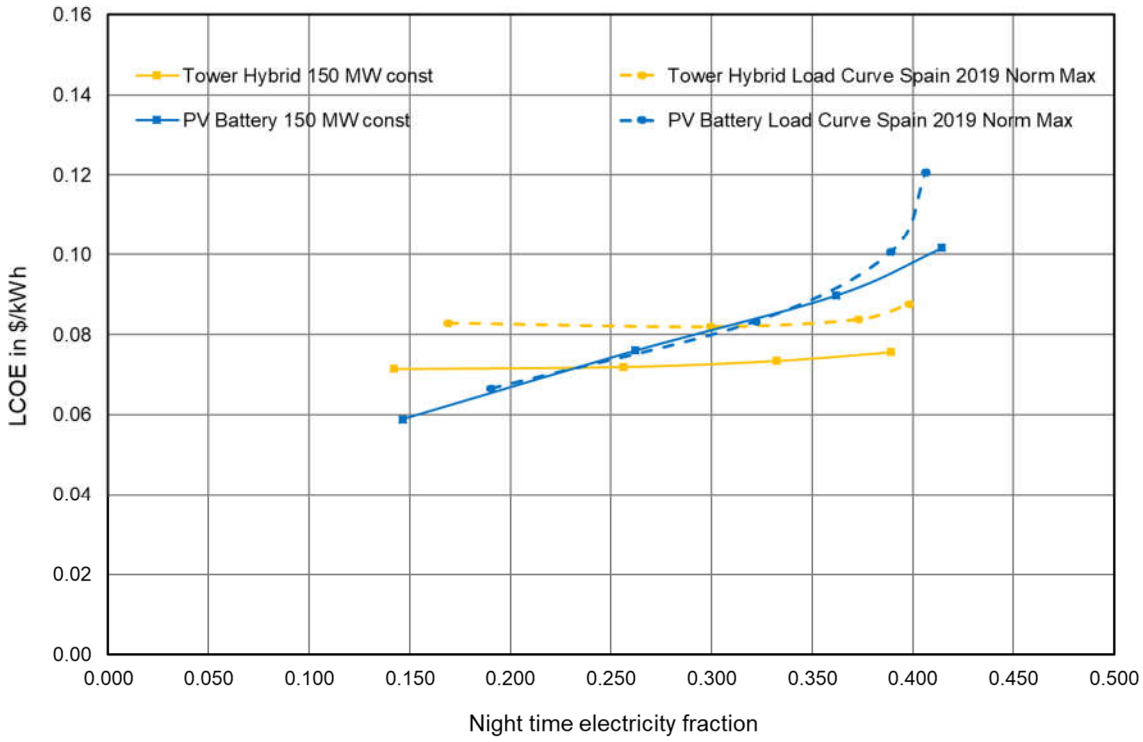

Figure 50: Results with load curve Spain 2019 for PSA

It can be seen how the results change for both technologies. Hybrid tower LCOEs slip up a bit (about one cent). This is mainly because of the lower demand during daytime hours that causes a smaller PV array with the corresponding electricity cost increase, but also to a lesser extent due to the partial load operation with the new load curve (lower efficiency). The lower demand during sunshine causes that the night share increases. There are some differences with the PV battery system too. The night share is increased because of the lower demand in the central hours. However, the curve remains similar because the battery can adapt quickly and flexibly to the load curve. For larger storage capacities, the dumping increases significantly and so does the LCOE.

In Figure 51 below the corresponding results from the HYPPO tool are presented. For all systems using a TES and power block applying a realistic load curve with curtailment of the turbine output leads to a slightly higher LCOE, at least for capacity factors lower than 80 to 90%. Only the PV-BESS system seems to benefit from the applied load curve. This is due to the higher flexibility of the BESS: reducing the output power below 150MW does not affect the BESS round-trip efficiency and the BESS is flexible in discharging at later hours during the night or even the early morning hours. At the same time, due to the generally reduced energy demand as defined per load curve, the PV field capacity can be reduced, while still leading to the same CF values.

Generally, systems using a TES seem to benefit from applying a load curve for higher CF values (above 70, 80 or 90% for PT standalone, PT-hybrid and CRT hybrid respectively) and show lower LCOEs for these CF values. This may be related to reduced solar field capacities and higher utilization rates of the storages, but this would have to be further analysed.

All systems are able to achieve higher capacity factors in this scenario. However, this does not have technical reasons, as the CF is calculated based on the maximum possible amount of annual energy injection, which is significantly reduced, if the load curve for Spain is applied.

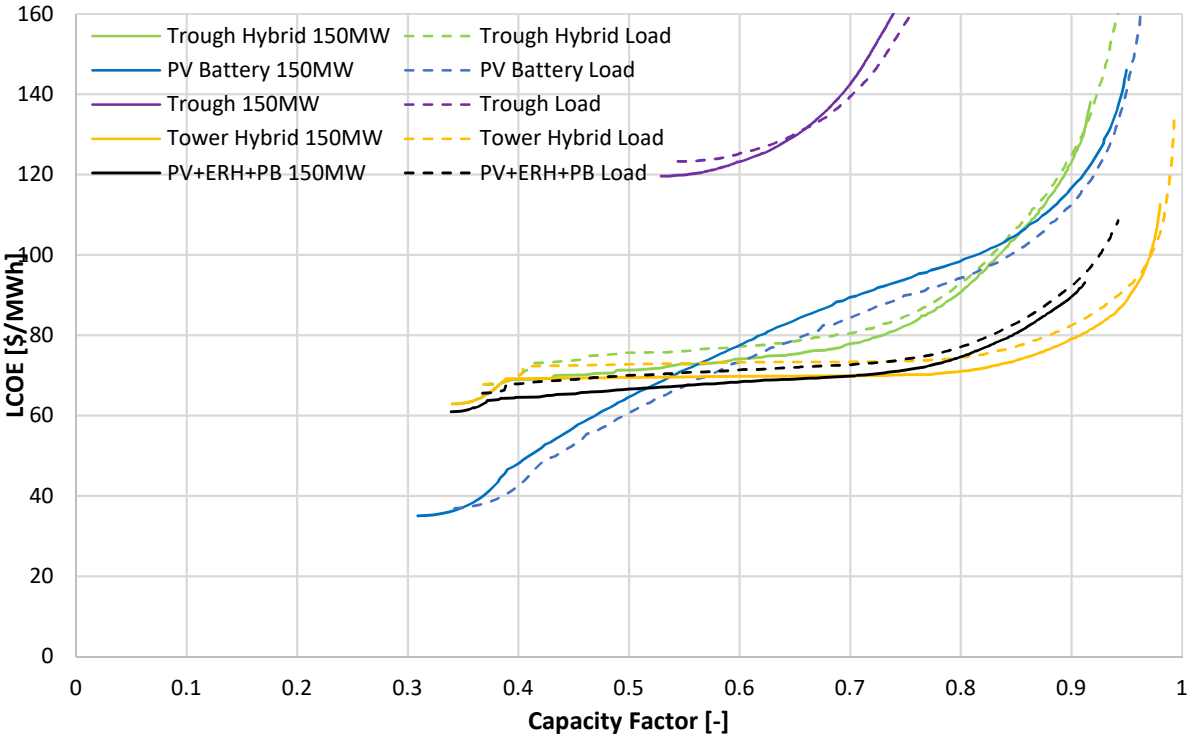

Figure 51: Results with Load Curve Spain 2019 for PSA (HYPPO results)

9.4.5. 15 minutes step simulation for PSA

The PSA site was simulated with a time step of 15 minutes instead of the usual 60 minutes. There is hardly any difference in the results and the higher accuracy obtained does not compensate for the longer computation time. In addition, there was less availability of meteorological data with this time step. Only the PV system with battery shows a minor difference when using a shorter time step. This is rather caused by the more precise definition of the night hours which causes the curve to move to the right. However, the yield of the plant does not improve. It is more noticeable for this technology just because the curve is steeper.

9.4.6. Calculation with start time power block set to 0

The influence of the start time of the power block on the night share was investigated. For this purpose, it was set to 0. The LCOE decreased because no energy was required for start-up. For an optimized 12h-storage hybrid trough the LCOE decreased from 0.0703 $/kW to 0.0683 $/kW. The 6h-storage system LCOE declined as well. There was no influence on the night share with this adjustment.

10. Comparison HYPPO and Greenius

Both simulation tools, greenius (DLR) and HYPPO were developed and used for the case studies independently. As both models use different approaches in calculating energy yields from the subcomponents, but also in distributing thermal and electrical energy flows (dispatch strategies), deviations in the results are to be expected. In this section the simulation results for the base case are compared and deviations are analysed. The purpose of this exercise is to give a better understanding of how each tool reflects certain boundary conditions and thus help potential software users to best interpret each model's simulation results.

As no operation data for a reference plant of this type is available, the models cannot be directly validated with data from existing plants. Therefore, the models used in this work are compared against each other and the results are critically checked for verification. As both models are based on existing, well validated single-plant models (greenius, SAM, PVSyst, Ebsilon®Professional), the purpose of comparing and verifying the results is to ensure the functioning of the hybrid modelling, which consists mainly of functions distributing energy streams coming from the different subcomponents going to storages and distribution to the grid. For both models consistency checks have been done such as checking the conservation of energy or testing the boundaries of the models for unrealistic behaviour.

10.1. Comparison of simulation models

All comparisons are made for the site in Riyadh with the 2021 cost assumptions. For the comparison, annual sums of different simulation results are compared. Furthermore, the hourly sums of a week with clear sky and a cloudy week are compared. The deviation x_{dev} between the annual sums of HYPPO AS_{HYPPO} and the annual sums of greenius $AS_{Greenius}$ are calculated with equation 10.1.

$$x_{dev} = \frac{AS_{HYPPO}}{AS_{Greenius}} - 1 \qquad \textbf{10.1}$$

10.1.1. Comparison of the PT-PV hybrid plant models as example for the Verification process

In this report the comparison of models is represented for the PT-PV hybrid topology only. The hybrid modelling of other topologies was based on it and the results are comparable. All topologies have been tested and compared individually but are not displayed in this report for reasons of clarity.

As greenius does not contain an optimization routine, the comparison is based on a parameter variation. For the comparison of the PT-PV hybrid plant model 137 scenarios are simulated and then compared. The scenarios were selected in order to reflect roughly the complete range of possible capacity combinations. The complete list of scenarios evaluated can be found in Table 20 below. A few cases were later eliminated due to erroneous simulation data related to cases at the very lower edge of component capacities. Of all cases displayed, scenario 114, being of special interest for having the lowest overall LCOE was selected for a direct comparison of weekly generation curves.

Table 20: Scenarios of PT-PV hybrid plant for comparison of HYPPO and Greenius simulation models

Scenario No	$\dot{Q}_{PT,nom}$ [MW$_{th}$]	$P_{PV,AC,nom}$ [MW$_{AC}$] (step size)	$\dot{Q}_{EH,nom}$ [MW$_{th}$]	$Q_{TES,nom}$ [MWh$_{th}$]
0 - 5	22.5	150 – 400 (50)	45	1033
6 - 11	45	150 – 400 (50)	90	1033
12 - 17	67.5	150 – 400 (50)	135	1033
18 - 22	45	200 – 400 (50)	90	2066
23 - 27	67.5	200 – 400 (50)	135	2066
28 - 33	90	250 – 500 (50)	180	2066
34 - 39	112.5	250 – 500 (50)	225	2066
40 - 45	135	300 – 550 (50)	270	2066
46 - 51	90	250 – 500 (50)	180	3099
52- 57	112.5	250 – 500 (50)	225	3099
58 - 63	135	300 – 550 (50)	270	3099
64 - 69	157.5	300 – 550 (50)	315	3099
70 - 75	180	350 – 600 (50)	360	3099
76 - 81	112.5	250 – 500 (50)	225	4132
82 - 87	135	300 – 550 (50)	270	4132
88 - 93	157.5	300 – 550 (50)	315	4132
94 - 99	180	350 – 600 (50)	360	4132
100 - 105	202.5	400 – 650 (50)	405	4132
106 - 110	45	250	60 – 100 (10)	1033
111 - 118	90	350	120 – 190 (10)	2066
119 - 127	112.5	400	160 – 220 (10), 225, 235	3099
128 - 136	157.5	450	250 – 310 (10), 315, 325	4132

In the first step the SF output of HYPPO and greenius is compared, first the annual sums of all PT-PV hybrid plant scenarios, then the hourly sums of scenario 114. The annual SF output is larger in HYPPO than in greenius for small systems with a nominal thermal power $\dot{Q}_{PT,nom}$ of 22.5 and 45 MW$_{th}$ and smaller for the larger systems. The annual sums of the SF output increase less in HYPPO with increasing nominal thermal power $\dot{Q}_{PT,nom}$ than in greenius. The deviation in the considered scenarios ranges from 2.1% for a SF with a nominal thermal power $\dot{Q}_{PT,nom}$ of $22.5\ \mathrm{MW_{th}}$ to -2.4% for a SF with a nominal thermal power $\dot{Q}_{PT,nom}$ of 202 MW$_{th}$.

Figure 52 presents the hourly sums of the SF output of scenario 114 for HYPPO and greenius for a week with clear sky, and a cloudy week. As can be seen, the SF output is clearly lower in HYPPO in the first hour of the day. On the other hand, the SF in HYPPO produces some thermal energy output in the evening hours. This can be explained with the different control strategies of the SF used in SAM compared to greenius. As mentioned above, SAM is used to create the surrogate model for HYPPO. In SAM some of the remaining thermal energy in the components of the SF is extracted after sunset. Therefore, the SF has a lower system temperature in next morning and needs more energy for the heat-up. It can also be seen in Figure 52 that the SF output is slightly lower in HYPPO then in greenius in the remaining hours of the day.

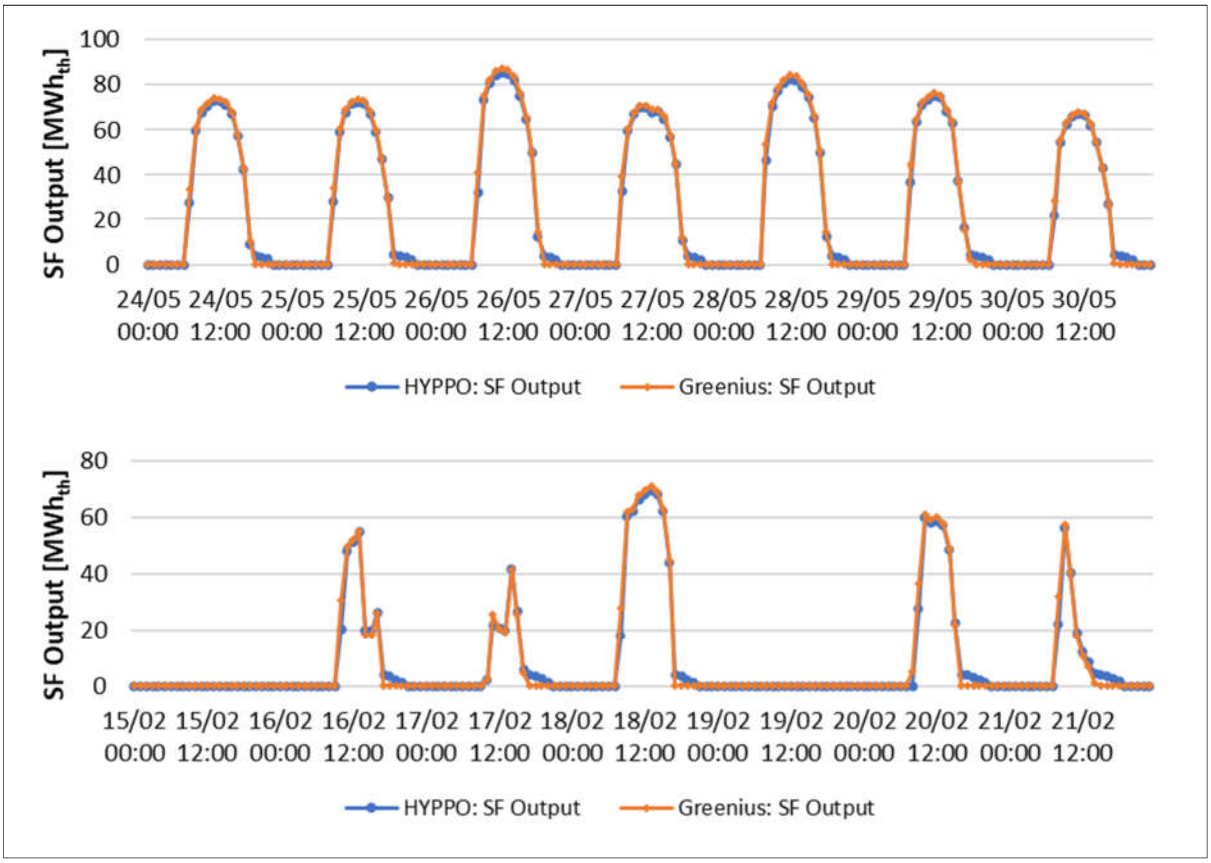

Figure 52: Hourly sums of the SF output of scenario 114 for HYPPO and Greenius for a week with clear sky (top), and a cloudy week (bottom)

In the second step, the PV output of HYPPO and greenius is compared. Again, first the annual sums of all PT-PV hybrid plant scenarios and then the hourly sums of scenario 114. The annual PV output is for all scenarios around 0.2%. higher in HYPPO than in greenius.

Comparing the hourly sums of the PV output of PT-PV plant scenario 114 for HYPPO and greenius for a week with clear sky, and a cloudy week in Figure 53, shows some differences between the two models. The PV output in HYPPO is lower in the morning and evening hours. For the rest of the day no tendency can be recognized: On some days the PV output is higher in HYPPO during midday, and on other days slightly lower. But it can be said that the difference between the hourly sums in HYPPO and greenius is larger on the days when HYPPO surpasses the PV output in greenius. The difference can be explained with the different tracking algorithms in PVSyst and greenius. However, it is assumed that results based on PVSyst are more accurate, as greenius does not consider backtracking and module mismatch losses due to self-shading, which is an important factor in the morning and evening hours. Furthermore, the PV model in greenius contains an error, as on the first day of the cloudy week between 6:00 and 7:00 the PV system has a power output equal to its nominal power.

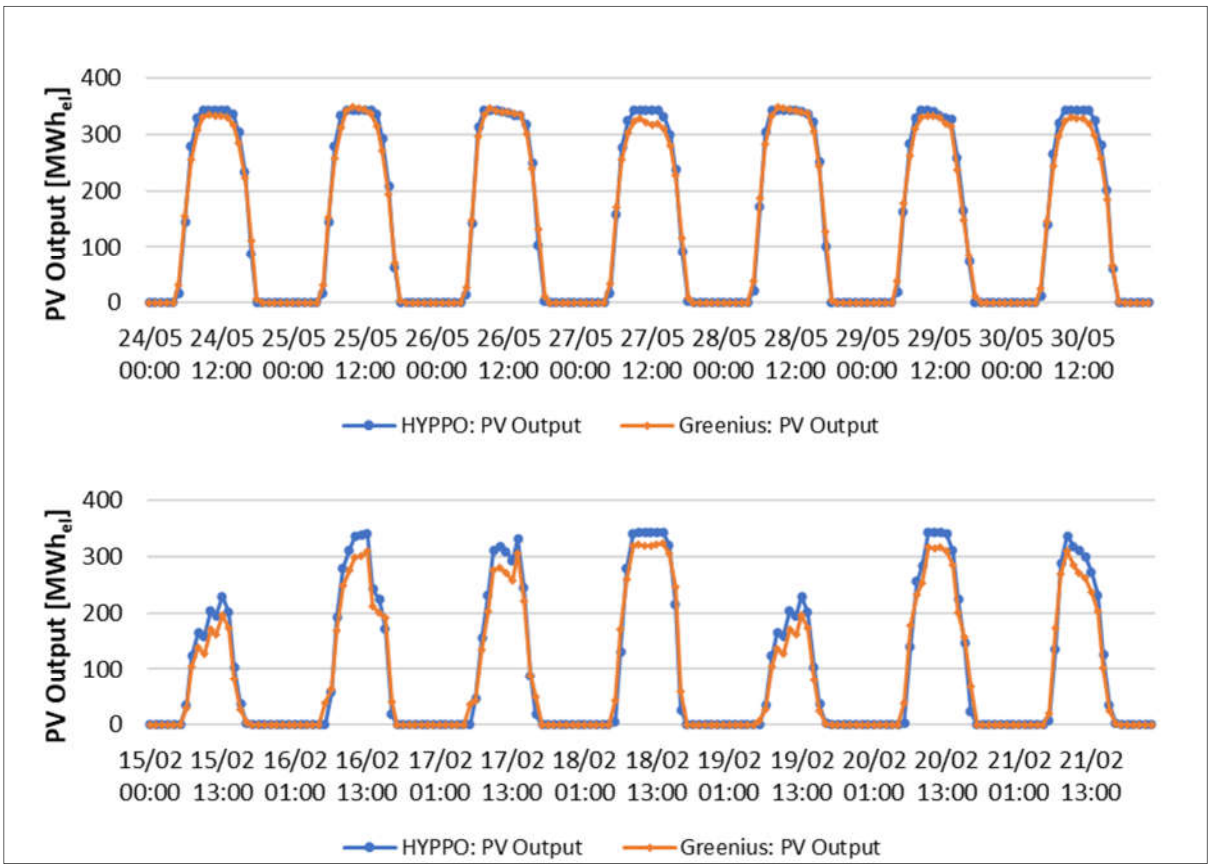

Figure 53: Hourly sums of the PV output of PT-PV hybrid plant scenario 114 for HYPPO and Greenius for a week with clear sky (top), and a cloudy week (bottom)

In the third step, the input into the EH from the SF and the PV system, as well as the resulting output is compared. All three energy flows are analyzed together, as they are linearly dependent from each other. Again, first the annual sums of all PT-PV hybrid plant scenarios as displayed in Figure 54 and then the hourly sums of scenario 114 as in Figure 55 are analyzed. The input into the EH not only depends on the available thermal energy from the SF and the available electrical energy from the PV system, but also on the maximal EH thermal power and the SOC of the TES. The annual sums of the thermal energy input from the SF into the EH is lower in HYPPO than in greenius. The deviation reaches values between -0.7% and -5.8%. Also, the electrical energy input from the PV system is lower in HYPPO. Here the deviation is between -2.6% and -7.6%. The higher deviation between HYPPO and greenius regarding the annual sums of the EH input from the PV system compared to the EH input from the SF, is due to the different definition if the EH nominal power in HYPPO and greenius. In HYPPO the EH nominal power refers to the EH thermal power, as most manufacturers do. Greenius on the other hand refers to the electrical power. Therefore, the maximum power output and input is around 1% higher in HYPPO. The difference is equal to the thermal losses of the EH. It is assumed that this difference can be neglected in the further course of the comparison. The deviation regarding the EH output between HYPPO and greenius is between -2.0% and -7.0% and therefore in between the deviation regarding the energy input from the SF and the deviation regarding the EH input from the PV system. To explain the higher deviation between HYPPO and

greenius regarding the annual sums of the thermal energy input from the SF into the EH compared to the deviation regarding the SF output, the hourly sums must be considered.

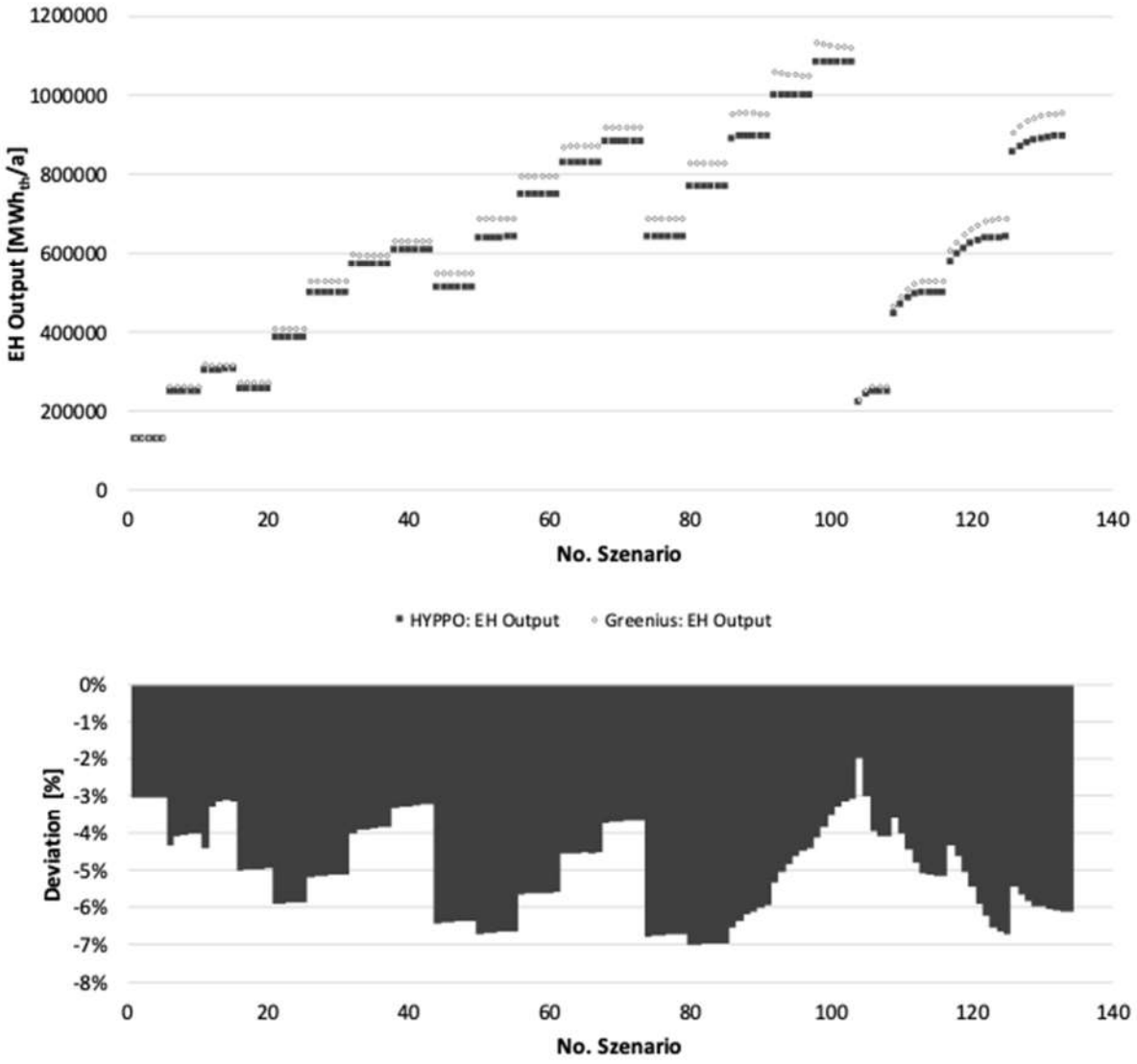

Figure 54: Annual sums of the thermal energy input from the SF into the EH of the different PT-PV hybrid plant scenarios for HYPPO and Greenius (top), and the deviation between both values (bottom)

After comparing the annual sums of the input into the EH from the SF and the PV system, as well as the resulting output, the hourly sums of PT-PV plant scenario 114 for HYPPO and Greenius for a week with clear sky, and a cloudy week are compared as per Figure 55.

It can be seen that the energy input into the EH and therefore the thermal energy output of the EH is clearly lower in HYPPO in the first hour of the day. This is due to the lower SF output in HYPPO in first hour of the day as explained based on Figure 52. The additional thermal energy produced by the SF in HYPPO in the evening hours cannot be used, as the PV system is not producing electrical energy at the same time. Without electrical energy, the EH cannot operate. This can be observed when comparing Figure 52 with Figure 55. Furthermore, the EH output is slightly higher in HYPPO than in greenius in the remaining hours of the day, except when the EH power limit is reached as can also be seen in Figure 55. This is due to the different definitions of the EH nominal power as explained above.

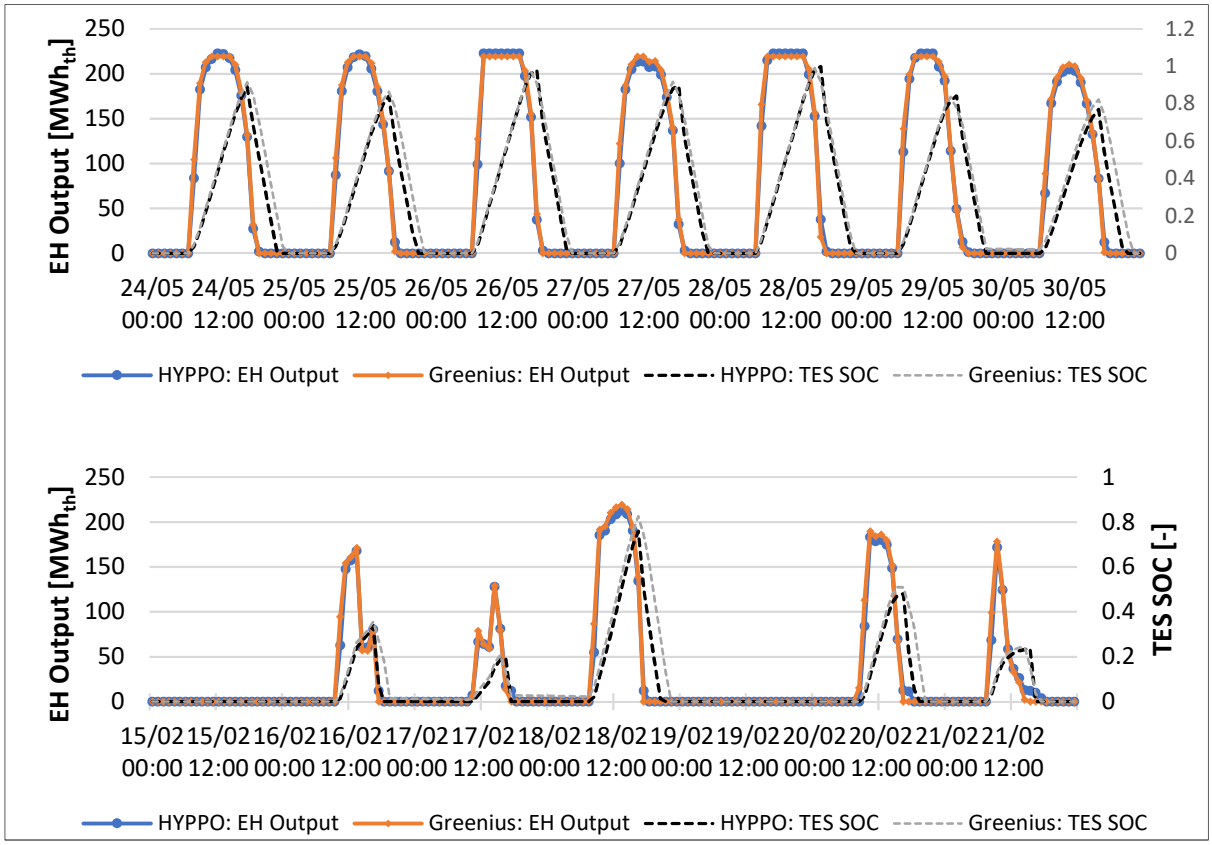

Figure 55: Hourly sums of the EH output of PT-PV hybrid plant scenario 114 for HYPPO and Greenius for a week with clear sky (top), and a cloudy week (bottom)

10.1.2. Impact of Deviations on Optimisation Results

The differences between both models are based on some structural differences in the underlying subcomponent models and some deviating parameter definitions as described above. This also applies for the other models not displayed here.

The overall impact of the model differences on the optimisation results can be seen in Figure 56 for all topologies. PV-BESS results match pretty well over the complete range, except for very extreme boundary cases that are not well covered by the HYPPO automated analysis. These extreme boundary cases, considering PV standalone systems without significant storage capacities should be evaluated manually instead, using separate tools like PVSyst or SAM or greenius in its basic version.

For the PT-hybrid and the CRT-hybrid models, deviations occur mostly for high CF values where the greenius model suggests slightly higher LCOEs.

The PV-ERH-PB models also shows greater discrepancies with high capacity factors. As with hybrid plants, greenius results present higher LCOEs for capacity factors above 85%. Note that the second operating strategy was used in this case [see also subsection 2.3]).

Overall, the models match pretty well, and the deviations can be considered as acceptable regarding the purpose of the tools to be used for high-level studies and general feasibility analysis.

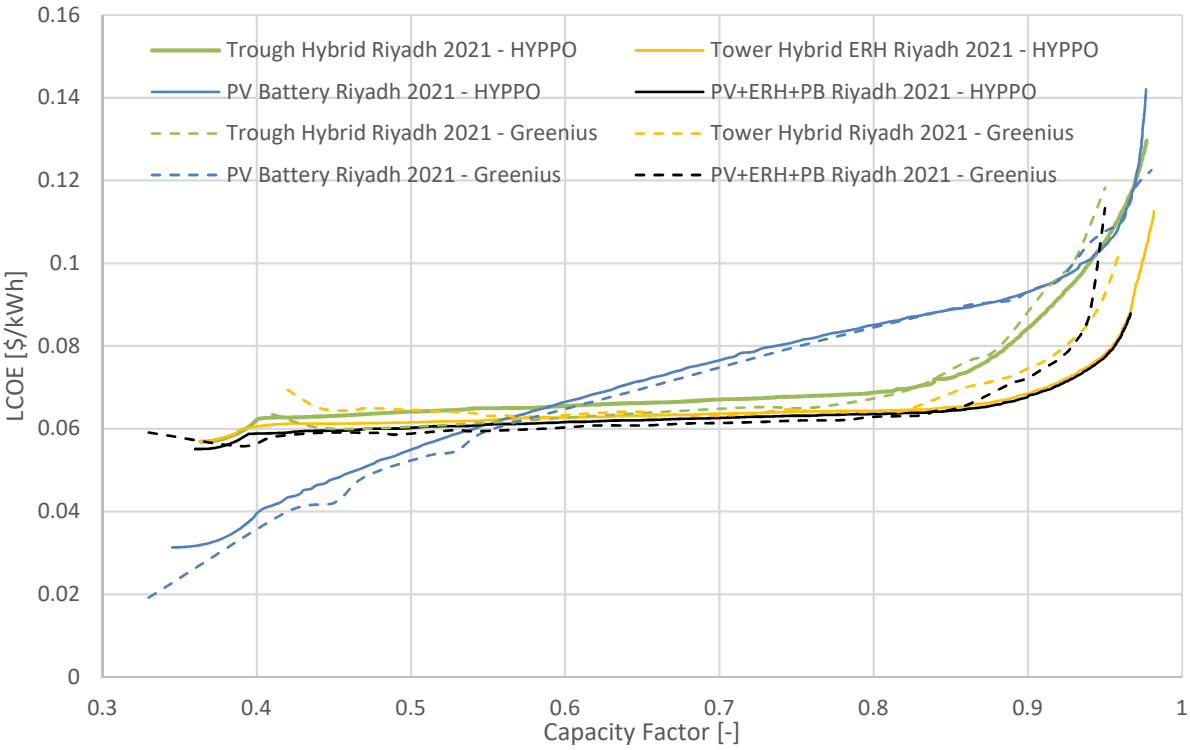

Figure 56: Comparison of greenius and HYPPO - Optimisation Results

11. Conclusions

General comments: In this study a wide range of scenarios has been evaluated. The results show that solar hybrid generation systems using either battery or thermal energy storages can be feasible for a wide range of applications. Which solution is the best in a specific case depends on multiple factors and is further discussed in the following paragraphs. LCOE is used as figure of merit to compare different systems and plotted vs. two parameters: capacity factor and night time electricity fraction. While capacity factor is commonly used and well known for power plant systems, the night time electricity fraction is defined in this report as part of the overall electricity which is produced during the time of day, when PV plants without storage cannot deliver significant electricity. Thus, both parameters are representing similar cases but cannot be converted directly. Night time electricity fraction is used here since it is postulated that developers and owners of hybrid PV-CSP power plants are primarily interested in an increased production of solar electricity during non-sunshine hours. Of course, there is some correlation between CF and night time electricity fraction but particularly for mid-range CF (0.5 – 0.8) the correlation is not very close. The same CF can be reached with different night time fractions. For very low and very high CF the correlation might be closer since this would mean also low and high night time fractions respectively (at least for the systems and operating conditions investigated in this study).

Base Case Riyadh: It could be shown that for CF values in a range between 40 and 55% and night time electricity fractions under 20-25% PV systems combined with a BESS can provide significantly lower LCOE values (40-60 $/MWh depending on discharge durations) compared to solar plants using TES. This range of CF values can be considered as “Peaker Plants” providing night-time power mainly for 3-5 evening hours. For higher CF values, thus longer durations of discharge during the night, the systems using TES provide cheaper LCOEs. These systems maintain very stable LCOE values (60-65 $/MWh) for a wide range of CFs (40-85%) and night time fractions, which seems related to the low marginal cost of increasing the storage capacity compared to BESS. Parabolic Trough hybrid systems have similar cost as Central Receiver hybrid systems. Hybridising CRT plants using additional P2H technology in parallel to the central receiver brings additional benefits. Surprisingly, the PV systems using P2H technology and TES show a very similar behaviour of the LCOE as the CRT hybrids and can reach high CF values in the range of 90% at stable LCOEs of 60-70$/MWh. Classical CSP plants not benefiting from direct injection of cheap PV electricity during the day cannot compete with the hybrid systems.

Projection of Cost 2030 and Sensitivity of Financial Parameters: Assuming moderate cost reductions for all related technologies, but predominantly for the PV and BESS technologies until 2030 the break-even point between systems using BESS and those using TES moves to higher CFs (from 55% in 2021 to 60% in 2030 for CRT and PV-ERH and from 58% to 65% for PT). This effect is solely cost driven and related to the marginal cost of storage. BESS can only compete with TES for longer discharge durations if their cost drops significantly. Price projections for 2030 generally can have the potential to reduce the LCOEs by 10-15$/MWh for TES technologies and 5-20$/MWh for BESS. The same effects were shown for separate cost sensitivities especially for the currently highly unstable PV and BESS cost assumptions. It is therefore strongly recommended to consider the development of prices in very early stages of solar hybrid project development. Compared to battery storages, TES solutions (either with or without CSP solar fields) can provide relatively stable LCOEs over a wide range of the capacity factor, thus providing a lower risk of fluctuating electricity prices during the development

stages of a plant. Ultimately, the project lifetime provides further cost reduction potentials and measures of extending the life of CSP solar field components should be further investigated.

Comparison Locations: The selection of a plant location will have a strong impact on the final project economics with a stronger impact on CSP technologies than on PV. For CSP plants locations with high DNI are clearly to be preferred, however, adding PV solar fields and hybridising the heat generation with P2H technology will dampen this effect. But still, high irradiation locations like Chile will still have significantly lower LCOEs compared to locations with higher shares or diffuse irradiation like China or Spain. It does not significantly depend on the project location (including ambient conditions) if battery or thermal storage solutions will have lower LCOEs, the decision for one or the other technology would rather have to be based on the required CF range and the current cost developments.

Cost of Heat (direct comparison): Comparing the direct heat generation cost reveals that PV+P2H technologies produce heat at very similar cost as CSP (central receiver systems). This conclusion deviates from earlier findings, but is also strongly depending on the cost assumptions. Parabolic trough system can provide heat cheaper but for the current commercial systems their temperature is limited to roughly 390°C resulting in lower conversion efficiencies in the power block and higher thermal storage cost compared to CRT and PV+P2H systems with roughly 565°C. PV+P2H systems have the benefit of being able to provide heat at a wide range of temperature levels.

Load Following Operation: Future energy systems with high renewable energy shares will require dispatchable generation to follow the grid loads and this may impact remuneration schemes compared to unlimited injection. It could be shown that PV-BESS plants are very flexible and that load following operation only impacts LCOEs if the plants need to reach very high capacity factors. For hybridised CRT systems the LCOE is higher, if they have to follow the load curve developed from Spain 2019, however the thermal storage systems show more stable and lower LCOEs for high capacity factors for load following.

Conclusion from comparing different models: Both models, greenius and HYPPO are suitable for modelling and optimising solar hybrid generation systems including both battery as well as thermal energy storages. They show realistic and comparable results. For detailed analysis of specific cases, simulation models with a higher grade of detail should be used, to gain higher accuracy of the results. For the high-level analysis of a wide range of component and capacity combinations, the developed tools are very useful.

12. References

[1] Guiliano, S. et al., THERMVOLT project: Systemvergleich von solarthermischen und photovoltaischen Kraftwerken für die Versorgungssicherheit, Abschlussbericht (BMWI, 2014 - 2016) https://www.tib.eu/en/suchen/id/TIBKAT:100051305X/

[2] Starke et al., Assessing the performance of hybrid CSP + PV plants in northern Chile, Solar Energy 138 (2016)

[3] Zhai et. al, The daily and annual technical-economic analysis of the thermal storage PVCSP system in two dispatch strategies, Energy Conversion and Management 154 (2017)

[4] Zurita et al., Techno-economic evaluation of a hybrid CSP + PV plant integrated with thermal energy storage and a large-scale battery energy storage system for base generation, Solar Energy 173 (2018)

[5] Riffelmann, K.J.; Weinrebe, G.; Balz, M.: Hybrid CSP-PV Plants with Integrated Thermal Storage, AIP Conference Proceedings 2445, 030020 (2022); https://doi.org/10.1063/5.0086610

[6] Mata-Torres et al., Multi-objective optimization of a Concentrating Solar Power + Photovoltaic + Multi-Effect Distillation plant: Understanding the impact of the solar irradiation and the plant location, Energy Conversion and Management X 11 (2021)

[7] Richter et al., Predictive storage strategy for optimal design of hybrid CSP-PV plants with immersion heater, Solar Energy 218 (2021)

[8] Acwa Power: https://www.acwapower.com/news/fourth-phase-of-mohammed-bin-rashid-al-maktoum-solar-park-is-the-first-cbi-certified-renewable-energy-project-financing-in-the-gcc-region/ (2019)

[9] Masdar: https://masdar.ae/Masdar-Clean-Energy/Projects/Noor-Midelt (2019)

[10] Acciona: https://www.acciona.com/updates/news/cerro-dominador-csp-plant-chile-officially-opens/ (2021)

[11] Heliocsp: https://helioscsp.com/4-concentrated-solar-power-projects-started-2-csp-projects-confirmed-epc-last-week-in-china/ (2022)

[12] DLR. (2020). greenius. Retrieved from http://freegreenius.dlr.de

[13] Hirsch, T. editor: SolarPACES Guideline for Bankable STE Yield Assessment http://www.solarpaces.org/wp-content/uploads/SolarPACES_Guideline_for_Bankable_STE_Yield_Assessment_-_Version_2017.pdf

[14] Dersch, J. et al., LCOE reduction potential of parabolic trough and solar tower technology in G20 countries until 2030. AIP Conference Proceedings 2303, 120002 (2020), https://doi.org/10.1063/5.0028883

[15] National Renewable Energy Laboratory (NREL), 2021 Annual Technology Baseline (ATB) Cost and Performance Data for Electricity Generation Technologies [data set] (2021), https://dx.doi.org/10.25984/1807473.

[16] Vignesh et al., 2021. U.S. Solar Photovoltaic System and Energy Storage Cost Benchmarks: Q1 2021. Golden, CO: National Renewable Energy Laboratory (2021). NREL/TP-7A40-80694

13. Abbreviations

BESS	Battery Energy Storage System
CF	Capacity Factor
CSP	Concentrated Solar Power
EPC	Engineering, Procurement and Construction
ERH	Electric Resistance Heater
LCOE	Levelized Cost of Electricity
PB	Power Block
PV	Photovoltaic
PV-BESS	Photovoltaic system with battery storage
PV+ERH+PB	Photovoltaic system with electric heater, thermal storage and power block
TES	Thermal energy storage

14. Annexes

14.1. HYPPO Results – Diagrams showing Capacity Factor

14.1.1. Comparison of Sites – Hyppo Results

The HYPPO Tool was only used to simulate 4 different sites: Riyadh (Kingdom of Saudi Arabia), PSA (Spain), De Aar (South Africa), Diego de Almagro (Chile). The results show LCOE over Capacity Factor.

Figure 57 depicts the pareto front for PSA with 2021 cost assumptions for all plant topologies. PSA has the lowest irradiation and the highest LCOE. The difference between the PT-PV plant's pareto front and the PV plant's pareto front is marginal between the first and second points of intersection. Because of its lower cost, CRT Hybrid is a cost-effective solution.

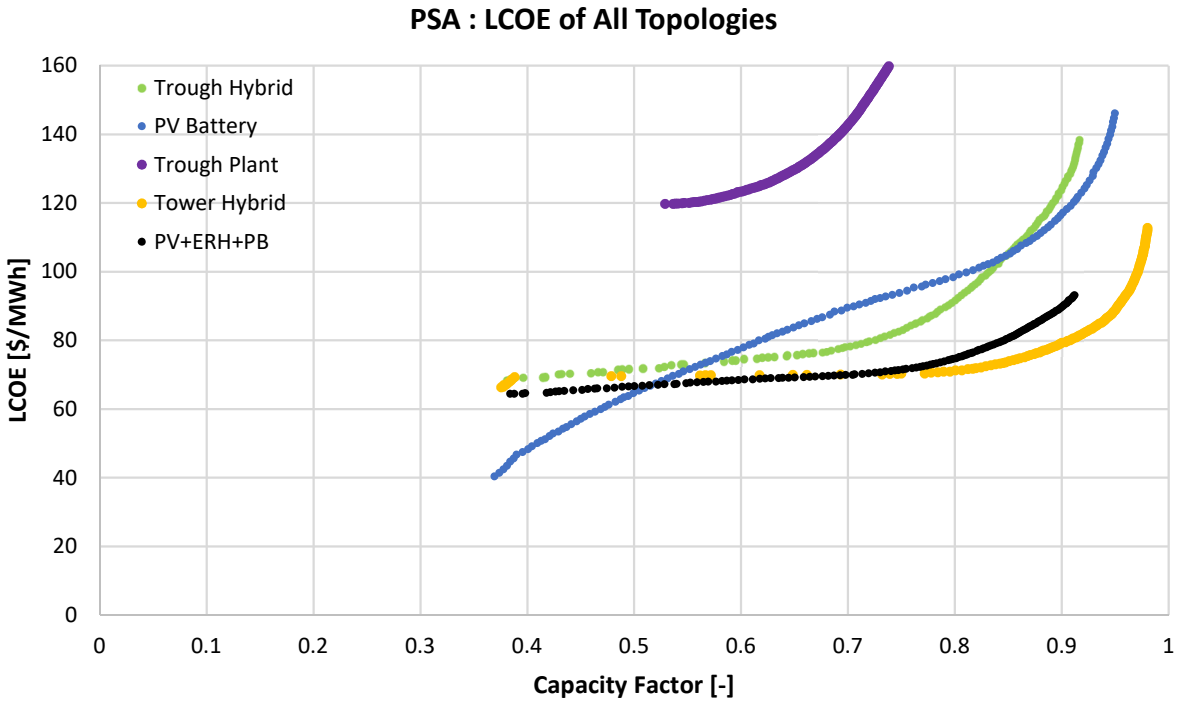

Figure 57: PSA (HYPPO results)

Figure 58 depicts the pareto front for Diego de Almagro's LCOE and CF with 2021 cost assumptions for all plant topologies. There is no second point of intersection between the PT-PV hybrid plant's pareto front and the PV plant. Furthermore, the pareto front of the PT plant is seen to be relatively close to the pareto front of the PV plant. However, in Diego de Almagro, as in all other locations, the PT plant is the least cost-effective solution for all CFs. The greater the DNI, the greater the CF range, and CSP plants are the more cost-effective solution when compared to PV-BESS hybrid plants. This becomes clearer when the pareto fronts of the two extreme cases, PSA with the lowest DNI and Diego de Almagro with the highest DNI, are compared.

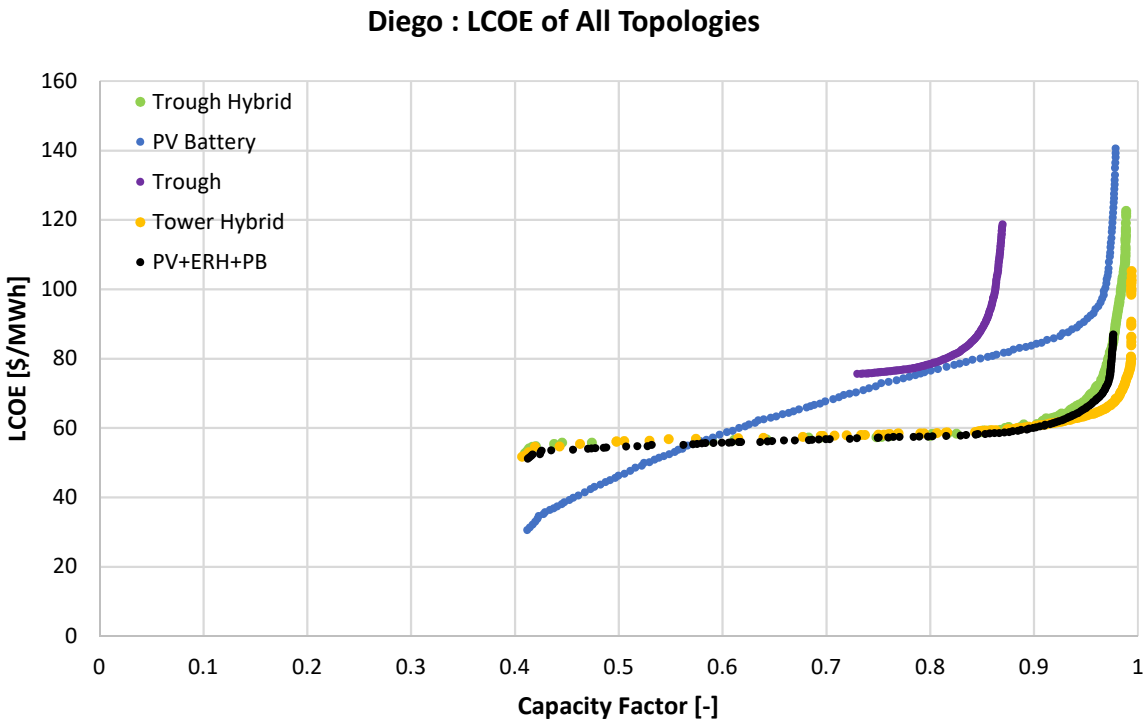

Figure 58: Diego (HYPPO results)

Figure 59 depicts the pareto front for De Aar with 2021 cost assumptions for all plant topologies. There is no second point of intersection between the PT-PV hybrid plant's pareto front and the PV plant. The only tendency for the position of the pareto front of the PT-PV hybrid plant in relation to the pareto front of the PV-BESS plant that can be recognized is regarding the DNI: The larger the annual sum of the DNI, the larger the range of CFs for which the CSP plants are the more cost-effective solution. This is directly linked to the efficiency of the PT-SF as it increases with increasing DNI. However, this cannot be defined as a reliable statement, as not only the DNI changes between the locations but also the GHI. Furthermore, the meteorological circumstances at a site are much more complex, than the annual sums of the DNI and GHI reveal.

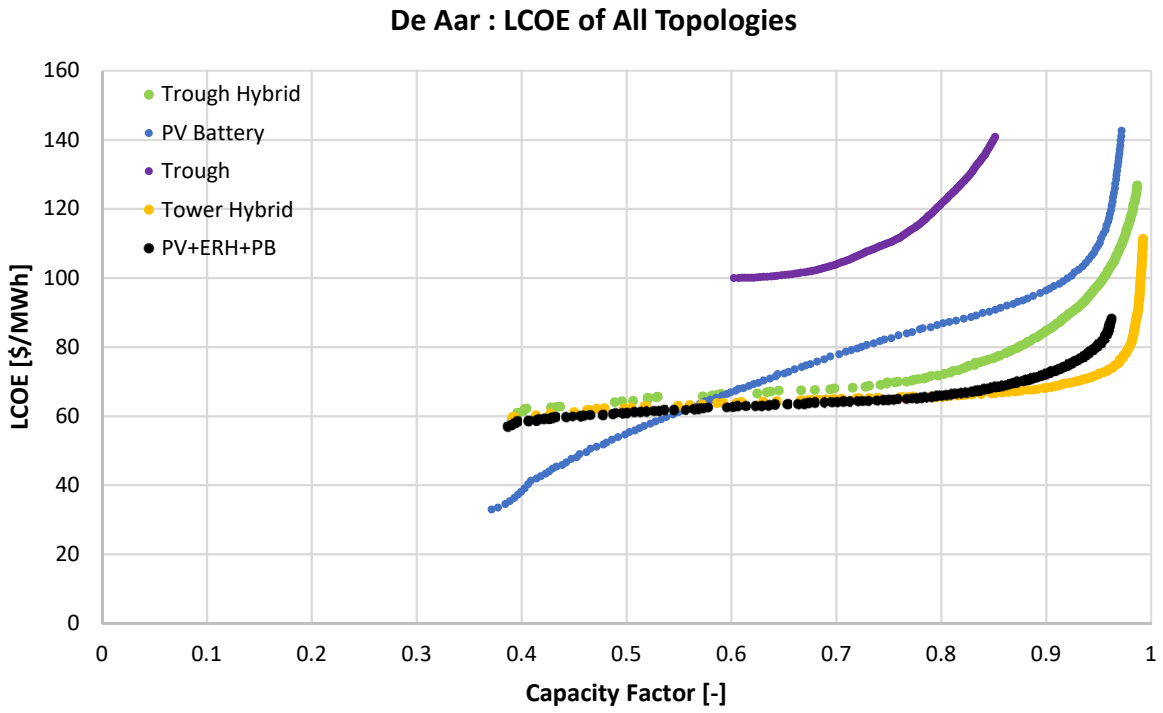

Figure 59: De Aar (HYPPO results)

All technologies were compared for all sites to properly assess the impact of the location. The figure explanations can be found in the respective chapter in the report. The same interpretations as in the report apply.

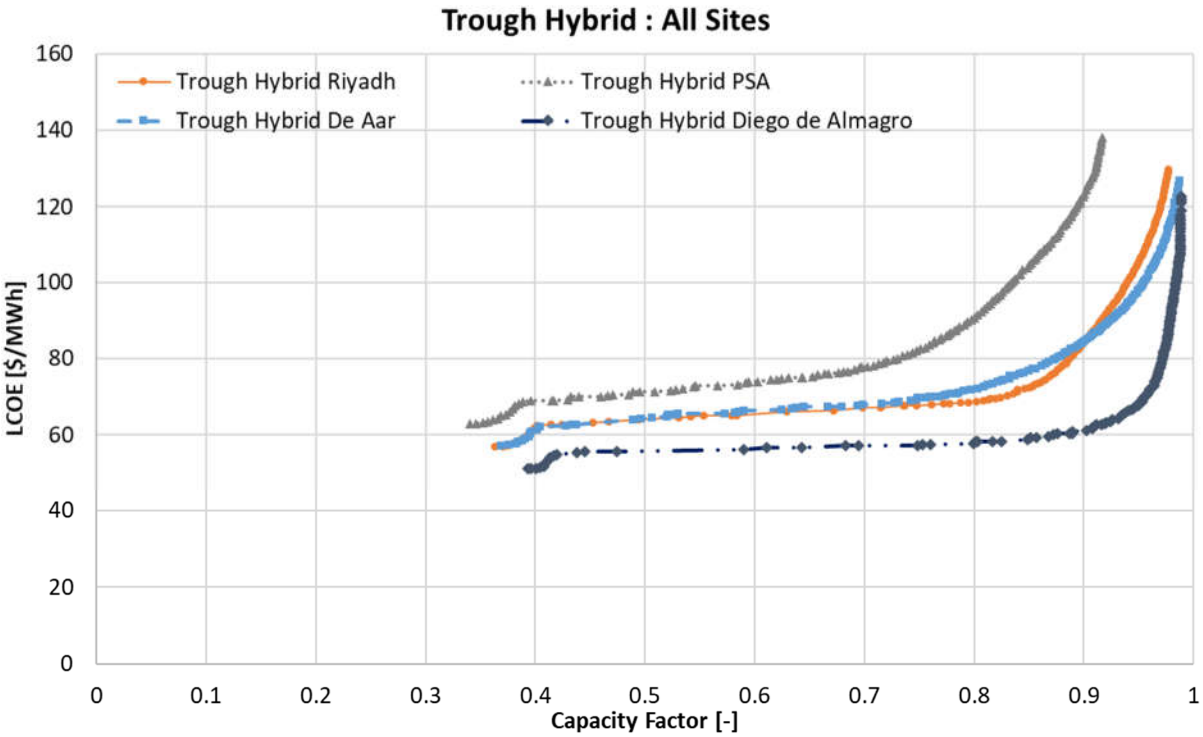

Figure 60: Trough Hybrid (HYPPO results)

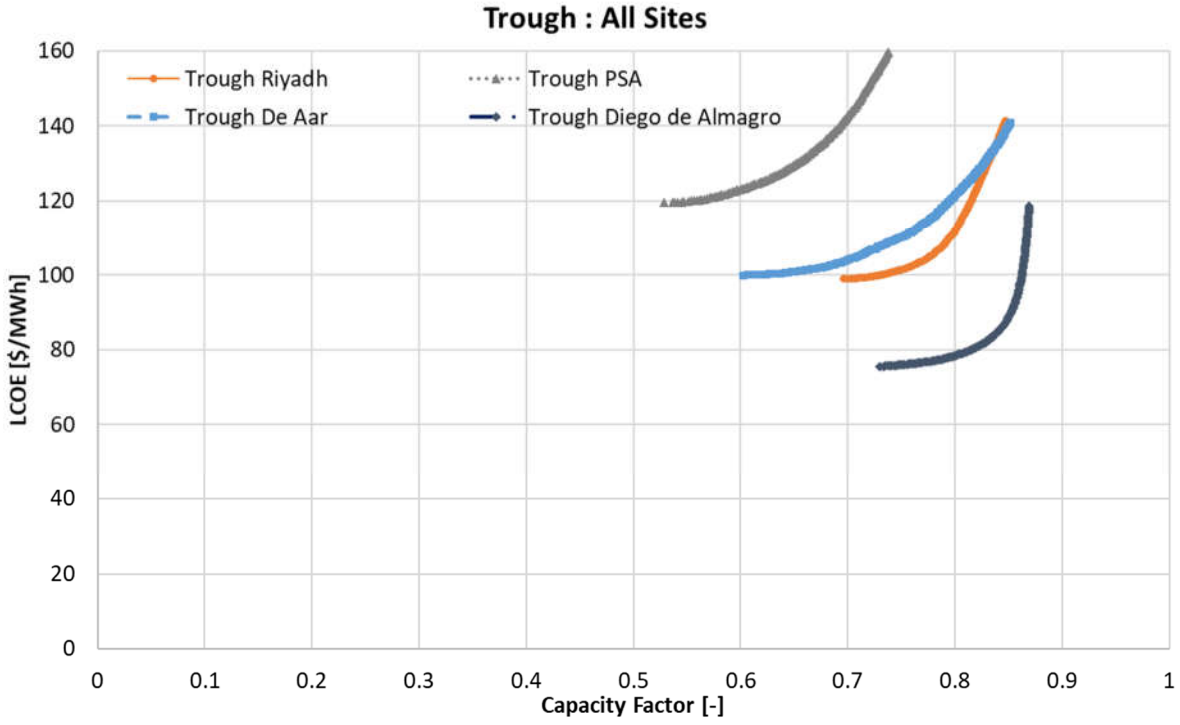

Figure 61: Trough (HYPPO results)

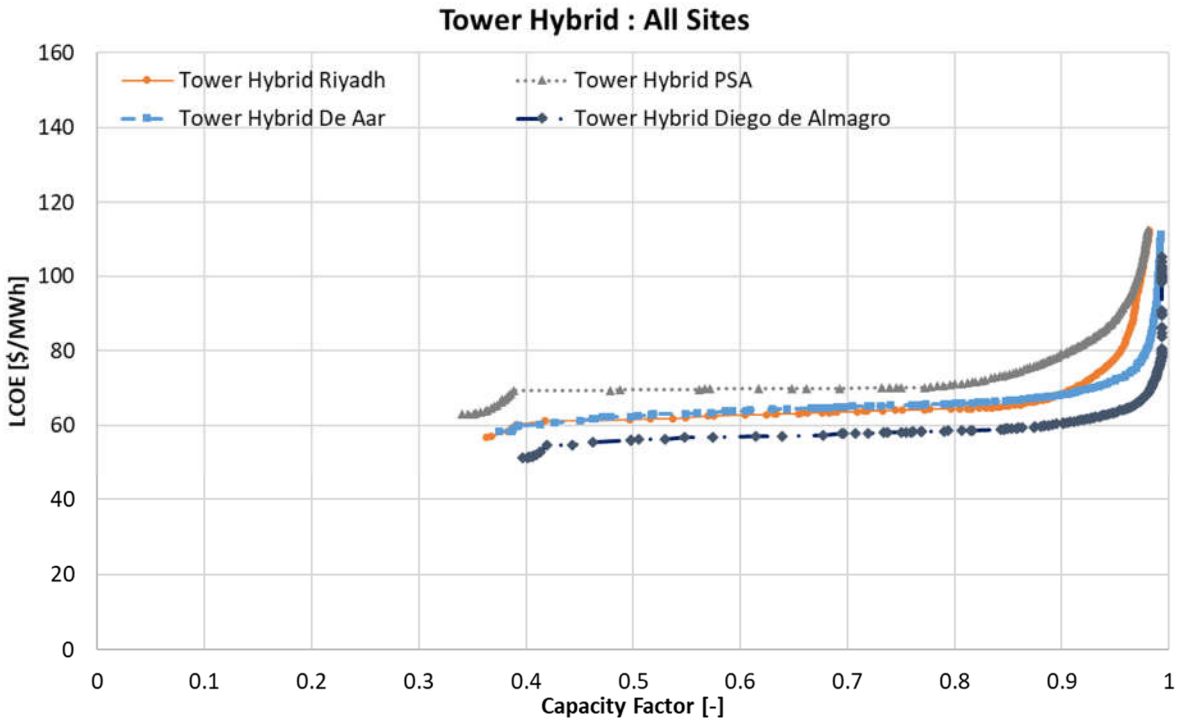

Figure 62: Tower Hybrid (HYPPO results)

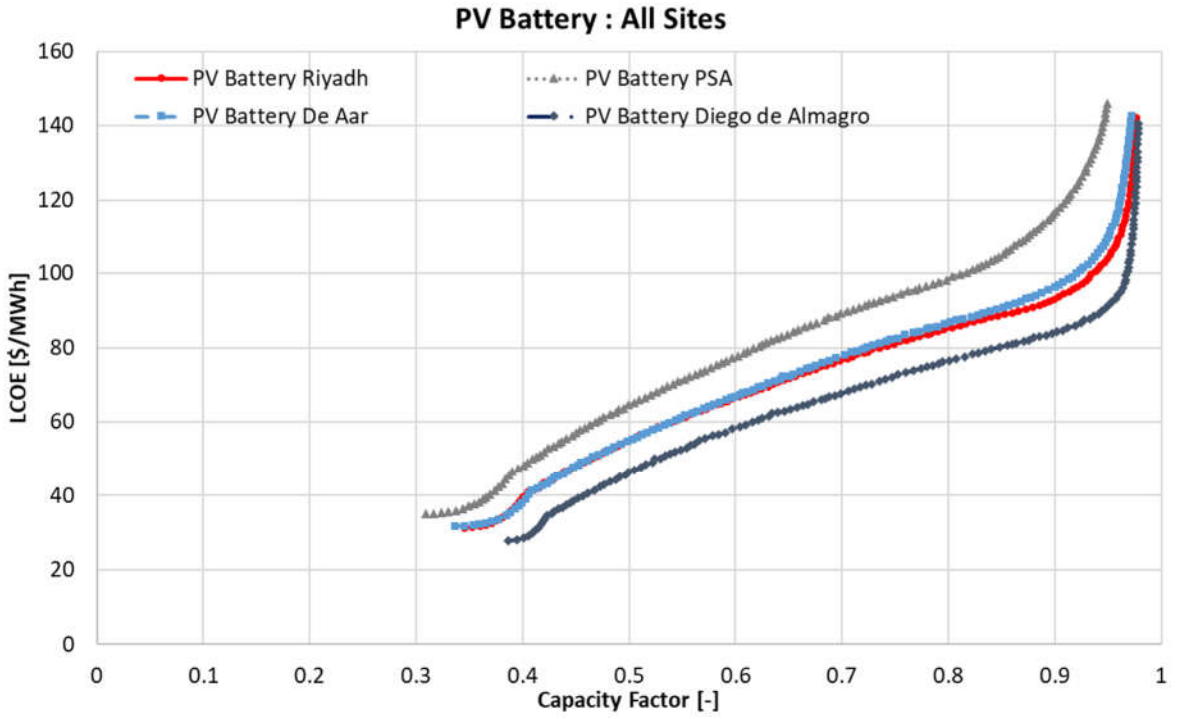

Figure 63: PV Battery (HYPPO results)

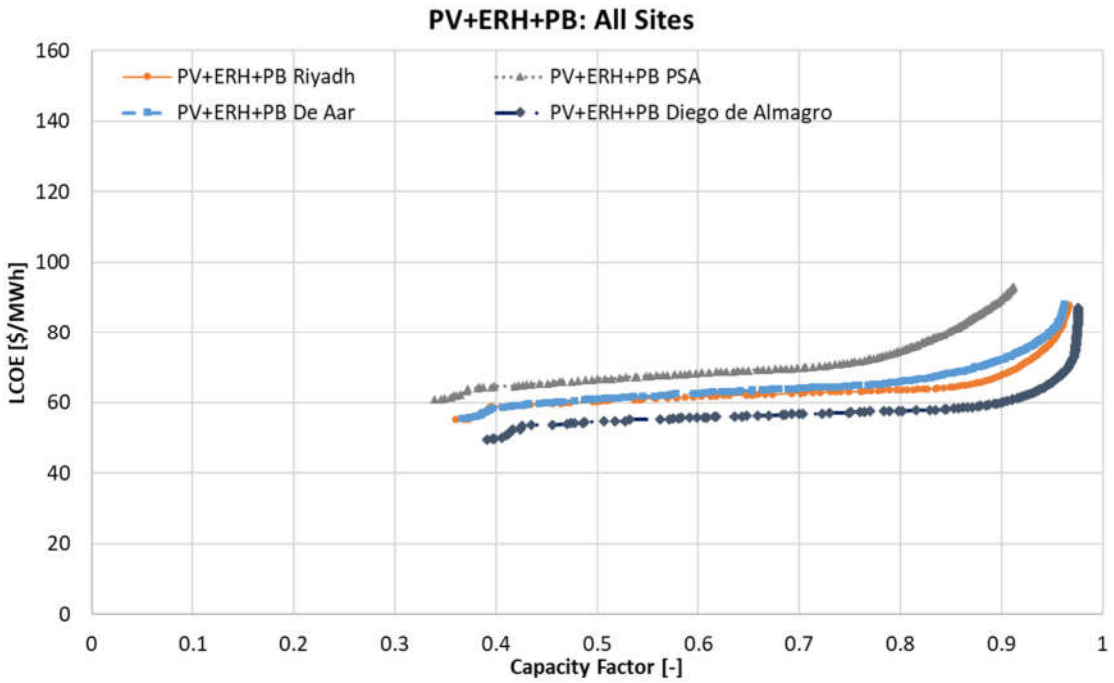

Figure 64: PV ERH (HYPPO results)

14.1.2. Projections 2030 – HYPPO Results

The figure explanations can be found in the respective chapter in the report.

In the below figure the HYPPO results for the base case side Riyadh using cost assumptions for 2021 and 2030 are compared. Figure 65 shows the Pareto front between CF and LCOE of all plant topologies for Riyadh with the cost assumptions of 2020 and 2030.

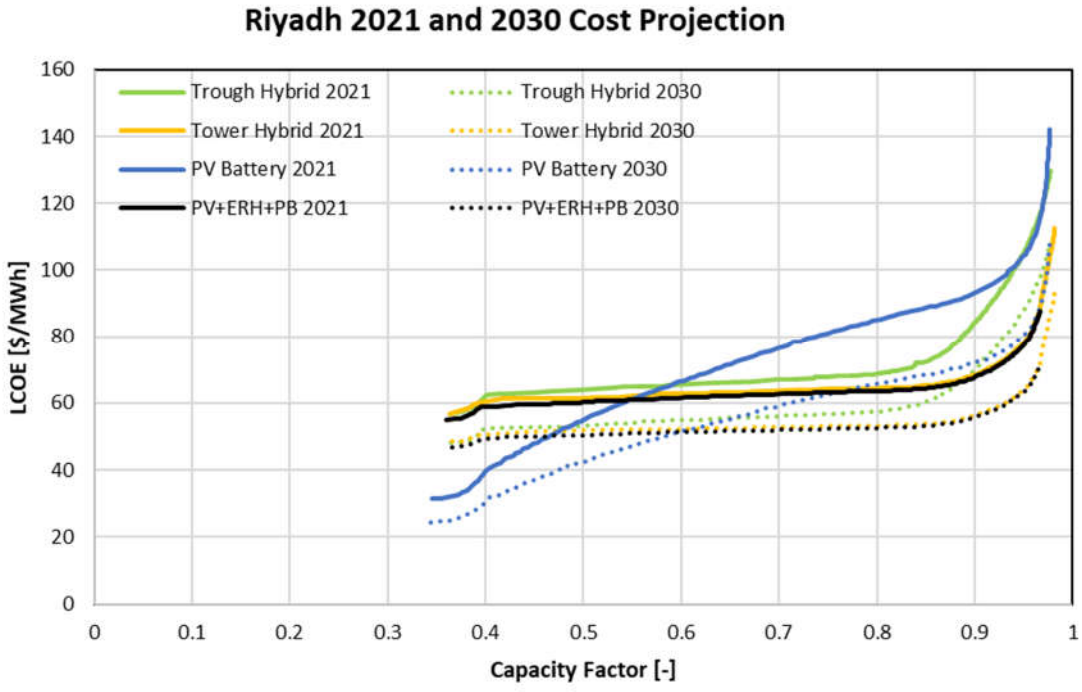

Figure 65: Cost projections 2030 (HYPPO results)